

AD737309

FINAL TECHNICAL REPORT\*

on

ANOMALOUS WATER AND OTHER POLYMERIC MATERIALS  
SPONSORED BY  
ADVANCED RESEARCH PROJECTS AGENCY  
ARPA ORDER NO. 1463

to

U. S. ARMY MISSILE COMMAND  
REDSTONE ARSENAL, ALABAMA

D D C  
RECORDED  
FEB 28 1972  
RECORDED  
B

\*This research was sponsored by the Advance Research Projects Agency of the Department of Defense under ARPA Order 1463 and was monitored by the U. S. Army Missile Command under Contract Number DAAHO1-71-C-0491. Views and conclusions expressed herein are the primary responsibility of the author or the contractor and should not be interpreted as representing the official opinion or policy of USAMICOM, ARPA, DOD, or any other agency of the Government.

SEE AD726761  
RECORDED

Reproduced by  
NATIONAL TECHNICAL  
INFORMATION SERVICE  
Springfield, Va. 22151

BATTELLE  
Columbus Laboratories  
505 King Avenue  
Columbus, Ohio 43201

DISTRIBUTION STATEMENT A

Approved for public release;  
Distribution Unlimited

**BEST  
AVAILABLE COPY**



Columbus Laboratories  
505 King Avenue  
Columbus, Ohio 43201  
Telephone (614) 299-3151  
Telex 24-5454

February 14, 1972

Commanding General  
U. S. Army Missile Command  
Redstone Arsenal, Alabama 35809

Attention AMSMI-RND

Dear Sir:

Enclosed are 46 copies of the Final Technical Report on "Anomalous Water and Other Polymeric Materials". This research is being carried out under Contract No. DAAHO1-71-C-0491. This report covers the period from December 30, 1970 to December 30, 1971.

Please do not hesitate to call us if you have any questions concerning this report.

Very truly yours,

R. J. Jakobsen  
Senior Research Chemist  
Organic Chemistry Division

RJJ:js  
Enc. (46)  
cc:  
Director  
Advanced Research Projects Agency  
1400 Wilson Boulevard  
Arlington, Virginia 22209 (3)

Defense Documentation Center  
Cameron Station  
Alexandria, Virginia 22314 (20)

Commanding General  
U. S. Army Material Command  
Washington, D. C. 20315 (1)

U. S. Army Missile Command  
Redstone Arsenal, Alabama  
Attention AMSMI-IWD (cover letter only)

DCASO, Columbus  
Building 1, Section 1  
Defense Construction Supply Center  
Columbus, Ohio 43215 (cover letter only)

## TABLE OF CONTENTS

	<u>Page</u>
SYNOPSIS . . . . .	i
INTRODUCTION AND BACKGROUND . . . . .	1
EXPERIMENTAL . . . . .	4
Liquid Water Cleaning of Capillary Tubes . . . . .	4
Preparation of Anomalous Materials from Water . . . . .	4
Preparation of Anomalous Material from $H_2O_2$ Solutions . . . . .	5
Vapor Water Cleaning of Capillary Tubes . . . . .	5
Liquid Propanol Cleaning of Capillary Tubes . . . . .	6
Liquid Water Extraction of Crushed Glasses . . . . .	6
Liquid Water Extraction of Glass Wool . . . . .	6
Synthesis of Carbonate Derivative . . . . .	7
Analyses . . . . .	7
Infrared Spectroscopy . . . . .	7
Electron Microprobe . . . . .	7
Emission Spectrography . . . . .	8
Other Analyses . . . . .	8
RESULTS . . . . .	9
Liquid Water Cleaning of Capillary Tubes and Preparation of Anomalous Materials from Water . . . . .	9
Infrared Spectra . . . . .	9
Emission Analysis . . . . .	17
Electron Microprobe Analysis . . . . .	20
C, H, N Analysis . . . . .	27
Preparation of Anomalous Material from $H_2O_2$ Solutions . . . . .	28
Infrared Spectra . . . . .	28
Emission Analysis . . . . .	30
Electron Microprobe Analysis . . . . .	30
Vapor Water Cleaning of Capillary Tubes . . . . .	42
Liquid Propanol-1 Cleaning of Capillary Tubes . . . . .	42
Infrared Spectra . . . . .	42
Emission Analysis . . . . .	45
Electron Microprobe Analysis . . . . .	45
Solvent Extractions . . . . .	45
Liquid Water Extractions of Crushed Glasses . . . . .	48
Infrared Spectra . . . . .	48
Emission Analysis . . . . .	48
Liquid Water Extraction of Glass Wool . . . . .	52
Carbonate Derivative . . . . .	54
Analysis . . . . .	54
Extraction . . . . .	70

TABLE OF CONTENTS  
(Continued)

	<u>Page</u>
DISCUSSION . . . . .	76
REFERENCES . . . . .	78
APPENDIX A - SAMPLE NOTATION . . . . .	A-1
APPENDIX B - NUMERICAL VALUES FOR THE RANGE OF THE RELATIVE INTENSITY DISTRIBUTION FROM ELECTRON MICROPROBE ANALYSIS . . . . .	B-1
APPENDIX C - WEIGHTS OF ELEMENTS DETECTED BY EMISSION SPECTROGRAPHIC ANALYSIS . . . . .	C-1

LIST OF TABLES

Table 1. Weights of Residues from Liquid Water Cleanings and Anomalous Material Preparations . . . . .	16
Table 2. Partial Emission Spectrographic Analyses for Liquid Water Cleaning Samples and Preparations of Anomalous Material from Water . . . . .	18
Table 3. C-H-N Analytical Results of Residue . . . . .	28
Table 4. Frequency Shifts (cm <sup>-1</sup> ) Due to Heating H O -P-1 . . . . .	31
Table 5. Partial Emission Spectrographic Analyses for Anomalous Material Preparations . . . . .	35
Table 6. Partial Emission Spectrographic Analysis for Liquid Washings of Capillary Tubes . . . . .	46
Table 7. Partial Emission Spectrographic Analyses for Water Extractions of Crushed Glasses . . . . .	52
Table 8. Emission Spectrographic Analyses . . . . .	62
Table 9. C-H-N-Na Analytical Results . . . . .	62

LIST OF FIGURES  
(Continued)

	<u>Page</u>
Figure 13. Electron Microprobe Analyses of H <sub>2</sub> O <sub>2</sub> -P-1 Showing the Back Scattered Electron Image of the Sample, and the X-ray Distribution Images for B, Na, and C. . . . .	32
Figure 14. Electron Microprobe Analysis of H <sub>2</sub> O <sub>2</sub> -P-1 Showing the X-ray Distribution Images for Mg and O, the Back Scattered Electron Image of the Sample, and the X-ray Distribution Image for K . . . . .	33
Figure 15. Electron Microprobe Analysis of H <sub>2</sub> O <sub>2</sub> -P-1 Showing the X-ray Distribution Images for Ca, Cl, S, and Si . . . . .	34
Figure 16. Electron Microprobe Analysis of the Black Portion of H <sub>2</sub> O <sub>2</sub> -P-1H Showing the Back Scattered Image of the Sample and the X-ray Distribution Images for B, Na, and C . . . . .	36
Figure 17. Electron Microprobe Analysis of the Black Portion of H <sub>2</sub> O <sub>2</sub> -P-1H Showing the X-ray Distribution Images for Mg and O, the Back Scattered Electron Image of the Sample, and the X-ray Distribution Image for K . . . . .	37
Figure 18. Electron Microprobe Analysis of the Black Portion of H <sub>2</sub> O <sub>2</sub> -P-1H Showing the X-ray Images for Ca, Cl, S, and Si . . . . .	38
Figure 19. Electron Microprobe Analysis of the White Portion of H <sub>2</sub> O <sub>2</sub> -P-1H Showing the Back Scattered Electron Image of the Sample and the X-ray Distribution Images for B, Na, and C . . . . .	39
Figure 20. Electron Microprobe Analyses of the White Portion of H <sub>2</sub> O <sub>2</sub> -P-1H Showing the X-ray Distribution Images for Mg and O, the Back Scattered Electron Image of the Sample, and the X-ray Distribution Image for K . . . . .	40
Figure 21. Electron Microprobe Analyses of the White Portion of H <sub>2</sub> O <sub>2</sub> -P-1 Showing the X-ray Distribution Images for Ca, Cl, S, and Si. . . . .	41

## LIST OF FIGURES

	<u>Page</u>
Figure 1. Infrared Spectra of (A) LW-H <sub>2</sub> O-1, (B) LW-H <sub>2</sub> O-2, (C) LW-H <sub>2</sub> O-12, and (D) LW-H <sub>2</sub> O-13 . . . . .	10
Figure 2. Infrared Spectra of (A) LW-H <sub>2</sub> O-14, (B) LW-H <sub>2</sub> O-15, (C) H <sub>2</sub> O-CP-1, and (D) LW-H <sub>2</sub> O-CP-2 . . . . .	11
Figure 3. Infrared Spectra of (A) LW-H <sub>2</sub> O-02, (B) H <sub>2</sub> O-CP-1, (C) H <sub>2</sub> O-UP-1, and (D) H <sub>2</sub> O-CP-2 . . . . .	12
Figure 4. Infrared Spectra of H <sub>2</sub> O-CP-3 (Top), H <sub>2</sub> O-CP-4 (Second from Top), H <sub>2</sub> O-CP-7 (Second from Bottom), and H <sub>2</sub> O-CP-8 (Bottom). . . . .	14
Figure 5. Infrared Spectra of H <sub>2</sub> O-UP-3 (Top), H <sub>2</sub> O-UP-5 (Second from Top), H <sub>2</sub> O-UP-6 (Second from Bottom), and H <sub>2</sub> O-UP-7 (Bottom) . . . . .	15
Figure 6. Electron Microprobe Analyses of LW-H <sub>2</sub> O-01 Showing the Back Scattered Electron Image of the Sample and the X-ray Distribution Image for B, Na, and C . . . . .	21
Figure 7. Electron Microprobe Analyses of LW-H <sub>2</sub> O-01 Showing the X-ray Distribution Images for Mg and O <sub>2</sub> , the Back Scattered Electron Image of the Sample, and the X-ray Distribution Image for K . . . . .	22
Figure 8. Electron Microprobe Analyses of LW-H <sub>2</sub> O-01 Showing the X-ray Distribution Images for Ca, Cl, S, and Si . . . . .	23
Figure 9. Electron Microprobe Analyses of H <sub>2</sub> O-CP-1 Showing the Back Scattered Electron Image of the Sample and the X-ray Distribution Images for B, Na, and C . . . . .	24
Figure 10. Electron Microprobe Analysis of H <sub>2</sub> O-CP-1 Showing the X-ray Distribution Images for Mg and O, the Back Scattered Electron Image of the Sample, and the X-ray Distribution Image for K . . . . .	25
Figure 11. Electron Microprobe Analyses of H <sub>2</sub> O-CP-1 Showing the X-ray Distribution Images for Ca, Cl, S, and Si . . . . .	26
Figure 12. Infrared Spectra of (A) H <sub>2</sub> O <sub>2</sub> -P-1, (B) A Thicker Sample of H <sub>2</sub> O <sub>2</sub> -P-1, (C) H <sub>2</sub> O <sub>2</sub> -P-1 Heated at 400 C for 5 Minutes, and (D) H <sub>2</sub> O <sub>2</sub> -P-1H Which is H <sub>2</sub> O <sub>2</sub> -P-1 Heated at 400 C for 60 Minutes . . . . .	29

LIST OF FIGURES  
(Continued)

	<u>Page</u>
Figure 22. Infrared Spectra of (A) VW-H <sub>2</sub> O-3, (B) VW-H <sub>2</sub> O-8, and (C) VW-H <sub>2</sub> O-5 . . . . .	43
Figure 23. Infrared Spectra of (A) LW-Pr-1, (B) LW-Pr-00, and (C) LW-Pr-01 . . . . .	44
Figure 24. Infrared Spectra of (A) LW-Pr-2, (B) the CCl <sub>4</sub> Soluble Portion of LW-Pr-2, and (C) the CCl <sub>4</sub> Insoluble Portion of LW-Pr-2 . . . . .	47
Figure 25. Infrared Spectra of (A) CG-N-1, (B) CG-7052-1, and CG-C-1 . . . . .	49
Figure 26. Infrared Spectra of (A) CG-U-1, (B) CG-V-1, and (C) CG-Q-1 . . . . .	50
Figure 27. Infrared Spectra of (A) CG-P-1, (B) CG-H <sub>2</sub> O-01 . . . . .	51
Figure 28. Infrared Spectra of GW-H <sub>2</sub> O-1 (Top), GW-P-H <sub>2</sub> O-1 (Middle), and GW-Q-H <sub>2</sub> O-1 (Bottom) . . . . .	53
Figure 29. Infrared Spectra NaHCO <sub>3</sub> in CH <sub>3</sub> OH (Top), Another Preparation of NaHCO <sub>3</sub> in CH <sub>3</sub> OH (Middle), and NaHCO <sub>3</sub> in C <sub>2</sub> H <sub>5</sub> OH (Bottom). . . . .	55
Figure 30. Infrared Spectra of NaHCO <sub>3</sub> in CH <sub>3</sub> OH Heated for Five Hours at 100 C (Top) and Residue from CCl <sub>4</sub> Extract of Above Sample (Bottom) . . . . .	56
Figure 31. Thermal Gravimetric Analysis Plot of the NaHCO <sub>3</sub> in CH <sub>3</sub> OH Product . . . . .	58
Figure 32. Infrared Spectrum of the Residue of the NaHCO <sub>3</sub> in CH <sub>3</sub> OH Product After TGA Run Shown in Figure 31 . . . . .	59
Figure 33. Mass Spectral Results (Mass Spectral Amplitude vs Temperature) for the NaHCO <sub>3</sub> in CH <sub>3</sub> OH Product. Masses 18-19 (Top), Masses 44-45 (Second from Top), Masses 31-32 (Second from Bottom), and Total Mass (Bottom) . . . . .	60
Figure 34. Mass Spectral Results for the NaHCO <sub>3</sub> in CH <sub>3</sub> OH Product at 83 C . . . . .	61

LIST OF FIGURES  
(Continued)

	<u>Page</u>
<b>Figure 35.</b> Infrared Spectra of the $\text{NaHCO}_3$ in $\text{CH}_3\text{OH}$ Product After Standing in Air for (A) 3 Days, (B) 5 Days, and (C) 7 Days . . . . .	64
<b>Figure 36.</b> Infrared Spectra of the $\text{NaHCO}_3$ in $\text{CH}_3\text{OH}$ Product After Standing in Air for (D) 10 Days, and (E) 24 Days . . . . .	65
<b>Figure 37.</b> Infrared Spectra of the $\text{NaHCO}_3$ in $\text{CH}_3\text{OH}$ Product After Standing in a Vacuum for 3 Days (Top) and 7 Days (Bottom). . . . .	66
<b>Figure 38.</b> Infrared Spectra of the $\text{NaHCO}_3$ in $\text{CH}_3\text{OH}$ Product After Standing in a Vacuum for 12 Days (Top) and 24 Days (Bottom) . . . . .	67
<b>Figure 39.</b> Infrared Spectra of the $\text{NaHCO}_3$ in $\text{CH}_3\text{OH}$ Product After Standing 10 Days in Air (Top) and 10 Days in a Vacuum (Bottom). . . . .	68
<b>Figure 40.</b> Infrared Spectra of the $\text{NaHCO}_3$ in $\text{CH}_3\text{OH}$ Product After Standing 24 Days in Air (Top) and 24 Days in a Vacuum (Bottom). . . . .	69
<b>Figure 41.</b> Infrared Spectra of the $\text{NaHCO}_3$ in $\text{CH}_3\text{OH}$ Product: Fresh Sample (Top) and After 21 Days in Air (Bottom) . . . . .	71
<b>Figure 42.</b> Infrared Spectra of the $\text{NaHCO}_3$ in $\text{CH}_3\text{OH}$ Product After Standing 21 Days in Air: Residue from $\text{CHCl}_3$ Extract (Top) and Residue from $\text{CCl}_4$ Extract (Bottom) . . . . .	72
<b>Figure 43.</b> Mass Spectra of the Residue from the $\text{CHCl}_3$ and $\text{CCl}_4$ Extracts of the $\text{NaHCO}_3$ in $\text{CH}_3\text{OH}$ Product at 50 C. . . . .	73
<b>Figure 44.</b> Mass Spectra of the Residue from the $\text{CHCl}_3$ and $\text{CCl}_4$ Extracts of the $\text{NaHCO}_3$ in $\text{CH}_3\text{OH}$ Product at 150 C . . . . .	74
<b>Figure 45.</b> Mass Spectra of the Residue from the $\text{CHCl}_3$ and $\text{CCl}_4$ Extracts of the $\text{NaHCO}_3$ in $\text{CH}_3\text{OH}$ Product at 200 C . . . . .	75

## SYNOPSIS

A better understanding of the infrared spectra of anomalous water coupled with extensive chemical analysis of water washes of glass systems and anomalous water preparations indicates that most of the material called anomalous water consists of substances either extracted from glass or that are residues of water. Thus no evidence has been found that anomalous water exists — at least as a form of water.

A material, synthesized in the laboratory (and likely to be sodium methyl carbonate) was identical to a material isolated from glass by extraction with methanol. This material exhibits unusual chemical behavior which can help explain some of the (anomalous) behavior of the material called anomalous water.

FINAL TECHNICAL REPORT

on

ANOMALOUS WATER AND OTHER POLYMERIC MATERIALS  
SPONSORED BY  
ADVANCED RESEARCH PROJECTS AGENCY  
ARPA ORDER NO. 1463

to

U. S. ARMY MISSILE COMMAND  
REDSTONE ARSENAL, ALABAMA

from

BATTELLE  
Columbus Laboratories

January 31, 1972

INTRODUCTION AND BACKGROUND

Few scientific reports in the last decade have attracted such widespread interest as has that of anomalous water. One result of this interest has been the experimental and theoretical investigations of anomalous materials by researchers who are expert in a wide range of technical disciplines. Yet even after these investigations, a number of basic questions concerning anomalous water remained either unanswered or incompletely answered.

Probably the most important of the unanswered questions was "Does water alone or water combined with another chemical moiety account for the anomalous water phenomenon?" From the experimental results obtained from samples of a few micrograms of anomalous water, one cannot answer this question unambiguously.

Chemical analyses by a number of laboratories strongly indicate that elements other than H and O have been present to varying degrees in the anomalous water samples. It is important to note, however, that excluding H and O, no combination of the elements detected to be present by chemical analysis of microgram samples has been conceived which will explain all of the experimental observations for anomalous water - especially the infrared spectrum.

The purpose of this research is the production of anomalous material prepared from water and anomalous materials prepared from selected organic compounds in amounts sufficiently large to enable their characterization, and to

permit an assessment to be made of the technological utility of the anomalous materials.

It is believed that a knowledge of the impurities present and the role such impurities play, if any, in the anomalous water phenomenon is critical for an accurate evaluation of data obtained by chemical analysis and for the optimization of synthesis techniques to be made. Therefore, the initial experimental work was designed to establish qualitatively and, where possible, quantitatively, the impurities which could be introduced during the preparation of anomalous materials.

It has been demonstrated that freshly drawn pyrex and quartz capillaries like those used for anomalous water preparations yield a water-soluble residue when they are washed with distilled water.<sup>(1)</sup> While the exact nature of this water-soluble residue was not characterized, it was shown that this residue from the water-soluble fraction appeared to be different from anomalous material prepared in the same capillaries. Also, as the number of washes of a group of capillaries was increased, it was observed that the amount of the residue from the water soluble fraction significantly decreased. However, after four washings, some water-soluble components were still being extracted.<sup>(1)</sup>

Therefore, an integral part of the present research program was to determine the nature of the water-soluble fraction and to test if all detectable water-soluble material could be removed from the capillaries\*. Experiments were conducted in which a group of pyrex capillaries was washed until no detectable water-soluble component was removed.

The residue from the water used for each wash was retained separately for analysis to determine the elemental composition of each residue and to approximate the relative rate at which each element was removed. These same "cleaned" capillaries were then used to prepare anomalous material and to investigate if additional components of the pyrex were extracted.

Exactly analogous experiments were performed using propanol-1 instead of water in the initial investigation of anomalous organics.

It has been observed by a number of researchers that anomalous water forms detectably only from water vapor.<sup>(2)</sup> Also, it has been reported that in some cases solubility can be increased by as much as 9 orders of magnitude in a thin layer of solvent, as opposed to the bulk solvent.<sup>(3)</sup> Thus research included experiments to test if such an abnormal solubility effect is involved in the formation of anomalous materials. Accordingly, capillaries were washed with water vapor in a pressure cooker.

It has been proposed that the anomalous character of anomalous water is due to the extraction of some unspecified component of the glass from which the capillaries are made.<sup>(4)</sup> Such an extract, like anomalous water, would have a density and index of refraction greater than those of water.

\*In this report, the terms capillary and tube are used interchangeably.

To investigate if some water-soluble fraction of a glass could account for the reported infrared spectrum of anomalous water, experiments were conducted to determine the kind and amounts of material which could be extracted from various glasses. Crushed portions of seven different glasses were extracted with water. In addition to recording their infrared spectra, the water-soluble fraction of each glass was analyzed by emission spectrography to determine the metallic composition of the residues. Other experiments to determine the water soluble portions of glass involved extraction of pyrex and quartz glass wool with water. Infrared spectra of these extracts were recorded.

Early anomalous water research at Battelle's Columbus Laboratories suggested that oxygen could play a key role in the formation of anomalous water.<sup>(5)</sup> In an attempt to test this hypothesis, the preparation of anomalous material from 3 percent aqueous H<sub>2</sub>O<sub>2</sub> instead of H<sub>2</sub>O was attempted.

During the final half of the research emphasis shifted from the preparation of anomalous water to the study of the identity and chemistry of a compound which could be either extracted from glass or synthesized in the laboratory [first done at the University of Maryland<sup>(6)</sup>]. The reason for this shift in emphasis was that the infrared spectrum of this compound indicated that if this compound could be identified in anomalous water, many of the questions concerning the infrared spectra of anomalous water could be answered.

EXPERIMENTALLiquid Water Cleaning of Capillary Tubes

For the liquid water cleaning experiments, about 500 freshly pulled pyrex capillary tubes were placed in a pyrex baking dish and the tubes were covered with 500 ml of demineralized water. The baking dish was then covered with Saran wrap and allowed to stand (with occasional shaking) for seven days. On the seventh day, the water was poured off into a round-bottomed pyrex flask. The baking dish and tubes were dried in an oven at 100 C and then a second cleaning was started by adding another 500 ml of demineralized water to the dish. This weekly cleaning cycle was repeated until the 500 tubes had been washed 15 times.

The flask containing a single washing was then placed on a rotary evaporator where most of the water was removed. At the point where a few ml of water remained in the flask, the evaporation was stopped and the water was transferred to a weighed pyrex vial. The remaining water was removed by evaporation with N<sub>2</sub> and the weight of the dry residue was obtained. A few drops of water were then added to the vial and aliquots of the solution were removed for infrared, emission, and electron microprobe analysis.

The washing was halted and the tubes were considered "cleaned" when the barely perceivable residue from the 15th washing gave no detectable weight (less than 0.1 mg) and no infrared spectrum could be obtained from the residue by the techniques used for the other washings. These samples of washings are designated LW-H<sub>2</sub>O-1\*, LW-H<sub>2</sub>O-2, etc. The letters stand for liquid wash with water and the numbers indicate which washing.

In addition, several standards or blanks were obtained. LW-H<sub>2</sub>O-00 is the residue obtained from the water used in these experiments. LW-H<sub>2</sub>O-01 and LW-H<sub>2</sub>O-02 are the first and second system blanks, respectively. A system blank is a duplicate of the washing experiments without the tubes being present. Thus the sample under consideration is the residue obtainable from a water wash of the baking dish, round-bottomed flask, and vial.

Preparation of Anomalous Materials from Water

The technique used in our laboratory for preparation of anomalous material has been described in detail<sup>(1)</sup> and will be only briefly described here. The capillary tubes are placed on pyrex Petri dishes resting on a porcelain plate in a greaseless desiccator. A pyrex evaporating dish containing demineralized water is placed

---

\*A complete list of sample notations is given in Appendix A.

below the porcelain plate and the desiccator is sealed with a vacuum of about 5 millimeters of pressure of mercury. After seven days the capillaries are removed from the desiccator and the anomalous material is removed from the tubes by washing with demineralized water. This wash water is then placed in a round-bottomed flask and the residue is obtained by the same procedure as used in the liquid washing experiments.

Two types of preparation were attempted. In one the pyrex tubes which had been washed 15 times (and designated "cleaned") were used for preparation of the anomalous material. This preparation is labeled  $H_2O$ -CP-1. The same tubes were then dried and placed in the desiccator for a second preparation. The sample resulting from this is labeled  $H_2O$ -CP-2. (CP stands for cleaned pyrex). This process was repeated for eight preparations. In the second type of experiment, pyrex tubes which had not been washed or "cleaned" were used for the preparation. The first sample is labeled  $H_2O$ -UP-1. (UP stands for uncleaned pyrex). This process was repeated for seven preparations.

#### Preparation of Anomalous Material from $H_2O_2$ Solutions

To test the role played by oxygen in the formation of anomalous material, a preparation was initiated using a 3 percent aqueous  $H_2O_2$  solution instead of  $H_2O$ . The method of preparation used was identical to that described above except the pyrex tubes were washed several times with water and several times with ethanol prior to being placed in the desiccator.

Upon removal from the desiccator the tubes were washed with quadruply distilled water. The major portion of the wash water (~80 ml total) was removed by evaporation under reduced pressure (~5 mm Hg). A water bath maintained at 40 C was used to warm the round-bottom flask containing the sample. Aliquots of the resulting concentrated solution (~4 ml) were used for analysis. The residue remaining after evaporation of the water from the 3 percent  $H_2O_2$  preparation is labeled  $H_2O_2$ -P-1. After casting a film on an Irtran plate from an aliquot of concentration solution for infrared analyses, the plate and sample were heated for 60 minutes at 400 C in air. This sample is designated  $H_2O_2$ -P-1H.

#### Vapor Water Cleaning of Capillary Tubes

Experiments were carried out in which capillary tubes were cleaned with water vapor in order to test the possibility that vapor water has a greater solvent power for glass than does liquid water. In this experiment a pressure cooker was used to generate the water vapor as steam. About 500 pyrex tubes were heated in the pressure cooker for periods up to eight hours. The residual water was poured off and the residue worked up via a rotary evaporator as in the liquid water wash experiments. These samples were labeled VW- $H_2O$ -1, VW- $H_2O$ -2, etc. The letters stand for vapor washing with water and the numbers indicate which washing.

Liquid Propanol Cleaning of Capillary Tubes

Prior to the preparation of other anomalous materials (such as from propanol instead of water), capillary tubes were repeatedly washed with liquid propanol. The procedure and experimental arrangement was identical to that described for the liquid water, except that 99 percent plus propanol was used for the washing instead of demineralized water. These samples are designated LW-Pr-1, LW-Pr-2, etc.

Sample LW-Pr-00 is the residue obtained from the propanol used in the washings. LW-Pr-01 is the residue from a propanol extraction of the Saran wrap used to cover the baking dish.

In addition, sample LW-Pr-2 was cross-extracted with carbon tetrachloride ( $CCl_4$ ) and infrared spectra obtained on both the  $CCl_4$  solubles and the  $CCl_4$  insolubles.

Liquid Water Extraction of Crushed Glasses

Experiments were designed to determine the composition of extractable material from various glasses. About 150 grams each of seven types of glass were crushed with a mortar and pestle and transferred rapidly into a new round-bottom flask containing about 150 grams of quadruply distilled water. The crushing was done on 30 to 50-g portions of glass. Each portion was transferred rapidly into the water to optimize contact of the freshly formed glass surfaces with the water. The glass was finely crushed, but no attempt to control particle size was made. Each crushed glass remained in contact with water for 10 days. The samples were periodically agitated. The water was decanted and filtered through a Gooch crucible, using a slurry of Whatman No. 1 filter paper to remove the fines. After filtration, the volume of the water was reduced to ~4 ml by the method described above for  $H_2O_2$ .

These samples are designated CG-V-1, CG-Q-1, etc. CG stands for crushed glass extraction and 1 signifies the first extraction. The middle letter indicates the type of glass: V=Vycor, Q=quartz, P=pyrex, N=Nonex, C=cobalt, U=uranium, and 7052=7052 glass. CG- $H_2O$ -01 is a system blank. The blank was a 150-g aliquot of the same water used for extracting crushed glass. The blank was carried through all operations described above except that it was never exposed to a crushed glass.

Liquid Water Extraction of Glass Wool

To further study the composition of extractable material from glass, 500 ml flasks were half filled with either pyrex or quartz glass wool. The flasks were then filled with 250 ml of demineralized water and allowed to stand (with occasional shaking) for 10 days. The water was decanted into a flask and was evaporated by the process used for the liquid water cleaning of capillary tubes. The original glass wool was then used for a second water extraction. These samples are designated:

GW-P-H<sub>2</sub>O-1 and -2 and GW-Q-H<sub>2</sub>O-1 and -2. In addition two standards or blanks were obtained. These blanks duplicated the experimental conditions except no glass wool was placed in the flasks. These samples are designated: GW-H<sub>2</sub>O-1 and -2.

### Synthesis of Carbonate Derivative

As explained in the Introduction, the research emphasis shifted when the University of Maryland group<sup>(5)</sup> extracted (with methanol) a compound from pyrex glass wool that gave an infrared spectrum that could be used to help explain the infrared spectra of anomalous water. Later the Maryland group found that it could synthesize this compound and the synthesis has since been repeated in our laboratory. In this saturated solution of sodium bicarbonate (NaHCO<sub>3</sub>) in methanol is prepared. After varying periods of time, the methanol is decanted from any residual NaHCO<sub>3</sub>. When this methanol is evaporated, the residual solid gives an infrared spectrum which is not that of NaHCO<sub>3</sub>. The infrared spectra of this residual solid and of the compound extracted from glass wool were identical. It is this residual solid, apparently a pure compound, which occupied most of the research effort in the latter half of the program. A product with a slightly different infrared spectrum can be prepared in a similar manner when ethanol is used as the solvent instead of methanol.

### Analyses

#### Infrared Spectroscopy

The infrared spectra were obtained on a Perkin-Elmer 521 spectrophotometer. Samples were run as films from water on Irtran plates or films from propanol on NaCl plates. It is significant that all samples were large enough so that spectra could be obtained without a beam condenser or the use of scale expansion.

#### Electron Microprobe

The microprobe analyses were done on a Model 400S Scanning Electron Microprobe manufactured by the Materials Analysis Company. The samples were prepared for the electron microprobe by laying films (from water or propanol) on high purity aluminum plates. X-ray images of the element distributions are shown in various figures throughout this report. The numerical value of the relative intensity counts for all elements and samples studied are given in Appendix B. These relative count values cover the range observed under the area of the electron beam. Two points of caution in the interpretation of results must be mentioned here. All samples showed varying amounts of browning or darkening under the electron beam. This coupled with the high vacuum used in the electron microprobe suggests that the electron microprobe sample might not be equivalent in composition to the samples used for other techniques of analysis. Secondly, the area shown in the photographs in the figures represents only a small portion of the total sample. As will be seen

later, all elements are not distributed evenly throughout the sample, and thus the electron microprobe analysis might not be representative of the entire sample.

### Emission Spectrography

The emission analysis was performed on an ARL 1.5 meter; 25,000 line/inch grating instrument. The spectra were recorded on photographic film in the region 2200A to 9400A.

Partial results of the emission analyses are listed in several tables throughout this report. The total emission results are listed in Appendix C. All values are expressed in micrograms with an accuracy of  $\pm 50$  percent. The weights of the samples used for emission analysis are not known; therefore some measure of sample amount is needed in order to be able to compare samples realistically. The next to last column of Appendix C gives the total weight of the elements detected. Values reported as <0.1, <1.0, <50.0, etc. are included in the total as 0.1, 1.0, 50.0, respectively. For some samples, a camera was used which did not give precise values for K (only reported as <50.0). For the same samples, no values are reported for Co, Sb, and As. Thus the last column of Appendix B gives the total weight of the elements detected minus the weight of K. Using the weights reported in this last column does not guarantee direct comparison of samples, but does give a better means of evaluating large scale changes in elemental composition; especially for samples containing equivalent amounts of K.

### Other Analyses

Conventional wet chemical C, H, and N analyses were done whenever the samples were large enough. These results are listed in Table 3. The weights of the residues obtained from the various washings and preparations are listed in Table 1.

Mass spectral data were obtained using both a Finnigan 1015 quadruple mass spectrometer and a high resolution instrument (MS-9) manufactured by Associated Electrical Instruments (AEI). The thermal gravimetric analyses were done on a Cahn-RG recording microbalance.

RESULTSLiquid Water Cleaning of Capillary Tubes and Preparation of Anomalous Materials from WaterInfrared Spectra

The infrared spectra of the samples obtained from the liquid water cleaning of capillary tubes are shown in Figures 1 and 2. The infrared spectra of some of the first preparations of anomalous materials from water utilizing these cleaned tubes are also shown in Figure 2.

All of these samples show some infrared absorption in the conventional OH stretching region from 3350 to 3500  $\text{cm}^{-1}$ . This appears to be typical of an anomalous water prepared in pyrex tubes. This, however, is a very, very small amount of OH absorption when compared to the OH band of water.

In addition all of these samples show a very weak CH absorption between 2850 and 3000  $\text{cm}^{-1}$ . This might indicate some fingerprint contamination (although gloves are always used) or absorption of organic vapors which are only slightly washed off each time because water is not a good solvent for many organics. On going from LW- $\text{H}_2\text{O}$ -1 through LW- $\text{H}_2\text{O}$ -15 the amount of CH material appears to be decreasing, but then it increases again, especially in  $\text{H}_2\text{O}$ -CP-2. In sample  $\text{H}_2\text{O}$ -CP-2 there is a weak 1730  $\text{cm}^{-1}$  absorption in addition to the CH absorption. A  $\text{CCl}_4$  extraction of  $\text{H}_2\text{O}$ -CP-2 gave a residue whose spectrum showed only 2850-3000  $\text{cm}^{-1}$  absorption and 1730  $\text{cm}^{-1}$  absorption of about the correct relative intensity to account for all the absorptions at these frequencies which are seen in the spectrum of  $\text{H}_2\text{O}$ -CP-2. Thus the organics can be removed without affecting the rest of the spectrum of anomalous water samples.

Most of the spectra of the liquid water washings show two absorption bands in the 1600  $\text{cm}^{-1}$  region. One is at 1640  $\text{cm}^{-1}$  and the other is at 1680  $\text{cm}^{-1}$ , with the 1680  $\text{cm}^{-1}$  band being, generally, the stronger absorption. It is interesting to note (although difficult to see in the figures) that the spectra of the anomalous water preparations also show two bands in this region. One is at 1680  $\text{cm}^{-1}$ , but the other is shifted to 1620  $\text{cm}^{-1}$ . In addition the 1620  $\text{cm}^{-1}$  band is always the stronger absorption in the spectra of the preparations. This observation strongly suggests that a different chemical species is present in the preparations than in the washings. All washings (LW- $\text{H}_2\text{O}$ -1 through LW- $\text{H}_2\text{O}$ -14) and the system blank (LW- $\text{H}_2\text{O}$ -02, Figure 3) show the absorption at 1640  $\text{cm}^{-1}$ . All preparations including  $\text{H}_2\text{O}$ -UP-1 (Figure 3) have this absorption at 1620  $\text{cm}^{-1}$ . This shift is quite consistent and is believed to be significant.

In the 1400  $\text{cm}^{-1}$  region, the infrared spectra of the liquid washings give very broad absorption which shows two peaks; one at 1350-1360  $\text{cm}^{-1}$  and one near 1410  $\text{cm}^{-1}$ . The peak near 1350  $\text{cm}^{-1}$  is generally the stronger absorption although occasionally the peaks are nearly equal in intensity. On the other hand, the spectra

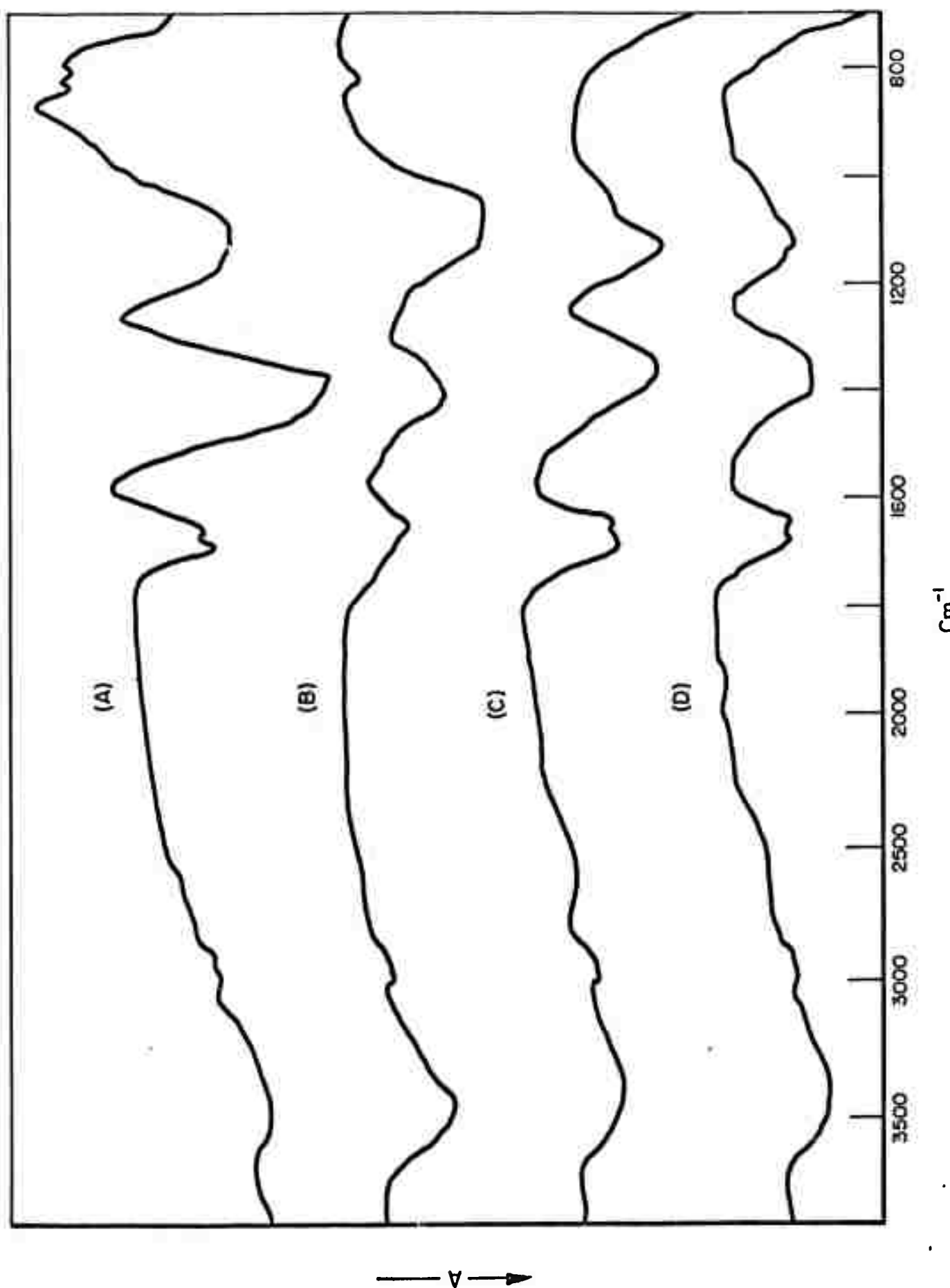


FIGURE 1. INFRARED SPECTRA OF (A) LW-H<sub>2</sub>O-1, (B) LW-H<sub>2</sub>O-2, (C) LW-H<sub>2</sub>O-12, AND (D) LW-H<sub>2</sub>O-13

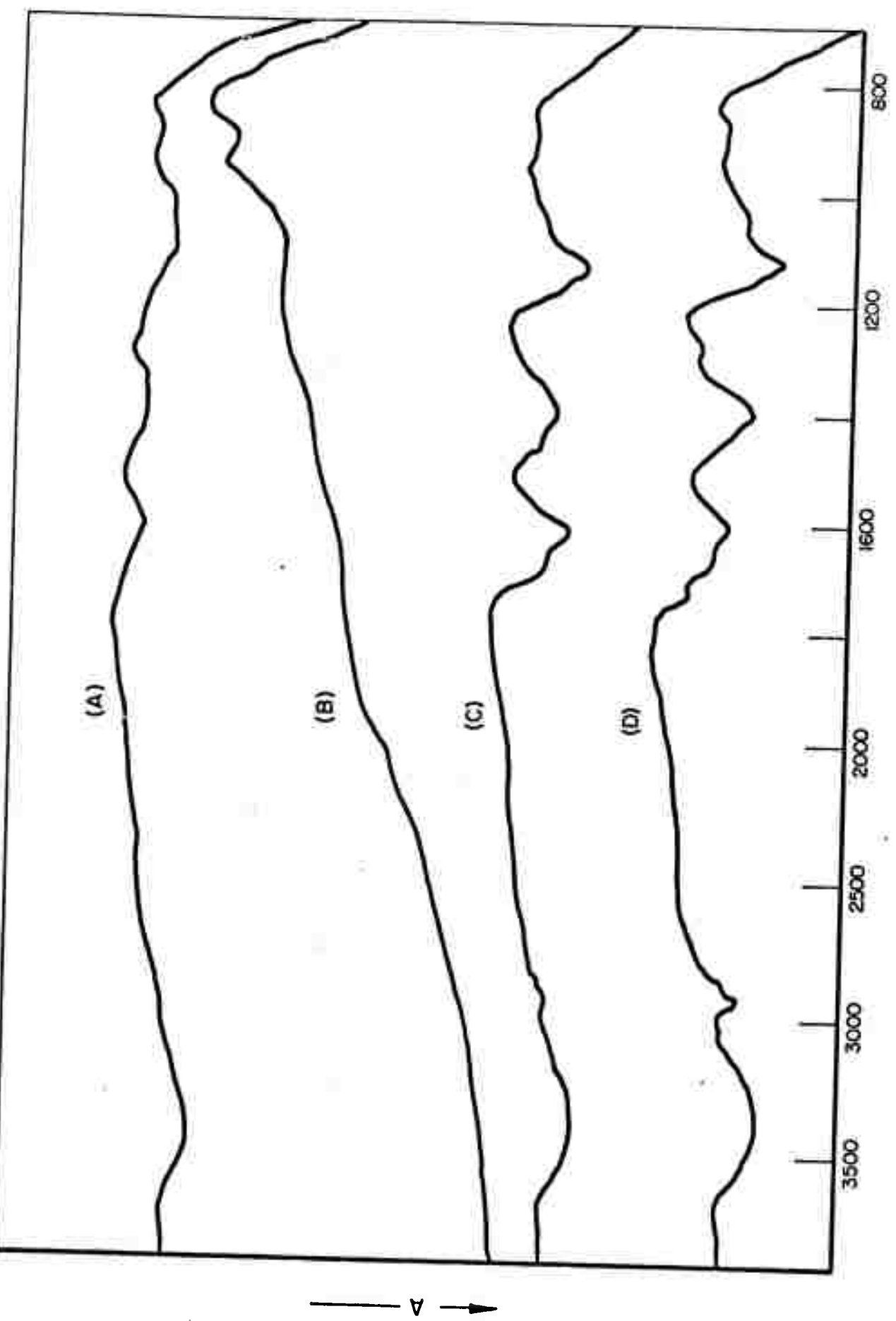


FIGURE 2. INFRARED SPECTRA OF (A) LW-H<sub>2</sub>O-14, (B) LW-H<sub>2</sub>O-15, (C) H<sub>2</sub>O-CP-1, AND (D) H<sub>2</sub>O-CP-2

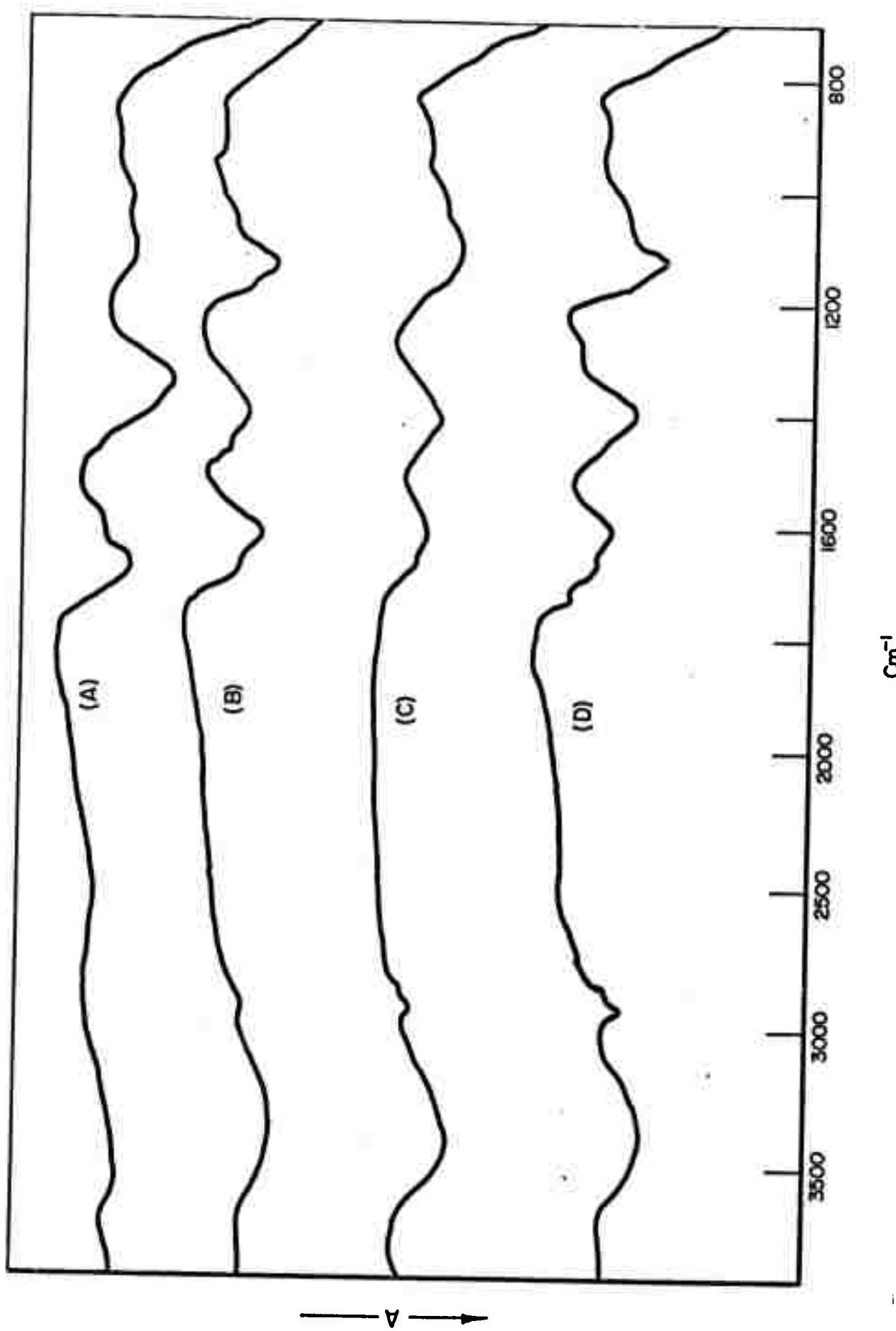


FIGURE 3. INFRARED SPECTRA OF (A) LW-H<sub>2</sub>O-02, (B) H<sub>2</sub>O-CP-1, (C) H<sub>2</sub>O-UP-1, AND (D) H<sub>2</sub>O-CP-2

of the anomalous water preparations show a strong  $1410\text{ cm}^{-1}$  absorption with, at best, a weak  $1350\text{ cm}^{-1}$  absorption (the width of the  $1410\text{ cm}^{-1}$  band makes it difficult to determine if a  $1350\text{ cm}^{-1}$  absorption is present). This shift between washings and preparations is best seen in Figure 3. The system blank or washing (LW- $\text{H}_2\text{O}$ -02) clearly shows strong absorption at  $1350\text{ cm}^{-1}$  while the preparations ( $\text{H}_2\text{O}$ -CP-1,  $\text{H}_2\text{O}$ -UP-1, and  $\text{H}_2\text{O}$ -CP-2) show strong  $1410\text{ cm}^{-1}$  absorption. Thus the  $1400\text{ cm}^{-1}$  spectral region also clearly shows differences between the liquid water washings and the preparations.

Spectral differences are also seen in the  $1100\text{ cm}^{-1}$  region. However, these are not differences between washings and preparations. For purposes of discussion consider two areas of infrared absorption in this spectral region; one from  $1040$  to  $1090\text{ cm}^{-1}$  and from  $1120$  to  $1140\text{ cm}^{-1}$ . In Figure 1 it can be seen that LW- $\text{H}_2\text{O}$ -1 and LW- $\text{H}_2\text{O}$ -2 show stronger absorption in the  $1040$  to  $1090\text{ cm}^{-1}$  range while LW- $\text{H}_2\text{O}$ -12 and LW- $\text{H}_2\text{O}$ -13 show a stronger band at  $1120$  to  $1140\text{ cm}^{-1}$ . This would seem to indicate that continual washing was removing the species giving rise to the  $1040$ - $90\text{ cm}^{-1}$  absorption more than the species giving rise to the  $1120$ - $40\text{ cm}^{-1}$  component. However in LW- $\text{H}_2\text{O}$ -14 (Figure 2) these bands are nearly of equal intensity again. From Figure 3 it can be seen that the preparations in cleaned tubes ( $\text{H}_2\text{O}$ -CP-1 and  $\text{H}_2\text{O}$ -CP-2) give a stronger  $1120$ - $40\text{ cm}^{-1}$  peak. However, while  $\text{H}_2\text{O}$ -UP-1 gives a stronger  $1120$ - $1140\text{ cm}^{-1}$  absorption there is definitely some  $1040$ - $90\text{ cm}^{-1}$  absorption also. The system blank or washing LW- $\text{H}_2\text{O}$ -02 gives mainly  $1040$ - $1090\text{ cm}^{-1}$  absorption.

Spectra of further preparations from cleaned tubes are shown in Figure 4 while spectra of further preparations from uncleaned tubes are shown in Figure 5. In general, the spectra in Figures 4 and 5 show the same trends discussed for the spectra in Figures 1 to 3. However there are certain exceptions; the major one being the spectrum of  $\text{H}_2\text{O}$ -CP-3 (Top Figure 4). This spectrum shows a high concentration of a nitrate and the frequencies are close to those of sodium nitrate. The reasons for the anomaly are not known, but it has been observed before<sup>(6)</sup>. This behavior is especially peculiar since the spectra of  $\text{H}_2\text{O}$ -CP-2 (Figure 3D) and  $\text{H}_2\text{O}$ -CP-4 (Figure 4, second from top) are typical of normal anomalous water preparations.

The only other major deviation is seen in the spectrum of  $\text{H}_2\text{O}$ -UP-5 (Figure 5, second from top) where there is considerable absorption in the  $1350$ - $1360\text{ cm}^{-1}$  region. This behavior is more typical of washings than of preparations.

The effectiveness of the washing procedure can be judged from the spectra of Figures 1 and 2. More than adequate residue was obtained to record the spectra of LW- $\text{H}_2\text{O}$ -1 and LW- $\text{H}_2\text{O}$ -2 (Figures 1A and -B). There was a significant decrease in the amount of residue available to obtain spectra of LW- $\text{H}_2\text{O}$ -12 and LW- $\text{H}_2\text{O}$ -13 (Figures 1C and -D). The sample LW- $\text{H}_2\text{O}$ -14 was very small; the resulting spectrum (Figure 2A) showed only weak bands. The residue LW- $\text{H}_2\text{O}$ -15 was barely perceptible and no spectrum (Figure 2B) could be obtained. The total weights of these residues and preparations are given in Table 1, and the weights give clearer indications of the above trends due to the washings.

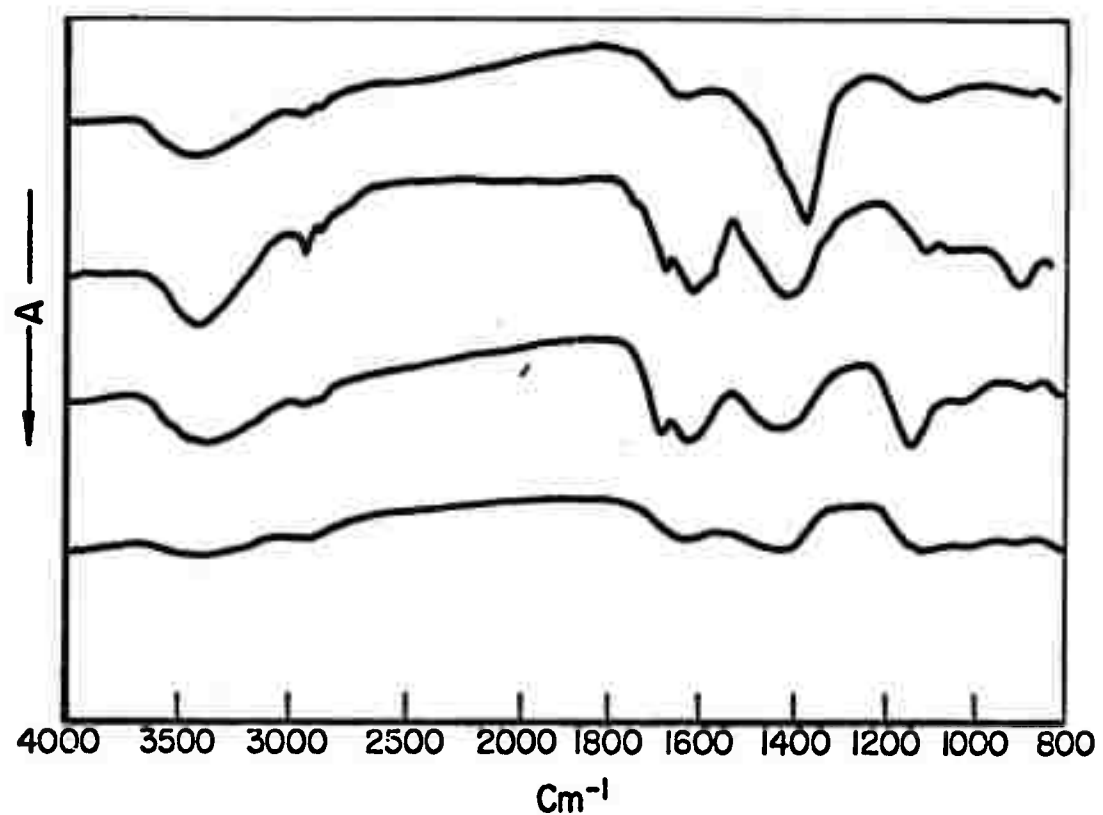


FIGURE 4. INFRARED SPECTRA OF  $\text{H}_2\text{O-CP-3}$  (TOP),  $\text{H}_2\text{O-CP-4}$  (SECOND FROM TOP),  $\text{H}_2\text{O-CP-7}$  (SECOND FROM BOTTOM), AND  $\text{H}_2\text{O-CP-8}$  (BOTTOM)

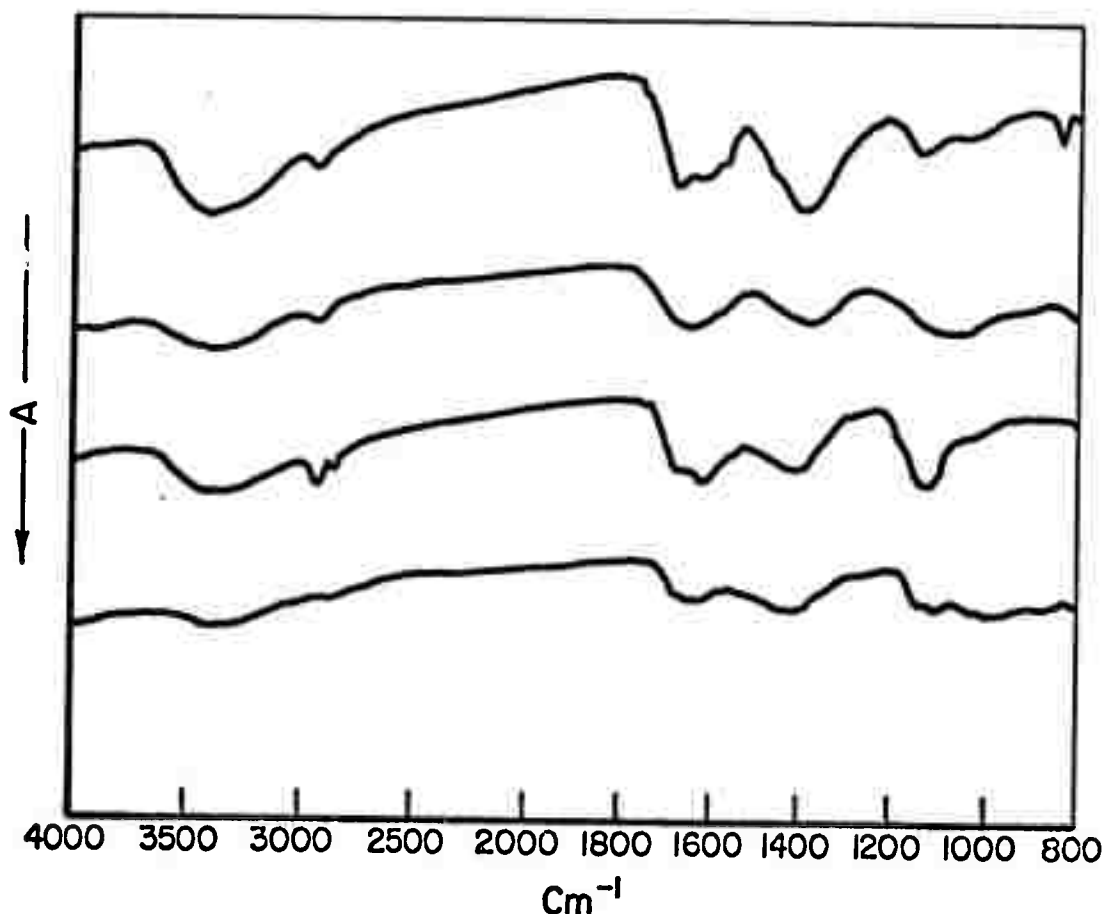


FIGURE 5. INFRARED SPECTRA OF  $\text{H}_2\text{O}$ -UP-3 (TOP),  $\text{H}_2\text{O}$ -UP-5 (SECOND FROM TOP),  $\text{H}_2\text{O}$ -UP-6 (SECOND FROM BOTTOM), AND  $\text{H}_2\text{O}$ -UP-7 (BOTTOM)

TABLE 1. WEIGHTS OF RESIDUES FROM LIQUID WATER  
CLEANINGS AND ANOMALOUS MATERIAL  
PREPARATIONS

Sample	Weight, (mg)
LW-H <sub>2</sub> O-02 (blank)	0.4
LW-H <sub>2</sub> O-1	3.6
LW-H <sub>2</sub> O-2	1.5
LW-H <sub>2</sub> O-10	0.5
LW-H <sub>2</sub> O-14	0.3
LW-H <sub>2</sub> O-15	no measurable weight, <0.1
H <sub>2</sub> O-CP-1	0.4
H <sub>2</sub> O-CP-2	0.3
H <sub>2</sub> O-CP-3	0.3
H <sub>2</sub> O-CP-4	1.3
H <sub>2</sub> O-CP-5	0.6
H <sub>2</sub> O-CP-6	1.0
H <sub>2</sub> O-CP-7	1.3
H <sub>2</sub> O-CP-8	0.5
H <sub>2</sub> O-UP-1	1.4
H <sub>2</sub> O-UP-2	1.3
H <sub>2</sub> O-UP-3	1.3
H <sub>2</sub> O-UP-4	0.8
H <sub>2</sub> O-UP-5	1.2
H <sub>2</sub> O-UP-6	0.5
H <sub>2</sub> O-UP-7	1.2

After the 15th wash, the tubes were judged to be "cleaned" and an anomalous material preparation using these tubes was started. Even though these were "cleaned" tubes, material was observed in the tubes after they were used for a preparation. When the material was removed from the tubes and the normal water evaporated, the weight of material from this first preparation was determined to be 0.4 mg. While this is greater than the non-measurable (<0.1 mg) weight of the 15th washing, it is not as much as had been produced in past preparations at Battelle, and is in the range of washings LW-H<sub>2</sub>O-10 to LW-H<sub>2</sub>O-14. This observation alone may indicate that a new material is formed in the tubes during the preparation process or it may only indicate that the vapor-like washing that goes on during the preparation can leach additional materials from the glass even after the glass tubes had been cleaned by the liquid washings. The variation in weights and the fact that material is continually produced (H<sub>2</sub>O-CP-2 to H<sub>2</sub>O-CP-8) lends weight to the vapor-like washing leaching additional material from the glass tubes.

The preparation in the uncleared tubes should give a weight in the range of the 3.6 mg obtained for the first washing (LW-H<sub>2</sub>O-1) if a vapor-like washing is as effective as a liquid washing. Since it did not, the formation of a material in the tubes during the preparation could be supported. However, again, varying weights of material are found in all these preparations (H<sub>2</sub>O-UP-2 to H<sub>2</sub>O-UP-7).

The spectra of virtually all the preparations are qualitatively similar. Thus, the differences in the weights of these preparations may only reflect amounts of available sample and not changes in composition. This will be discussed further in following sections.

The spectra of the washings in Figures 1 and 2 all show the 1600 cm<sup>-1</sup> band to be weaker than the 1400 cm<sup>-1</sup> band. The spectrum of the first preparation in these cleaned tubes (H<sub>2</sub>O-CP-1) shows an intensity reversal, i. e., the 1600 cm<sup>-1</sup> band is stronger than the 1400 cm<sup>-1</sup> band. In the past<sup>(1)</sup> we have used the latter intensity relationship as one indication of the formation of a new material during the preparation process. At the present time it would appear that the relationship based on the stronger 1600 cm<sup>-1</sup> versus 1400 cm<sup>-1</sup> band must be qualified since in Figure 3, it is clearly seen that the spectra of both H<sub>2</sub>O-CP-2 and H<sub>2</sub>O-UP-1 show the 1600 cm<sup>-1</sup> band to be weaker than the 1400 cm<sup>-1</sup> band (as in the H<sub>2</sub>O washing samples). This reversal of intensity of the 1600 and 1400 cm<sup>-1</sup> bands is also seen in some of the spectra of Figures 4 and 5.

### Emission Analysis

Emission spectrographic analyses have been obtained on all the liquid washing samples and on the first few preparations of anomalous materials from water. Complete emission results on all samples are given in Appendix C. Partial emission results for the washings and preparations are given in Table 2. The elements listed in Table 2 are those which show weight changes on going from sample to sample. With this criterion elements such as Ba, Mn, Fe, Sn, Ni, Cu, Ti, and Cr are not included in Table 2. Note that the numbers represent the total weight in micrograms of each of the elements observed. Since all of the elements present

TABLE 2. PARTIAL EMISSION SPECTROGRAPHIC ANALYSES FOR LIQUID  
WATER CLEANING SAMPLES AND PREPARATIONS OF  
ANOMALOUS MATERIAL FROM WATER

Sample	B	Si	Mg	Elements ( $\mu\text{g}$ )			
				Al	Na	Ca	K
LW-H <sub>2</sub> O-00	<0.1	0.1	0.02	<0.1	<1.0	0.1	<50.0
LW-H <sub>2</sub> O-01	2.0	5.0	0.5	0.2	1.0	1.0	<50.0
LW-H <sub>2</sub> O-02	0.1	1.0	0.2	<0.1	<1.0	0.3	<1.0
LW-H <sub>2</sub> O-1	15.1	10.0	2.0	1.0	50.0	5.0	<50.0
LW-H <sub>2</sub> O-2	3.0	3.0	0.3	0.2	>100.0	3.0	>100.0
LW-H <sub>2</sub> O-12	0.2	2.0	0.3	0.1	<1.0	1.0	<50.0
LW-H <sub>2</sub> O-13	0.3	2.0	0.3	<0.1	<0.1	1.0	<50.0
LW-H <sub>2</sub> O-14	2.0	5.0	0.5	0.2	10.0	1.0	<50.0
H <sub>2</sub> O-CP-1	0.3	2.0	1.0	0.2	20.0	2.0	<50.0
H <sub>2</sub> O-CP-2	3.0	20.0	3.0	3.0	30.0	5.0	10.0
H <sub>2</sub> O-CP-3	1.0	10.0	2.0	1.0	20.0	5.0	2.0
H <sub>2</sub> O-UP-1	5.0	10.0	5.0	1.0	30.0	5.0	<50.0
H <sub>2</sub> O-UP-2	1.0	7.0	1.0	0.5	10.0	2.0	1.0

in the sample (such as C, O, S, Cl) are not observed and since the total weight of the sample is not known, comparisons between samples must be made with some caution.

The water (LW-H<sub>2</sub>O-00) used in the washings is comparatively clean, i. e., comparatively free of the elements listed in Table 2. Comparing the analysis of the water (LW-H<sub>2</sub>O-00) to the analysis of the system blanks or washings (LW-H<sub>2</sub>O-01 and LW-H<sub>2</sub>O-02) shows that additional elements are being extracted from the system (the baking dish, flask, and vial). Principal among these appear to be B, Si, Mg, and Ca. The differences between the two system blanks (LW-H<sub>2</sub>O-01 and LW-H<sub>2</sub>O-02), can reasonably be used to indicate the limits of accuracy between any two samples. The analysis of the first tube washing (LW-H<sub>2</sub>O-1) shows a large increase in some elements when compared to the analyses of the system blanks. This observation shows that comparatively large amounts of B, Si, Ca, and especially Na are being extracted from the pyrex capillary tubes. In fact, comparison of the analyses of LW-H<sub>2</sub>O-01 and LW-H<sub>2</sub>O-14 indicates that except for Na the quantity of elements present in LW-H<sub>2</sub>O-14, the last listed tube washing, is similar to that of the system blank. However it must be mentioned here that in LW-H<sub>2</sub>O-14 some of the material present must still be coming from the tubes since at this point the system has also gone through 14 washings. Therefore the 14th system blank should, in theory, yield less material than LW-H<sub>2</sub>O-01.

Some of the numerical values from the emission analyses of the residues from tube washing are not yet understood; for example the exceptionally high Na and K values in LW-H<sub>2</sub>O-2, or the low values for all elements in LW-H<sub>2</sub>O-12 and LW-H<sub>2</sub>O-13. Part, but not all, of the low values can be explained by a much smaller total sample for LW-H<sub>2</sub>O-12 and LW-H<sub>2</sub>O-13.

The first preparation using the cleaned tubes (H<sub>2</sub>O-CP-1) gives emission analysis values that, except for Na, are below the values for the last listed tube washing (LW-H<sub>2</sub>O-14). In fact the emission values for the first preparation are within the range (again except for Na) of the elements of the two system blanks (LW-H<sub>2</sub>O-01 and LW-H<sub>2</sub>O-02) and are distinctly lower than the emission values found for the first preparation in uncleaned tubes (H<sub>2</sub>O-UP-1). As would be expected the values found for H<sub>2</sub>O-UP-1 are most similar to those found for the first tube washing (LW-H<sub>2</sub>O-1).

The second and third preparations in cleaned tubes give values for the elements which are distinctly higher than those of the first preparation. On the other hand the second preparation in uncleaned tubes gives elemental values that are below the first preparation in uncleaned tubes and in the range of some of the preparation in cleaned tubes. In addition all preparations are qualitatively similar in elemental composition whether from cleaned or uncleaned tubes. Since the tube washings demonstrate that material can be extracted from the tubes, the results for all preparations would tend to indicate further extraction rather than formation of a new substance.

Electron Microprobe Analysis

In addition to the metals detected by emission spectroscopy, electron microprobe microanalysis is also capable of detecting many nonmetals. Electron microprobe analyses have been obtained on all the liquid washing samples and on some of the preparations of anomalous materials from water. The complete electron microprobe results are listed in Appendix B. These results are given in numerical values which represent the density counts per second for each element studied. In most cases a range is given for the extremes observed over the area covered by the electron beam. Use of these numerical values can often provide a better basis for comparison of the overall composition of samples than X-ray images.

However, the X-ray images often provide information on the distribution of elements within a specific sample area. Such X-ray images are shown for two samples in Figures 6 through 11. X-ray images are shown for only two samples since these two are fairly representative of the remainder of the samples.

Figures 6 to 8 are X-ray images of the first system blank, sample LW-H<sub>2</sub>O-01. X-ray images of the first preparation from cleaned tubes, sample H<sub>2</sub>O-CP-1, are shown in Figures 9 to 11. It was previously stated that based on emission analysis results LW-H<sub>2</sub>O-01 and H<sub>2</sub>O-CP-1 had similar elemental compositions except for the Na content. The X-ray images and Appendix B support most of the emission results. The B X-ray images in Figures 6 and 9 indicate a slightly higher boron or B content in LW-H<sub>2</sub>O-01 than in H<sub>2</sub>O-CP-1; consistent with the emission results in Table 2. The X-ray images in Figures 6 to 11 also show roughly equal amounts of C, K, Ca, S, and Mg for the two samples which agrees with the count per second values in Appendix B and with the emission values for K, Ca and Mg in Table 2. The X-ray images (and the numerical values from Appendix B) indicate a higher concentration of both Si and O in the system blank (LW-H<sub>2</sub>O-01) than in the residue from the clean tube preparation (H<sub>2</sub>O-CP-1); consistent with the emission values for Si. There are no emission values for O.

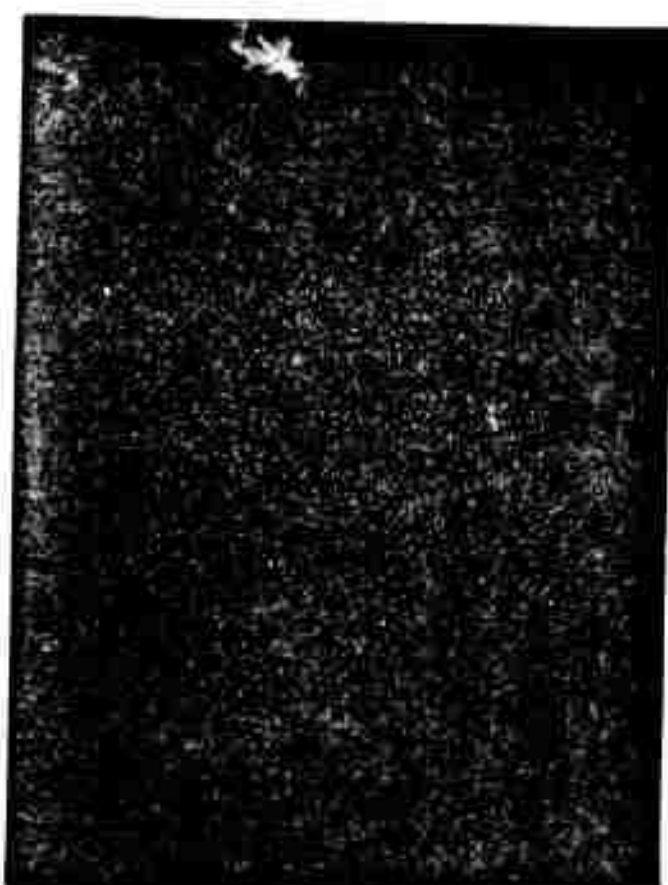
For Cl, the X-ray images indicate approximately equal quantities in the two samples except that H<sub>2</sub>O-CP-1 shows a very heavy concentration of Cl in certain spots, some of which are observed as a cross pattern. However for Na, the electron microprobe results do not agree with the emission results. Both the X-ray images and the numerical values in Appendix B indicate a higher concentration of Na in LW-H<sub>2</sub>O-01 than in H<sub>2</sub>O-CP-1, yet the emission results in Table 2 indicate much more Na in H<sub>2</sub>O-CP-1 than in LW-H<sub>2</sub>O-01. This discrepancy may result (as noted in the Experimental section) from the fact that the electron microprobe beam covers only part of the sample. Thus if Na is not evenly distributed in one of the samples, it would be possible for the electron microprobe and emission analyses to differ since the emission analysis is a function of the total sample. In fact, it is somewhat surprising that there are not more such differences.

Uneven distribution of elements has been noted in several samples and these can be discerned from the numerical values in Appendix B. Most notable of these is LW-H<sub>2</sub>O-2. In this sample large crystals resembling pentagons are observed around the edge of the sample. These large crystals have not been detected in any

**FIGURE 6.** ELECTRON MICROPROBE ANALYSES OF LW-H<sub>2</sub>O-01 SHOWING THE BACK SCATTERED ELECTRON IMAGE OF THE SAMPLE AND THE X-RAY DISTRIBUTION IMAGE FOR B, Na, AND C

LW-H<sub>2</sub>O-01

21B



B



Na

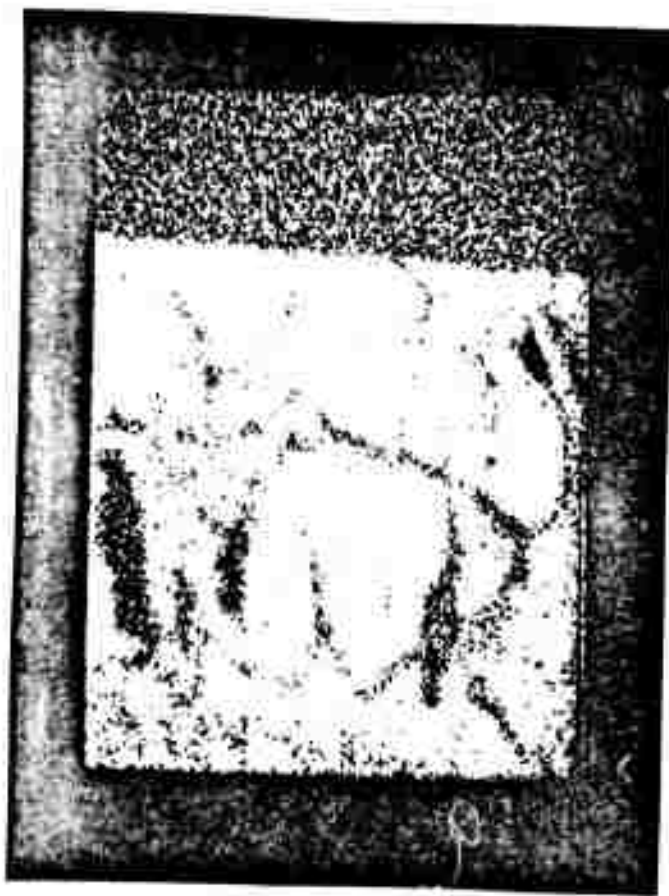


C

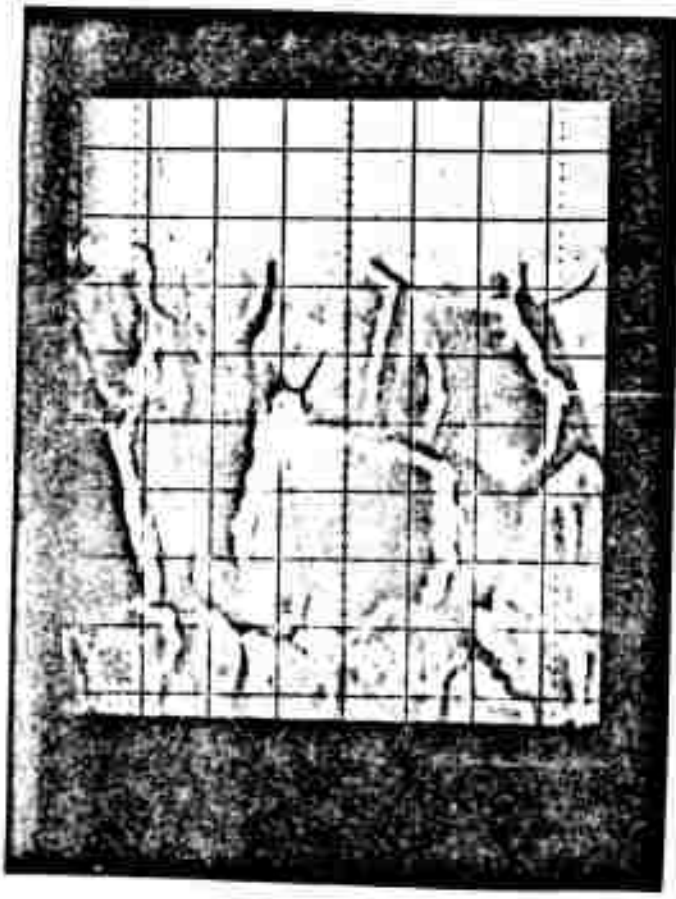
FIGURE 7. ELECTRON MICROPROBE ANALYSES OF LW-H<sub>2</sub>O-01 SHOWING THE X-RAY DISTRIBUTION IMAGES FOR Mg AND O<sub>2</sub>, THE BACK SCATTERED ELECTRON IMAGE OF THE SAMPLE, AND THE X-RAY DISTRIBUTION IMAGE FOR K

LW-H<sub>2</sub>O-01

22B



Mg

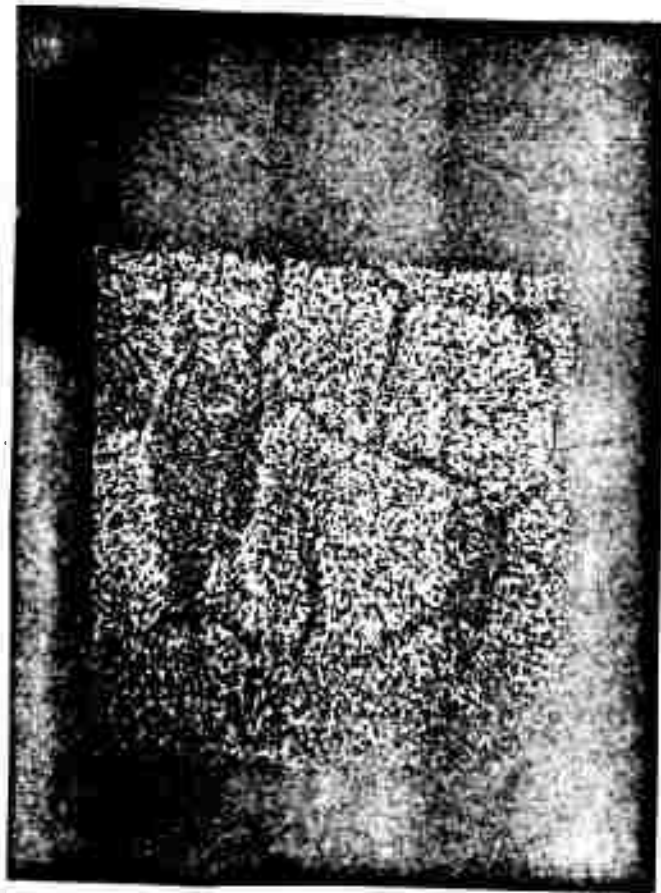


O<sub>2</sub>



K

**FIGURE 8. ELECTRON MICROPROBE ANALYSES OF LW-H<sub>2</sub>O-01 SHOWING THE X-RAY DISTRIBUTION IMAGES FOR Ca, Cl, S, AND Si**



Ca



Cl

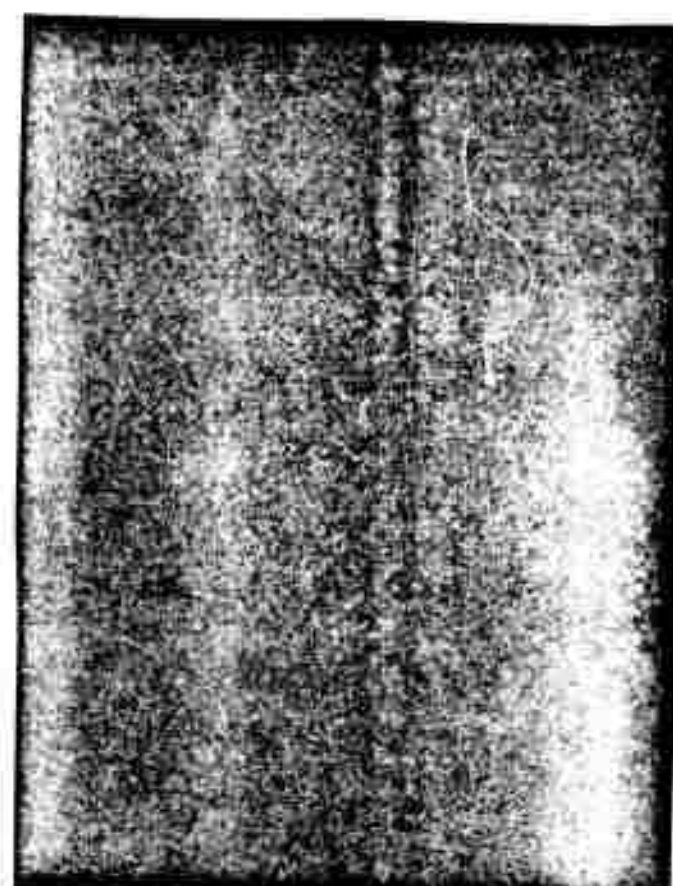


S



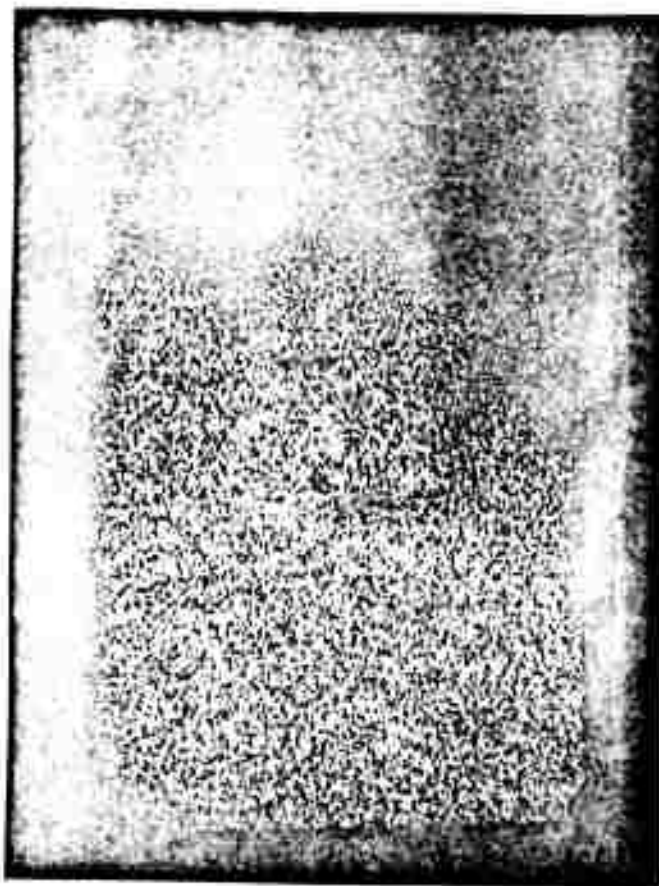
Si

**FIGURE 9. ELECTRON MICROPROBE ANALYSES OF H<sub>2</sub>O-CP-1 SHOWING THE BACK SCATTERED ELECTRON IMAGE OF THE SAMPLE AND THE X-RAY DISTRIBUTION IMAGES FOR B, Na, AND C**

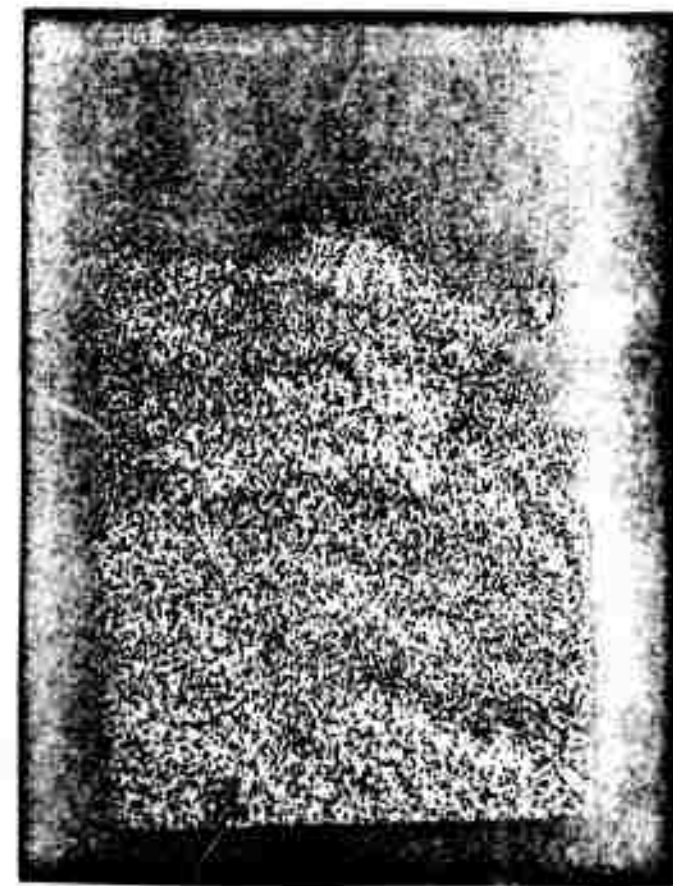


NOT REPRODUCIBLE

B



Na



C

FIGURE 10. ELECTRON MICROPROBE ANALYSIS OF H<sub>2</sub>O-CP-1 SHOWING THE X-RAY DISTRIBUTION IMAGES FOR Mg AND O, THE BACK SCATTERED ELECTRON IMAGE OF THE SAMPLE, AND THE X-RAY DISTRIBUTION IMAGE FOR K

$H_2O-CP-1$

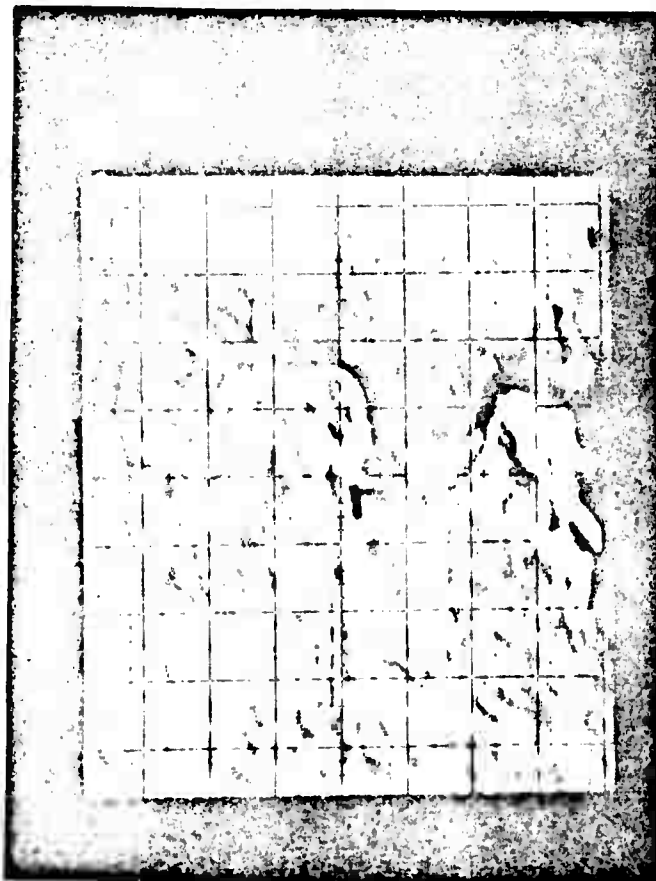
25B



$Mg$

NOT REPRODUCIBLE

$O_2$



$K$

FIGURE 11. ELECTRON MICROPROBE ANALYSES OF H<sub>2</sub>O-CP-1 SHOWING THE X-RAY DISTRIBUTION IMAGES FOR Ca, Cl, S, AND Si

$H_2O-CP-1$  26B



Ca

NOT REPRODUCIBLE



Cl



S



Si

other sample. The crystals contain a very heavy concentration of K and some Cl, but not nearly enough Cl to satisfy stoichiometry with the K. All the other elements reported were detected in the area away from the large crystals.

As can be seen in Appendix B, Cl was found to be concentrated in spots for most of the samples rather than being evenly distributed. Most of the time (as in the X-ray images of H<sub>2</sub>O-CP-1) no cationic element was detected which showed a pattern of spots similar to that found for Cl. Occasionally, however, some of the Si distribution patterns were similar to that of Cl.

Silicon, like Cl, many times was found to be unevenly distributed, i.e., heavily concentrated, at the edge of the sample. K and Ca were found in heavier concentrations at the edges for the beginning tube washings (LW-H<sub>2</sub>O-1, 2, and 12), but were more uniformly distributed for the other samples.

For any given element, the electron microprobe analyses can be used to detect changes in concentration of that specific element among the various samples. However the greatest benefit of the electron microprobe work to this point in the research came from the detection of elements that cannot be studied by emission spectroscopy, i.e., C, O, Cl, and S. Quantitative values of the concentration of these elements cannot be obtained. However it is important to note that these elements were detected in all of the system blanks, all of the liquid washings, and all of the preparations from cleaned or uncleaned tubes alike. The only possible exceptions are those of LW-H<sub>2</sub>O-2 and LW-H<sub>2</sub>O-14 where the S content appears to be near trace quantities.

It is especially important (for purposes of interpreting the infrared spectra) to note that C was detected in every sample. Based on a count of about 2475 (per second) for carbon in a graphite standard, it can be estimated that the carbon weight percentage in these samples of residues is in the 5 to 15% range. The total quantity of elements may be decreased with washing, but all elements originally detected in the blanks and first wash (LW-H<sub>2</sub>O-1) are present at all stages to varying degrees. Thus no element originally detected was completely removed by washing - even for tubes which had been cleaned 15 times.

### C, H, N Analysis

Wet chemical or combustion C, H, N analyses were obtained whenever the sample was large enough. These values are listed in Table 3. Such analyses were obtained for three samples of which only one (LW-H<sub>2</sub>O-1) is in the group of samples being presently discussed. Even for these samples, the amount of material was small enough that it is difficult to state accuracy limits for these analyses. However for LW-H<sub>2</sub>O-1, the carbon percentage is at the extreme upper limit deduced from the electron microprobe analyses.

It is interesting here to note that N was detected in sample LW-H<sub>2</sub>O-1. The C, H, N analyses for the other samples will be discussed in later sections.

TABLE 3. C-H-N ANALYTICAL RESULTS OF RESIDUES

Sample	%C	%H	%N
LW-H <sub>2</sub> O-1	16.2	2.2	2.5
H <sub>2</sub> O <sub>2</sub> -P-1	12.1	2.5	4.2
LW-Pr-1	38.9	5.6	2.0

### Preparation of Anomalous Material From H<sub>2</sub>O<sub>2</sub> Solutions

#### Infrared Spectra

A preparation of anomalous material using 3 percent aqueous H<sub>2</sub>O<sub>2</sub> was completed. The purpose of this preparation was to learn more about the role oxygen might play in the formation of anomalous material. Some surprising results were obtained. First, the yield from the 3 percent H<sub>2</sub>O<sub>2</sub> preparation was about 5 mg, a fairly large yield. In addition, the infrared spectra (shown in Figure 12) of the residue from the 3 percent H<sub>2</sub>O<sub>2</sub> preparation are similar, yet have distinct differences, when compared to the spectra of anomalous material prepared from 100 percent water. The film prepared for the infrared analyses was distinctly stick to the touch, differing from most preparations from 100 percent water. The top spectrum (A) of Figure 12 shows the residue obtained from the 3 percent H<sub>2</sub>O<sub>2</sub> preparation. Spectrum (b) is that of a much thicker run of the first spectrum. That such intense spectra are easily recorded is an indication of the large quantity of material available. In addition, the absorption bands are sharper and at more distinct frequencies than in any previous spectrum of anomalous material.

Instead of the usual broad OH stretching vibration (seen in preparations from pyrex tubes), the spectrum of this material shows three OH peaks near 3460, 3380, and 3230 cm<sup>-1</sup>. This observation indicates that three types of OH groups are present in the sample. The two bands in the 1600 cm<sup>-1</sup> region are very strong and at 1680 and 1640 cm<sup>-1</sup>; not 1620 cm<sup>-1</sup> as in the preparations from pure water. In the 1400 cm<sup>-1</sup> region a band can be seen at 1470 cm<sup>-1</sup> with shoulder near 1390 or 1400 cm<sup>-1</sup>. The 1470 cm<sup>-1</sup> frequency is high compared to 1410 cm<sup>-1</sup> in the preparations from pure water. A band is observed at 1175 cm<sup>-1</sup> with some additional absorption on the low frequency side near 1090 cm<sup>-1</sup>. In addition, a weak band at 787 cm<sup>-1</sup> is observed in the spectrum of the thicker sample.

Spectrum (C) of Figure 12 shows the results of heating (b) of Figure 10 at 400 C for five minutes. The three OH peaks in the 3400 cm<sup>-1</sup> region have disappeared and a more normal broad OH band is observed. The intensity of the bands in the 1600 and 1400 cm<sup>-1</sup> region are diminished compared to the 1100 cm<sup>-1</sup> band. The 1680 cm<sup>-1</sup> has disappeared and the 1640 cm<sup>-1</sup> band has shifted to 1630 cm<sup>-1</sup>.

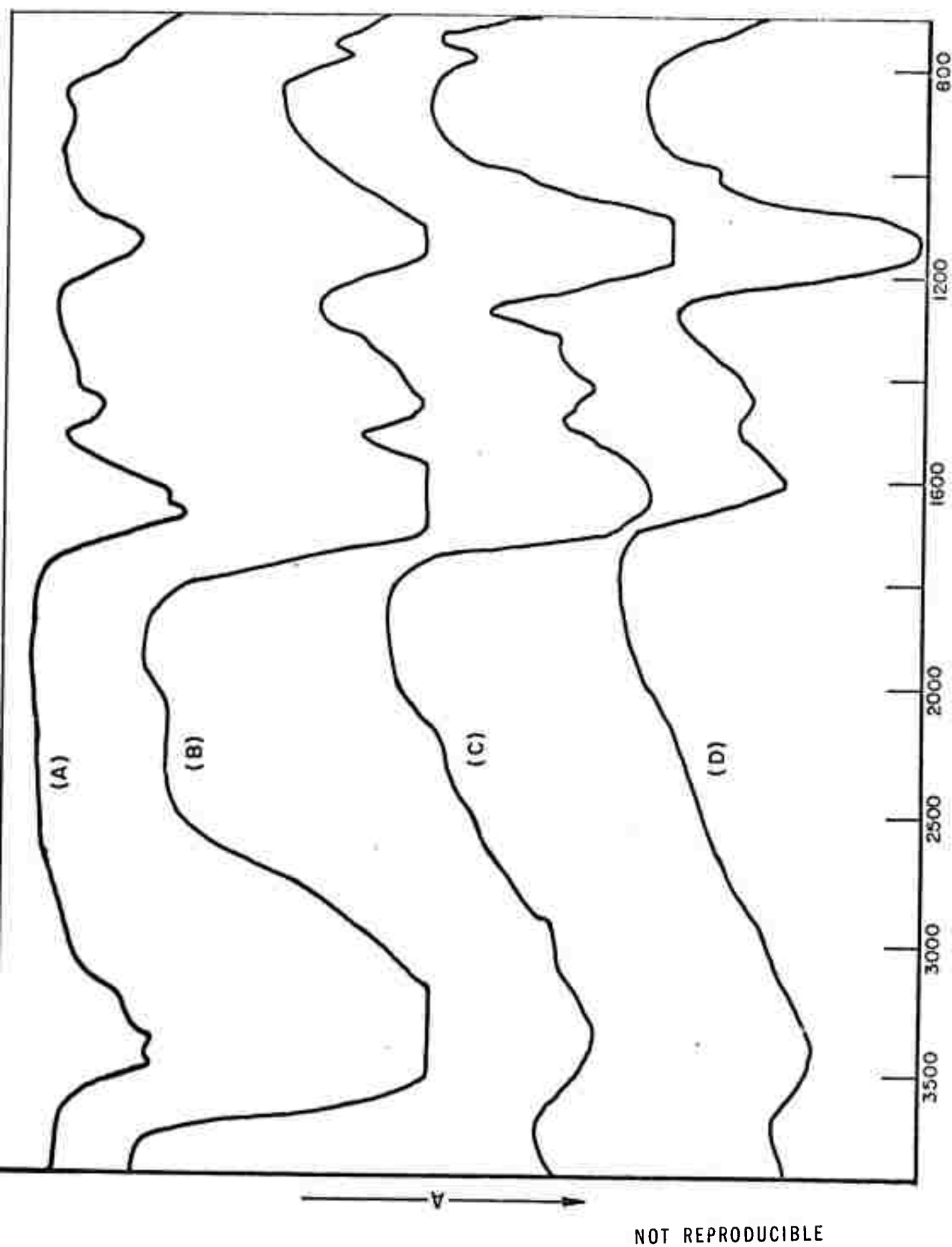


FIGURE 1. INFRARED SPECTRA OF (A)  $\text{H}_3\text{O}^+\text{-P}(=\text{O})(\text{OH})_2$ , (B) A TRIMERIC SAMPLE OF  $\text{H}_3\text{O}^+\text{-P}(=\text{O})(\text{OH})_2$ , (C)  $\text{H}_3\text{O}^+\text{-P}(=\text{O})(\text{OH})_2$  TREATED AT 400°C FOR

The  $1470\text{ cm}^{-1}$  peak shows a large shift to  $1425\text{ cm}^{-1}$  and a peak at  $1325\text{ cm}^{-1}$  can now be clearly seen. The appearance of a band near  $1425\text{ cm}^{-1}$  could signify carbonate formation, but no confirming band near  $880\text{ cm}^{-1}$  can be detected as is the usual case. The  $1100\text{ cm}^{-1}$  absorption of (C) appears unchanged.

After heating (C) of Figure 12 at  $400\text{ C}$  for an additional 60 minutes, spectrum (D) is obtained ( $\text{H}_2\text{O}_2\text{-P-1H}$ ). Upon heating, the sample begins to brown and after 60 minutes at  $400\text{ C}$ , it appears to be a black powder. The  $1640\text{ cm}^{-1}$  absorption of spectrum (B) now appears at  $1615\text{ cm}^{-1}$ . The band in the  $1400\text{ cm}^{-1}$  range has broadened, reversed the original direction of its shift and now appears near  $1450\text{ cm}^{-1}$ . The band at  $1325\text{ cm}^{-1}$  can no longer be seen. The  $1145\text{ cm}^{-1}$  band has decreased in intensity, but is still very strong. The  $787\text{ cm}^{-1}$  band is missing from the spectrum of (D), but a new band appears at  $1000\text{ cm}^{-1}$ . The frequency shifts due to heating this ample are summarized in Table 4. From these frequencies it can be seen that even though the frequencies of the unheated sample ( $\text{H}_2\text{O}_2\text{-P-1}$ ) are somewhat different than those of preparations from pure water the frequencies of the heated sample ( $\text{H}_2\text{O}_2\text{-P-1H}$ ) are quite similar to those of preparations from water. In fact, the spectrum of  $\text{H}_2\text{O}_2\text{-P-1H}$  would compare quite well to spectra of samples such as  $\text{H}_2\text{O}_2\text{-CP-1}$  and  $\text{H}_2\text{O-UP-1}$ , except for the intensity of the  $1145\text{ cm}^{-1}$  band.

### Emission Analysis

As an aid to interpreting the infrared spectral changes due to heating  $\text{H}_2\text{O}_2\text{-P-1}$ , emission analyses of  $\text{H}_2\text{O}_2\text{-P-1}$  and  $\text{H}_2\text{O}_2\text{-P-1H}$  were obtained. Partial results of these analyses are given in Table 5 together with the emission values obtained for preparations from pure water ( $\text{H}_2\text{O-CP-1}$  and  $\text{H}_2\text{O-UP-1}$ ) for comparison. Complete emission results are given in Appendix C. Considering the drastic spectral changes between  $\text{H}_2\text{O}_2\text{-P-1}$  and  $\text{H}_2\text{O}_2\text{-P-1H}$ , the differences in elemental composition are surprisingly small. Some Na and K are lost by heating the sample, but this is offset by a gain in Ca upon heating. (It is at present difficult to understand how Ca increases by heating a sample.) Comparing the  $\text{H}_2\text{O}_2$  preparations ( $\text{H}_2\text{O}_2\text{-P-1}$ ) to the preparations from pure water shows that the  $\text{H}_2\text{O}_2$  residue contains much less Na than the  $\text{H}_2\text{O}$  residues. For other elements the  $\text{H}_2\text{O}_2$  residue is closer to  $\text{H}_2\text{O-CP-1}$  (except for Mg and possibly B) than to  $\text{H}_2\text{O-UP-1}$ . This is somewhat understandable since the pyrex tubes used for the  $\text{H}_2\text{O}_2$  preparation were washed several times with water and several times with ethanol before the preparation was started. Thus the  $\text{H}_2\text{O}_2$  tubes are probably nearer the condition of the cleaned tubes used for  $\text{H}_2\text{O-CP-1}$  rather than the uncleaned tubes used for  $\text{H}_2\text{O-UP-1}$ .

### Electron Microprobe Analysis

The electron microprobe results for  $\text{H}_2\text{O}_2\text{-P-1}$  and  $\text{H}_2\text{O}_2\text{-P-1H}$  tend to support the emission spectrographic results for these two samples and give information about changes in concentrating of elements not analyzed by emission spectrography. Numerical values of the electron microprobe analyses are given in Appendix B. Figures 13, 14, and 15 are X-ray images of an edge of  $\text{H}_2\text{O}_2\text{-P-1}$ . The sample

TABLE 4. FREQUENCY SHIFTS ( $\text{cm}^{-1}$ ) DUE TO HEATING  $\text{H}_2\text{O}_2\text{-P-1}$ 

$\text{H}_2\text{O}_2\text{-P-1}$	$\text{H}_2\text{O}_2\text{-P-1}$ (5 min., 400 C)	$\text{H}_2\text{O}_2\text{-P-1H}$ (60 min., 400 C)
3460		
3380	3360	3400
3230		
1680		
1640	1625	1615
1470	1425	1450
1400 (Sh)		
1325 (Sh)	1325	
1145	1145	1145
1090 (Sh)		
787	787	1000

FIGURE 13. ELECTRON MICROPROBE ANALYSES OF  $H_2O_2$ -P-1 SHOWING THE BACK SCATTERED ELECTRON IMAGE OF THE SAMPLE AND THE X-RAY DISTRIBUTION IMAGES FOR B, Na, AND C

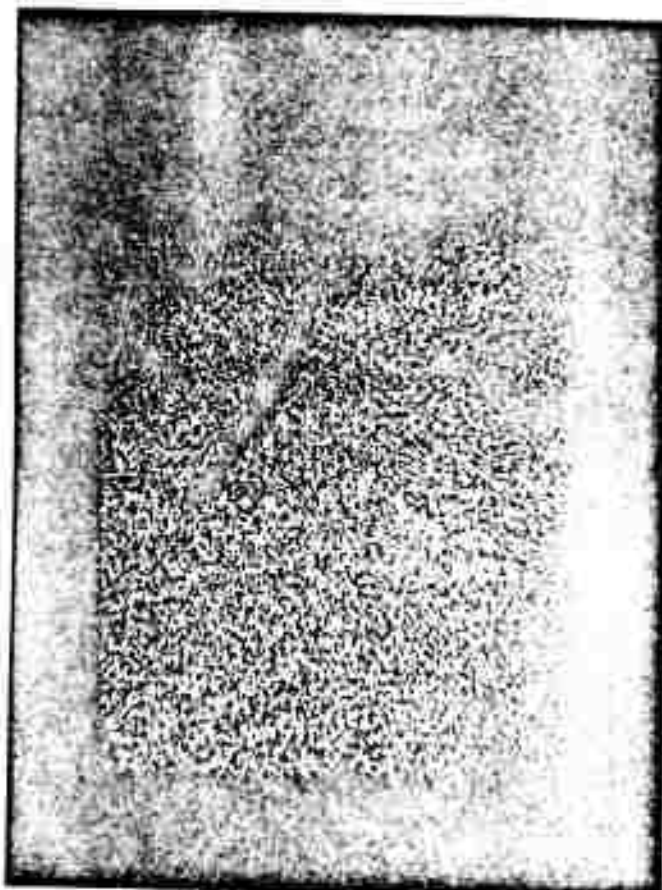
$H_2O_2 - P - 1$

323



NOT REPRODUCIBLE

B



Na

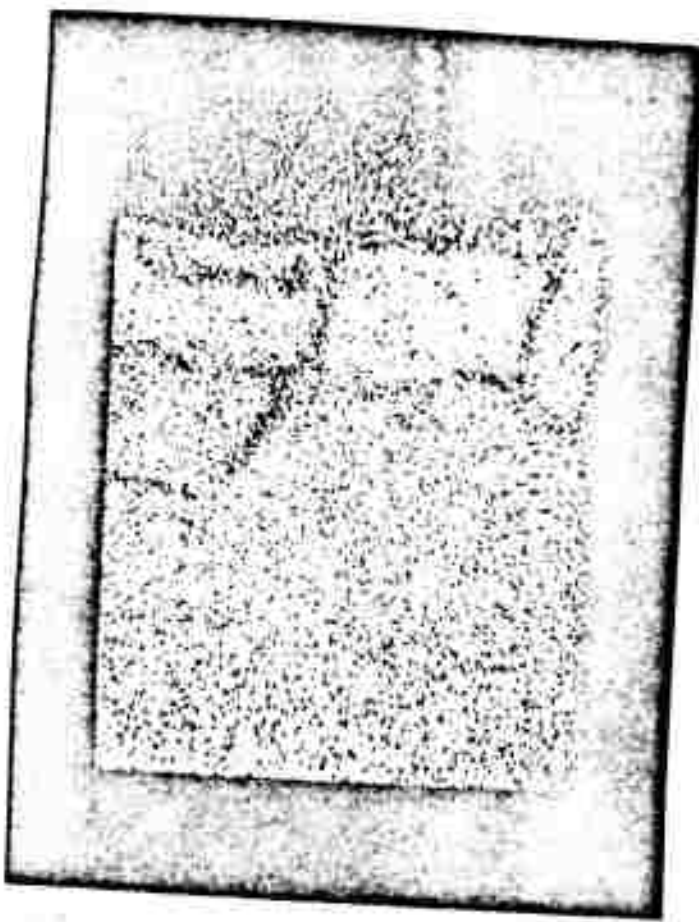


C

FIGURE 14. ELECTRON MICROPROBE ANALYSIS OF H<sub>2</sub>O<sub>2</sub>-P-1 SHOWING THE X-RAY DISTRIBUTION IMAGES FOR Mg AND O, THE BACK SCATTERED ELECTRON IMAGE OF THE SAMPLE, AND THE X-RAY DISTRIBUTION IMAGE FOR K

$H_2O_2-P-1$

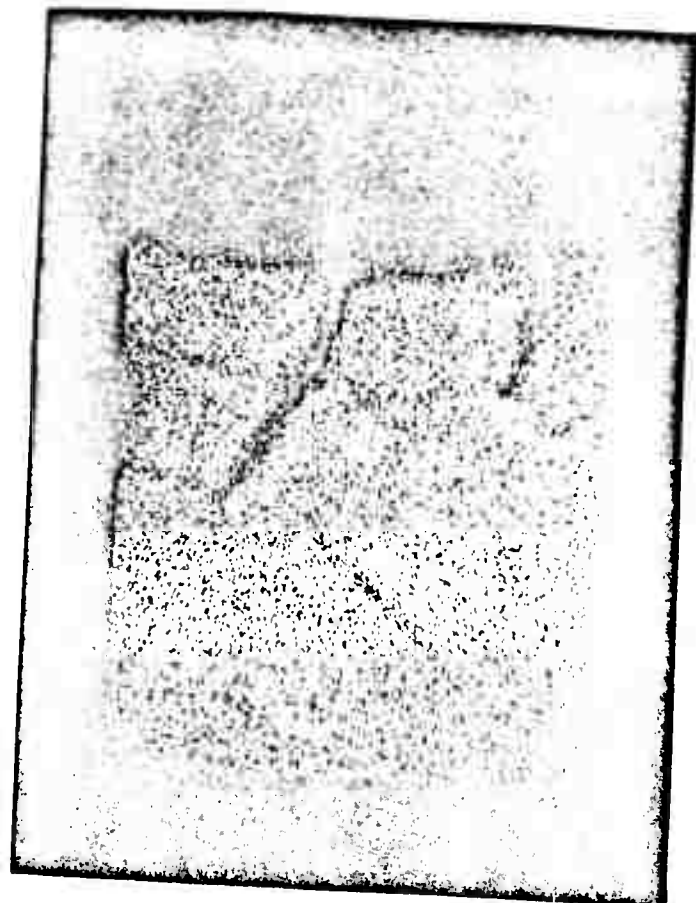
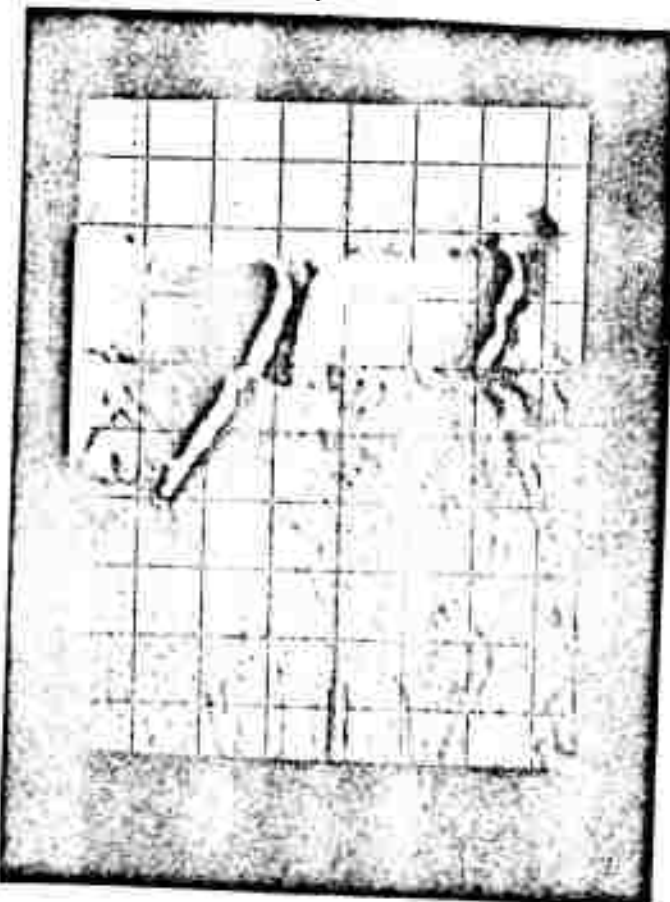
33B



$Mg$

NOT REPRODUCIBLE

$O_2$



$K$

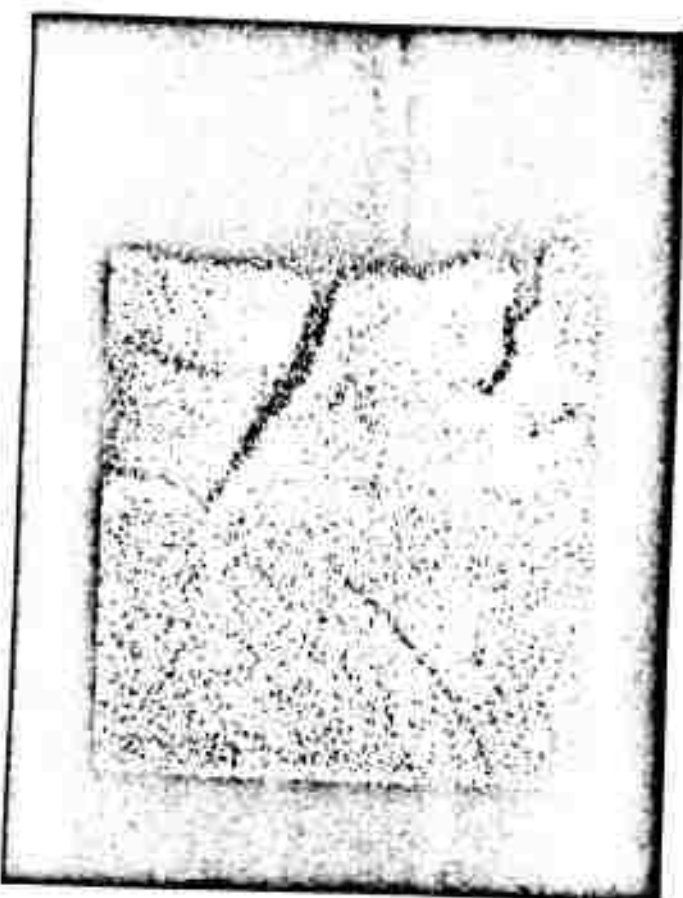
FIGURE 15. ELECTRON MICROPROBE ANALYSIS OF  $H_2O_2$ -P-1 SHOWING THE X-RAY DISTRIBUTION IMAGES FOR Ca, C1, S AND Si

$H_2O_2 - P - 1$

543



Ca

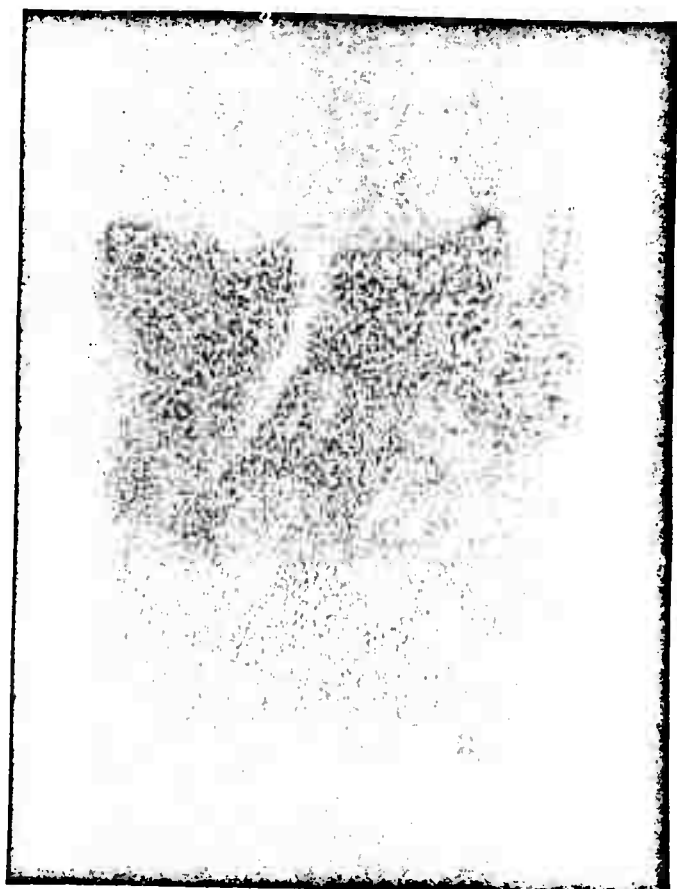


Cl

NOT REPRODUCIBLE



S



Si

TABLE 5. PARTIAL EMISSION SPECTROGRAPHIC ANALYSES FOR ANOMALOUS MATERIAL PREPARATIONS

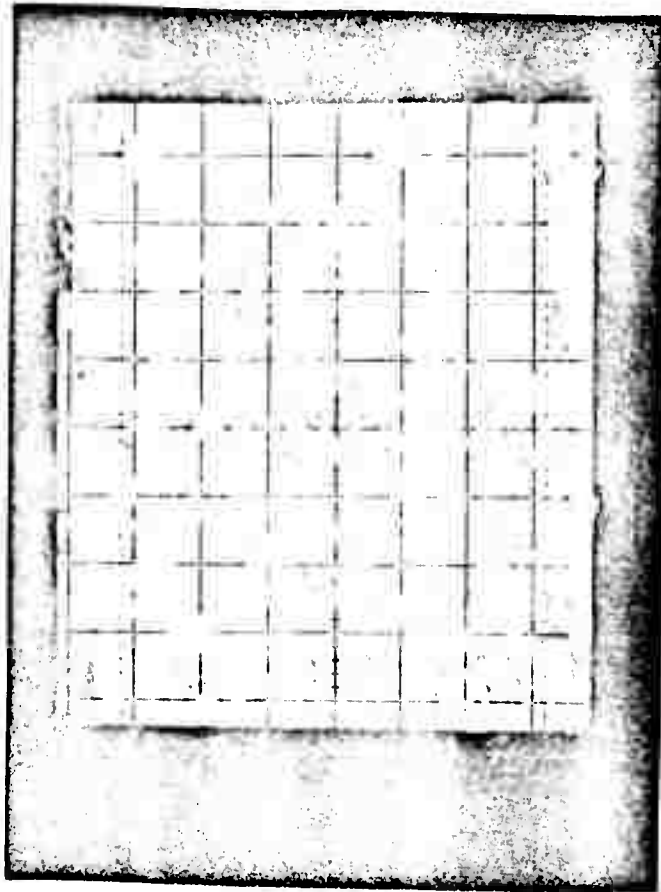
Sample	Elements ( $\mu\text{g}$ )							
	B	Si	Fe	Mg	Al	Na	Ca	K
$\text{H}_2\text{O}_2\text{-P-1}$	2.0	3.0	0.1	5.0	0.1	5.0	1.0	5.0
$\text{H}_2\text{O}_2\text{-P-1H}$	1.0	3.0	0.1	5.0	0.5	2.0	8.0	1.0
$\text{H}_2\text{O-CP-1}$	0.3	2.0	0.1	1.0	0.2	20.0	2.0	<50.0
$\text{H}_2\text{O-UP-1}$	5.0	10.0	0.5	5.0	1.0	30.0	5.0	<50.0

$\text{H}_2\text{O}_2\text{-P-1H}$  was prepared for the electron microprobe study by scraping the black powder off the Irtran plate used for the infrared study onto an Al disc. In anticipation of fixing the black powder to the Al plate, a drop of water was placed on the black powder. The area of the drop of water was many times larger than the area of the black powder. After the water had evaporated, the black powder was observed in approximately its original position. However, a heavy white film covered the area where the drop of water had been. The film was many orders of magnitude more residue than could be obtained from just a drop of water. Therefore part of the original black powder is believed to have dissolved in the water and thus spread out over the area of the drop. Figures 16, 17, and 18 are X-ray images of the black portion of this sample ( $\text{H}_2\text{O-P-1H}$ ). Some of the white portion could be under the black powder particles. Figures 19, 20, and 21 are the X-ray images of the white portion of the sample. There does not appear to be any of the black material mixed in with the white material. Appendix B and Figures 13 to 21 suggest that the carbon concentration, if anything, increases upon heating from the 12.1 percent for  $\text{H}_2\text{O}_2\text{-P-1}$  indicated by Table 3. The carbon is much more heavily concentrated in the black powder particles than in the white portion of the heated sample. This increase upon heating is also true of O and Cl, with O more heavily concentrated in the white portion and Cl fairly evenly distributed. The microprobe results confirm the Ca increase on heating  $\text{H}_2\text{O}_2\text{-P-1}$ . In summary, C, O, Cl and Ca all apparently increase upon heating. Since it is impossible to see how these elements could form during the heating process, it must mean that the concentration of the other elements decreased and C, O, Cl, and Ca became a bigger percentage of the total sample. The microprobe results indicate that S concentration remains about constant, but is heavier in the white portion of the sample than the black. The Si content is not affected by heating (as emission indicates), the white portion of the heated sample has almost no Si.

FIGURE 16. ELECTRON MICROPROBE ANALYSIS OF THE BLACK PORTION OF H<sub>2</sub>O<sub>2</sub>-P-II SHOWING THE BACK SCATTERED IMAGE OF THE SAMPLE AND THE X-RAY DISTRIBUTION IMAGES FOR B, Na, AND C

$H_2O_2-P-1H$  (BLACK)

36B



NOT REPRODUCIBLE

B



Na

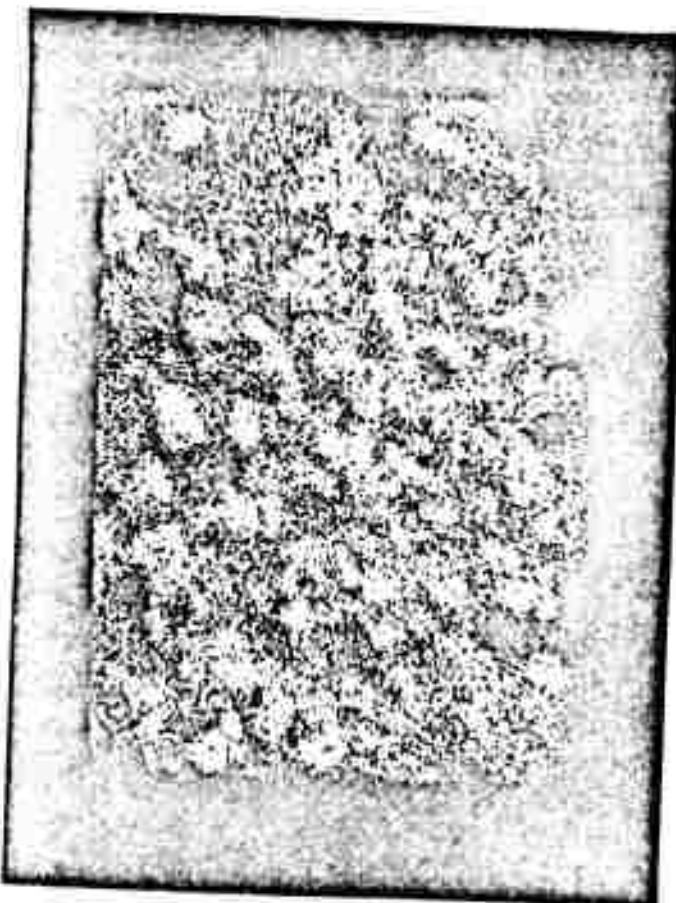


C

FIGURE 17. ELECTRON MICROPROBE ANALYSIS OF THE BLACK PORTION OF  $\text{H}_2\text{O}_2\text{-P-1H}$  SHOWING THE X-RAY DISTRIBUTION IMAGES FOR Mg AND O, THE BACK SCATTERED ELECTRON IMAGE OF THE SAMPLE, AND THE X-RAY DISTRIBUTION IMAGE FOR K

$H_2O_2-P-14$  (BLACK)

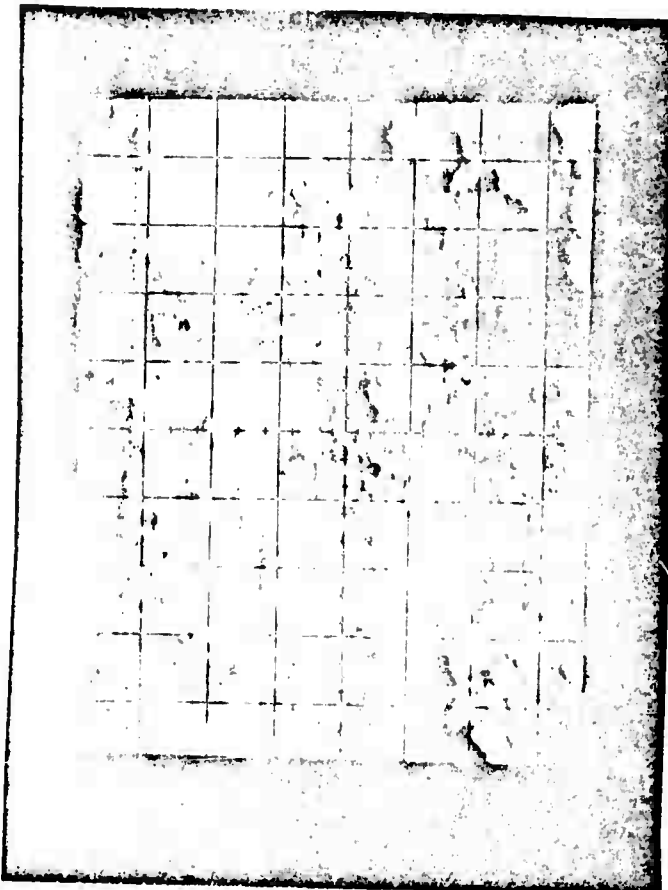
37B



Mg

NOT REPRODUCIBLE

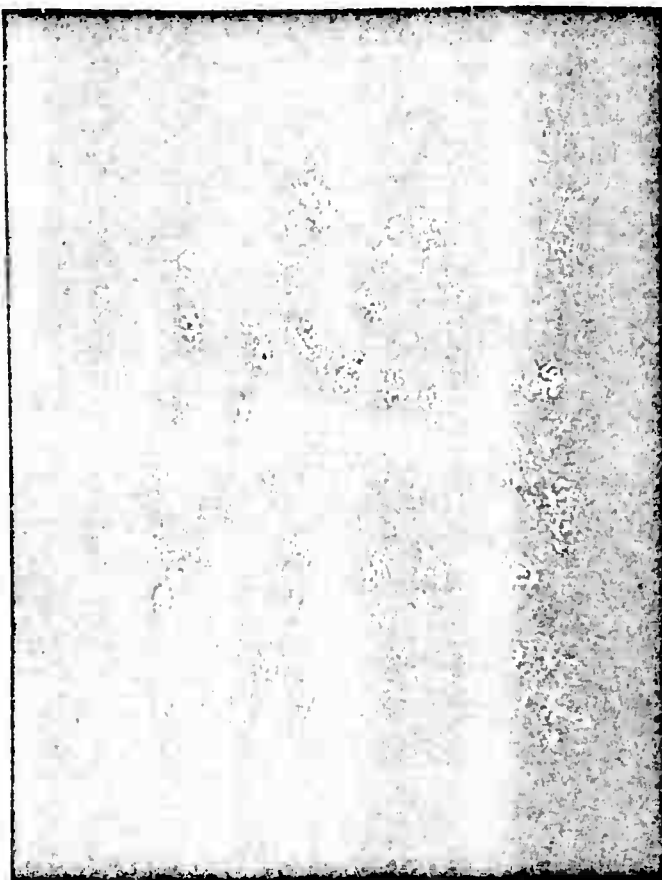
O<sub>2</sub>



K

**FIGURE 18.** ELECTRON MICROPROBE ANALYSIS OF THE BLACK PORTION OF  $H_2O_2$ -P-1H SHOWING THE X-RAY IMAGES FOR Ca, C1, S AND Si

$H_2O_2 - P - 1H$  (BLACK) 388



Ca



Cl

NOT REPRODUCIBLE



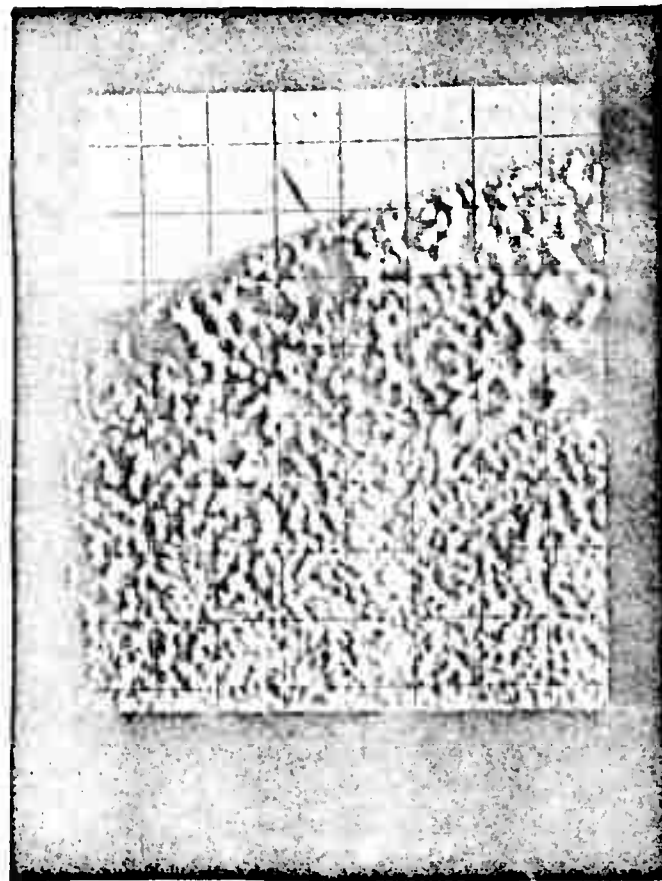
S



Si

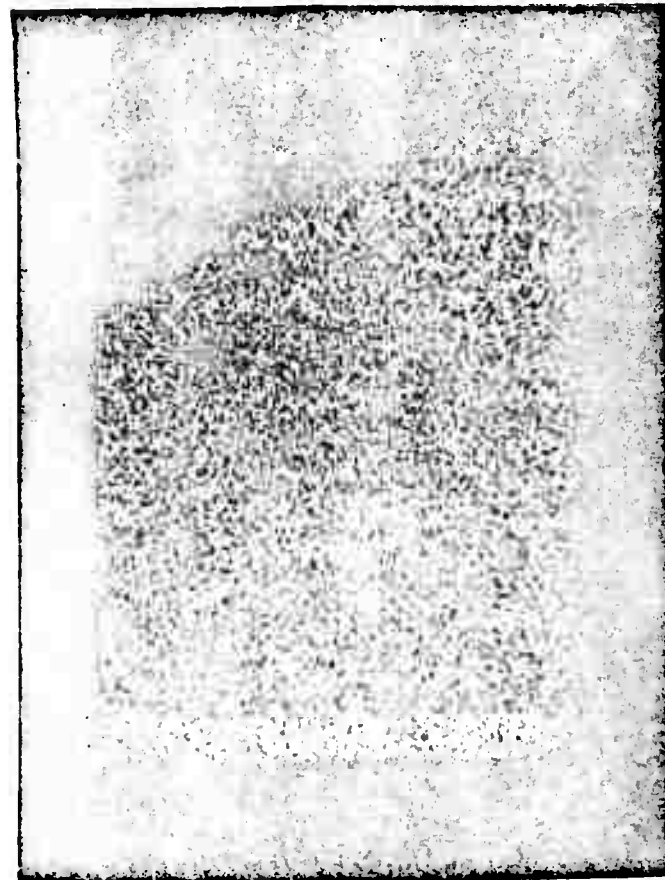
FIGURE 19. ELECTRON MICROPROBE ANALYSIS OF THE WHITE PORTION OF H<sub>2</sub>O<sub>2</sub>-P-1H SHOWING THE BACK SCATTERED ELECTRON IMAGE OF THE SAMPLE AND THE X-RAY DISTRIBUTION IMAGES FOR B, Na, AND C

$H_2O_2 - P-1H$  (WHITE) 39B

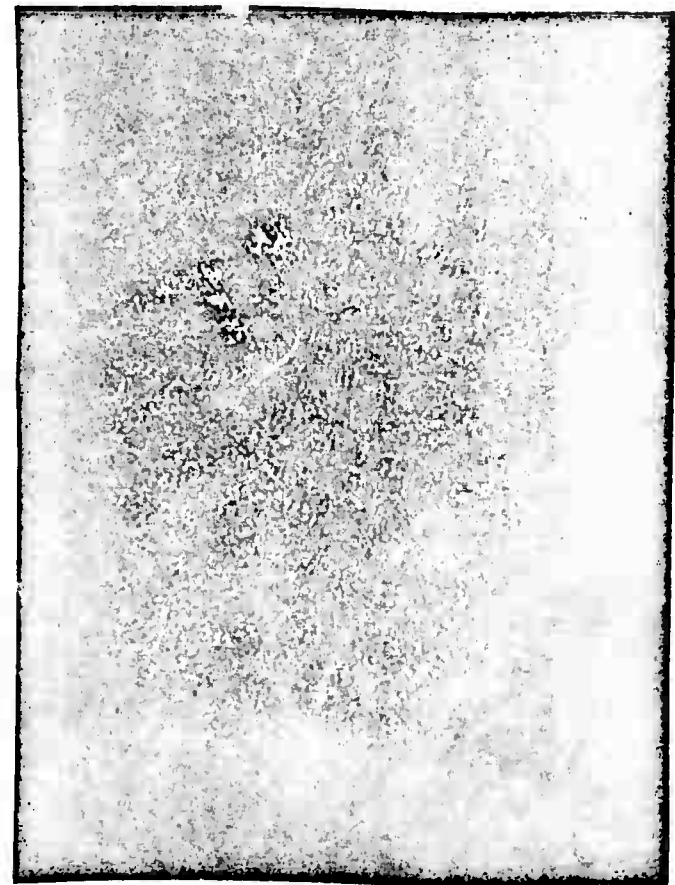


NOT REPRODUCIBLE

B



N

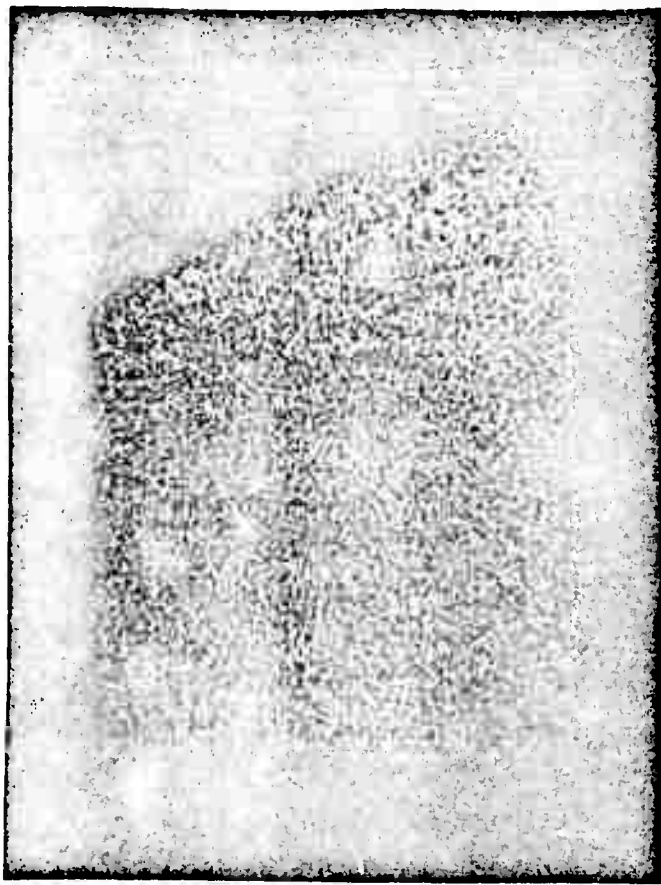


C

40A

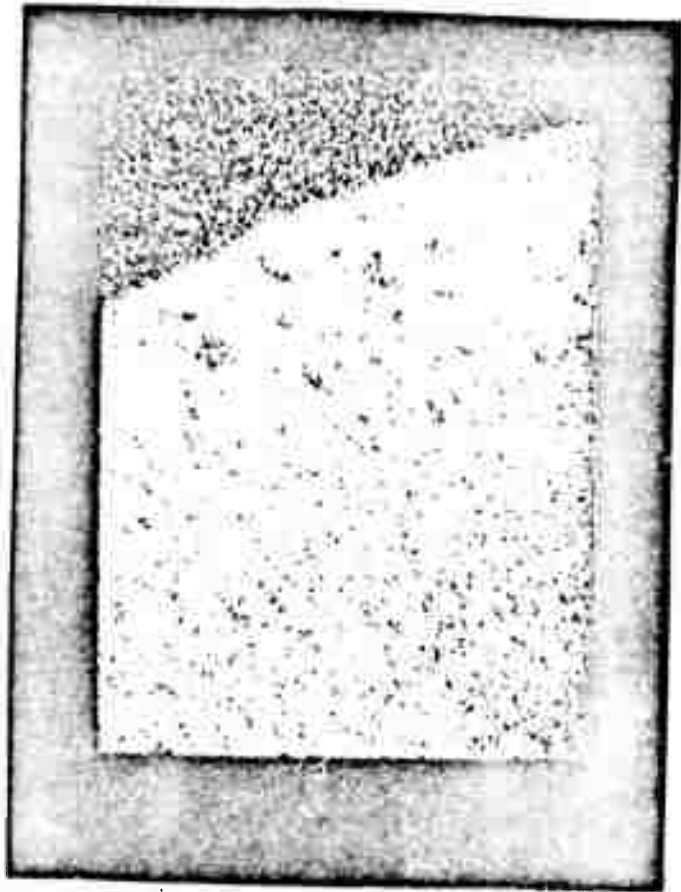
FIGURE 20. ELECTRON MICROPROBE ANALYSES OF TiIW WHITE PORTION OF  $H_2O_2$ -P-111 SHOWING THE X-RAY DISTRIBUTION IMAGES FOR Mg AND O, THE BACK SCATTERED ELECTRON IMAGE OF THE SAMPLE, AND THE X-RAY DISTRIBUTION IMAGE FOR K

H<sub>2</sub>O<sub>2</sub>-P-1H (WHITE) 40B

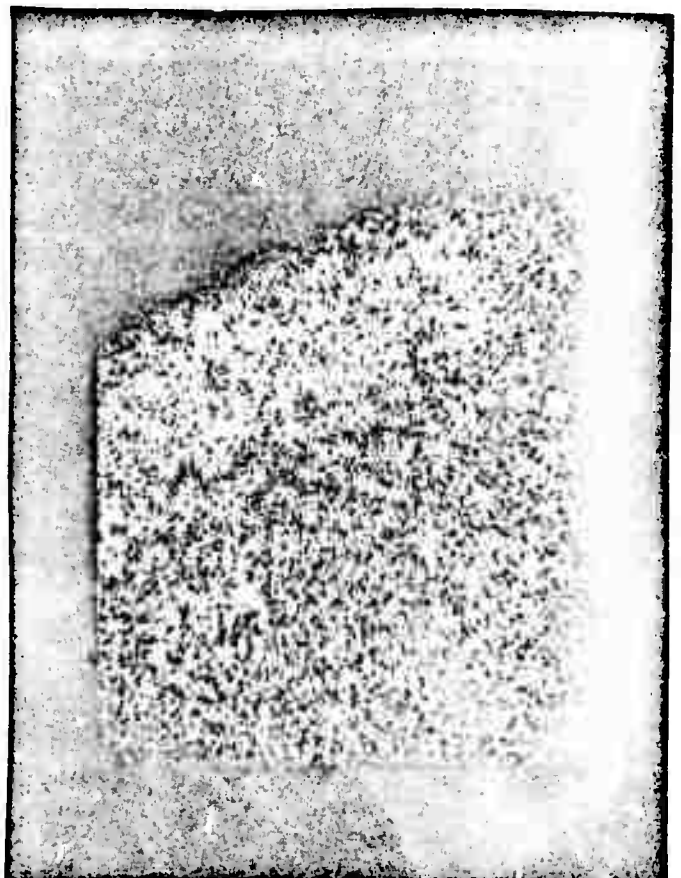
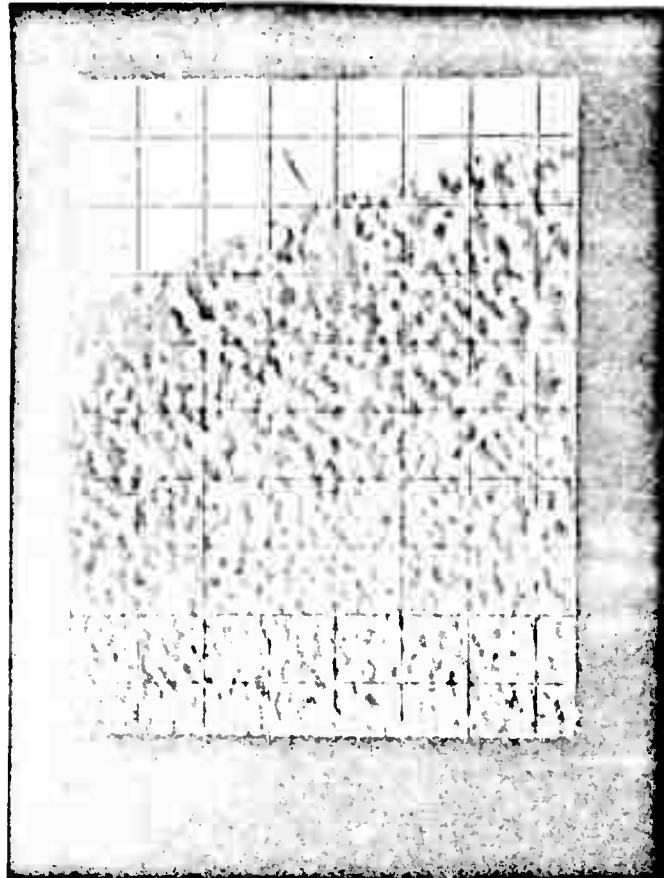


Mg

NOT REPRODUCIBLE



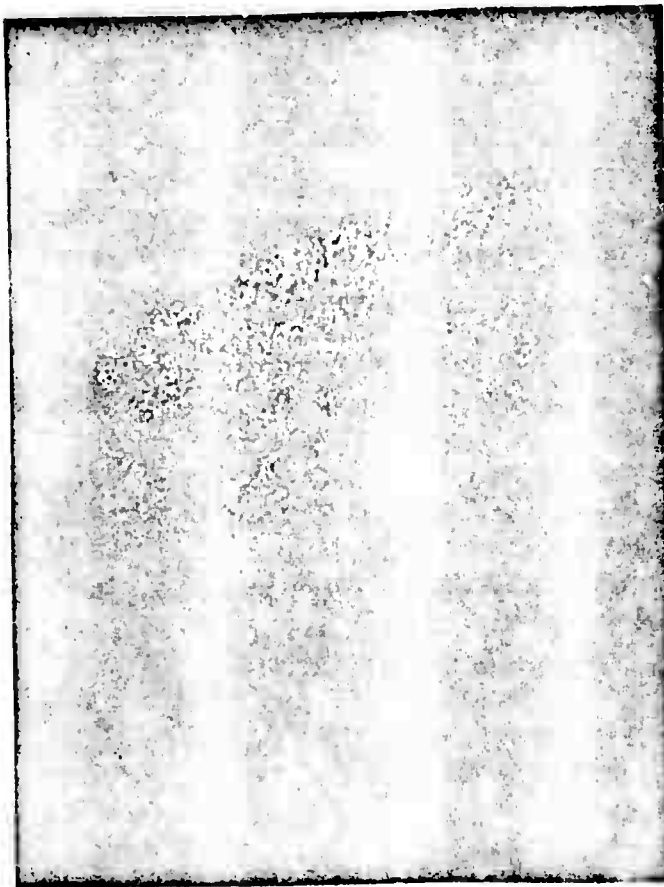
O<sub>2</sub>



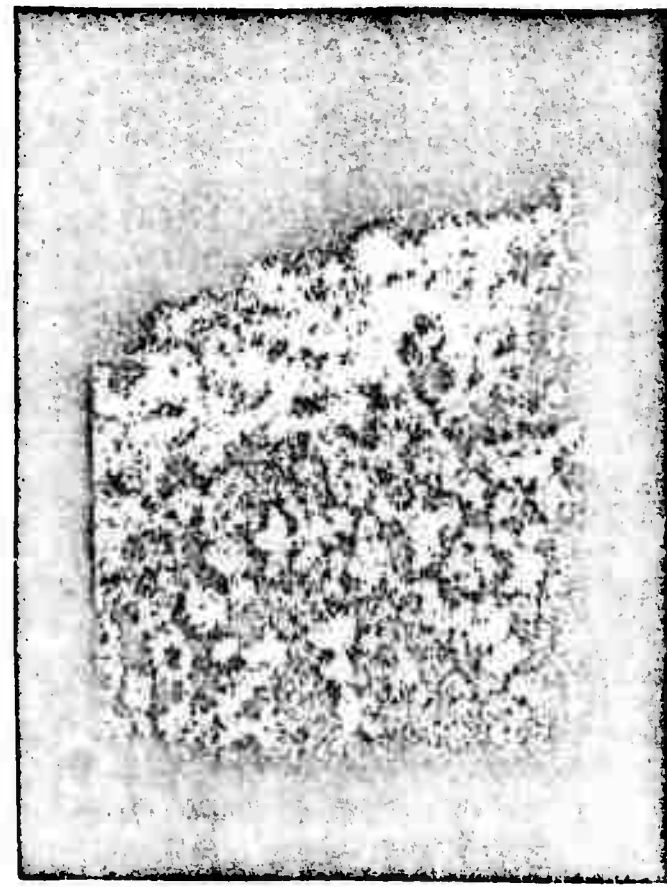
K

FIGURE 21. ELECTRON MICROPROBE ANALYSES OF THE WHITE PORTION OF H<sub>2</sub>O<sub>2</sub>-P-1 SHOWING THE X-RAY DISTRIBUTION IMAGES FOR Ca, C1, S, AND Si

$H_2O_2 - P - 1H$  (WHITE) 41B



Ca

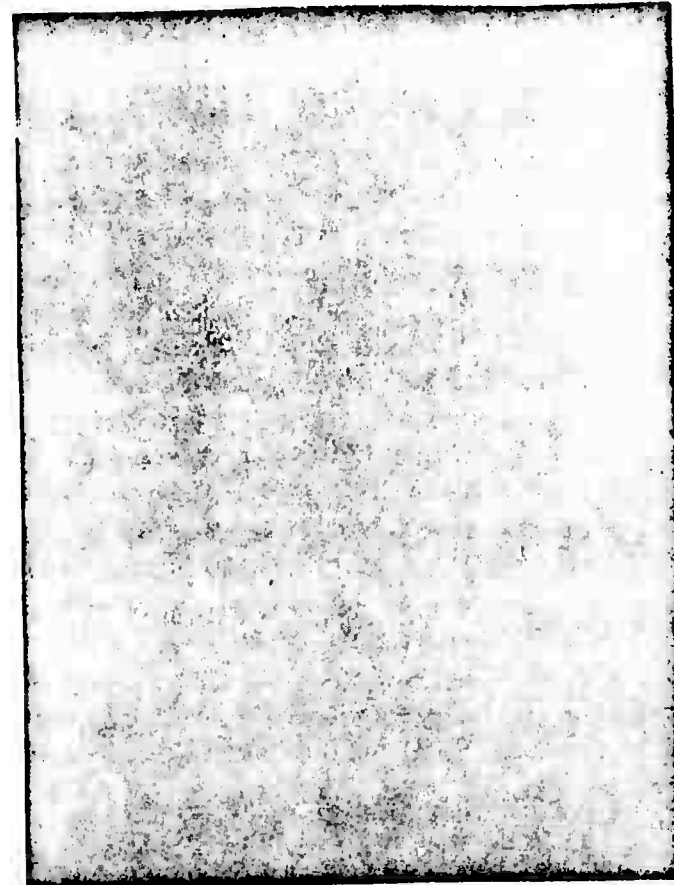


Cl

NOT REPRODUCIBLE



S



Si

### Vapor Water Cleaning of Capillary Tubes

Since the preparation of anomalous materials is essentially a vapor process, it was deemed advisable to repeat the liquid cleaning procedure, but using vapor water instead of liquid water. This was done by producing the vapor (as steam) in a typical pressure cooker.

The results were discouraging and somewhat unproductive. The reasons for this statement can be seen in Figure 22, which shows the spectra obtained from the three vapor washings of capillary tubes. The top (a) spectrum (VW-H<sub>2</sub>O-3) is totally that of an organic molecule which is unlikely to come from the pyrex tubes. Water extraction of the rubber gasket of the pressure cooker yielded a residue which gave a spectrum identical to (A). Spectrum (B) indicates the presence of more inorganic material than (A), but still shows the presence of the gasket extract. The bottom (C) spectrum (VW-H<sub>2</sub>O-5) is much like that of liquid water extracts of glass tubes and shows no organic gasket extract. However, even after a lengthy water extraction of the gasket, residues were sometimes obtained which gave spectra like (C): but sometimes (and randomly) the residues give spectra like either (A) or (B). Because of this gasket contamination and because repeated preparations in both cleaned and uncleaned tubes (which in a sense is a vapor cleaning were carried out, the pressure cooker cleaning experiments were discontinued.

### Liquid Propanol-1 Cleaning of Capillary Tubes

#### Infrared Spectra

Some of the same type problems encountered in the vapor cleaning experiments gave problems in the propanol-1 washing experiments. The detection of these problems can be seen in Figure 23. The top spectrum (A) is of the residue from the first tube washing with propanol-1 (LW-Pr-1). While other materials are also present, the major component is an organic phthalate.

At first it was suspected that the phthalate might originate from the propanol-1 used for the washing. Thus the residue was obtained from evaporation of an amount of propanol-1 equal to that used for the washings. The spectrum of this material (LW-Pr-00) is shown in the middle spectrum (B) of Figure 23. While a surprisingly large residue from 99+ percent pure propanol-1 is indicated, only a small portion of this material is a phthalate. The spectrum of this propanol-1 residue does confirm where some of the other materials in spectrum (A) originate. However, another source of phthalate contamination is indicated. The only remaining possibility is the Saran wrap used to cover the baking dish which holds the propanol and the glass tubes. Accordingly we extracted some Saran wrap with propanol-1 and, after evaporation of the propanol-1, obtained the bottom (C) spectrum in Figure 23. This is clearly the spectrum of a phthalate and establishes the source of the additional phthalate contamination.

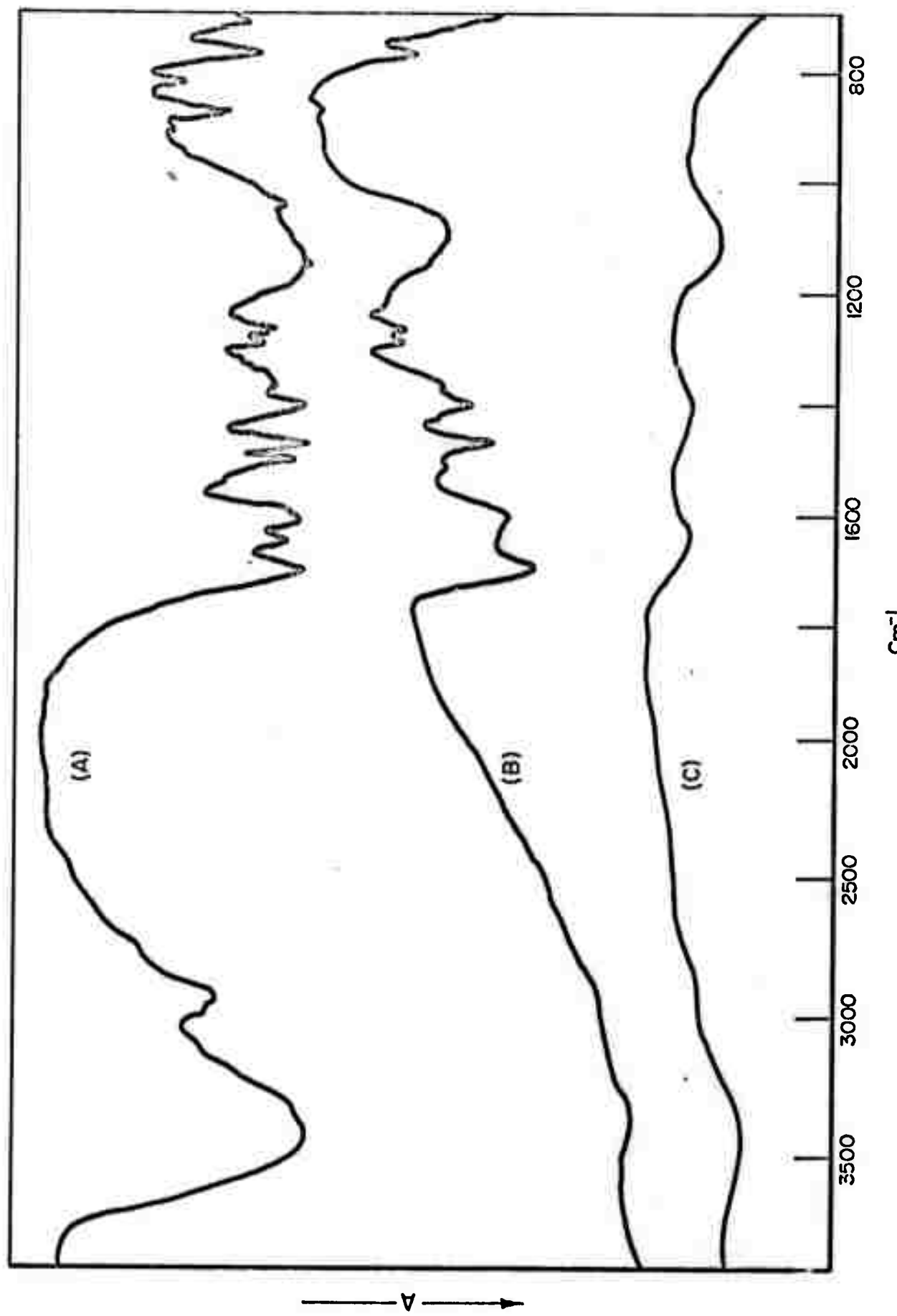


FIGURE 22. INFRARED SPECTRA OF (A)  $\text{Vn-H}_2\text{O-3}$ , (B)  $\text{Vn-H}_2\text{O-8}$ , AND (C)  $\text{Vn-H}_2\text{O-5}$

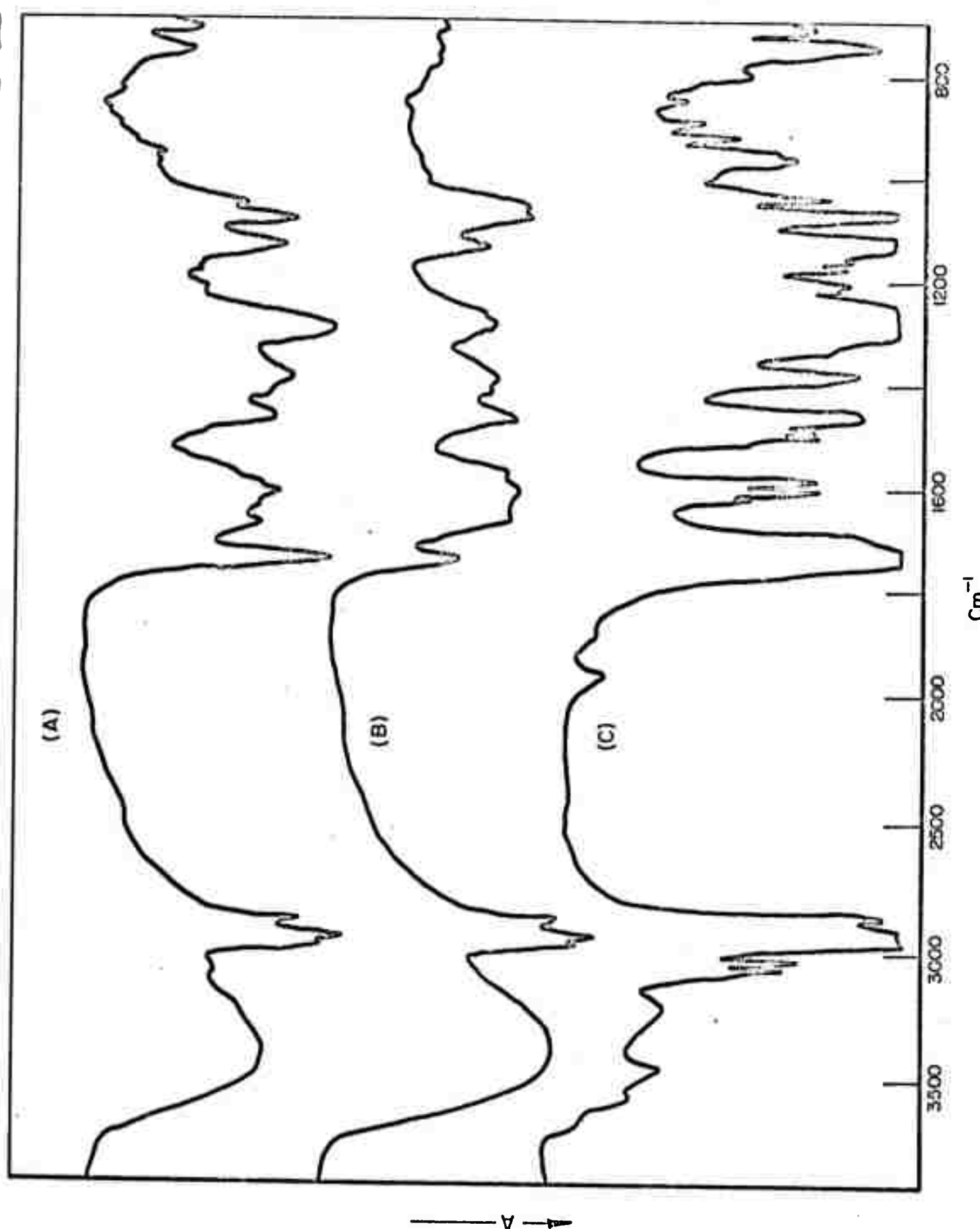


FIGURE 3. INFRARED SPECTRA OF (A) IM-Pr-1, (B) IM-Pr-00, AND (C) IM-Pr-01

### Emission Analysis

While the propanol-1 washing samples, LW-Pr-1 and LW-Pr-2 are heavily contaminated with an organic phthalate that does not come from the washed tubes, one can still obtain much valuable information from these experiments. Partial emission values for the first two propanol-1 washes are listed in Table 6 together with those for the first two water washes.

It was anticipated that propanol-1 would be a better solvent for elements in the tubes such as carbon, but a poorer solvent than water for inorganic ions. Because of the phthalate impurity it is not possible to learn anything about elements such as carbon. However, it is obvious from Table 6 that propanol-1 is as good a solvent for inorganic ions as is water at the concentrations under consideration; maybe an even better solvent. Based on the analyses in Table 6, propanol-1 certainly seems to be a better solvent for Si, Fe, Mg, Sn, Al, and Cr, while water is a better solvent for Na, Cu, and maybe K. The second propanol-1 wash, LW-Pr-2, extracted much more material from the tubes than did the first wash, LW-Pr-1. This is especially true for B, Si, Fe, and Al. The reasons for higher solubility in the second wash are not understood. Note, however, that the second water wash extracted much more Na and K than did the first water wash.

### Electron Microprobe Analysis

The electron microprobe results listed in Appendix B for LW-Pr-1 and LW-Pr-2 do not appear to be as useful as for other samples because of the phthalate impurity. However the results do confirm that water is a better solvent for K and S in pyrex than is propanol-1, but propanol-1 is as good or better solvent for Cl than is water.

### Solvent Extractions

The observation that propanol-1 can extract inorganic ions from glass can be verified by the infrared spectra of cross-extracted portions of propanol-1 wash residues. These spectra are shown in Figure 24. The top spectrum (A) is that of the second propanol-1 residue, LW-Pr-2. Most of the spectrum is due to the phthalate contaminant. Spectrum B is that of the  $CCl_4$  soluble portion of LW-Pr-2 and appears to be almost pure phthalate. The bottom spectrum (C) is that of the  $CCl_4$  insoluble portion of LW-Pr-2 which closely resembles the spectra of the  $H_2O$  washes of glass tubes. Thus it appears that rather clean separations of the organic and inorganic portions of these residues can be made. For the same reasons the organics could be separated from water washing.

TABLE 6. PARTIAL EMISSION SPECTROGRAPHIC ANALYSIS FOR  
LIQUID WASHINGS OF CAPILLARY TUBES

Sample	B	Elements ( $\mu\text{g}$ )							Cr	K
		Si	Fe	Mg	Sn	Al	Na			
LW-PR-1	2.0	10.0	2.0	2.0	3.0	3.0	30.0	2.0	1.0	<50.0
LW-Pr-2	10.0	100.0	5.0	3.0	3.0	15.0	30.0	1.0	2.0	5.0
LW-H <sub>2</sub> O-1	15.0	10.0	0.2	2.0	0.5	1.0	50.0	5.0	0.1	<50.0
LW-H <sub>2</sub> O-2	3.0	3.0	0.1	0.3	0.5	0.2	>100.0	3.0	0.1	>100.0

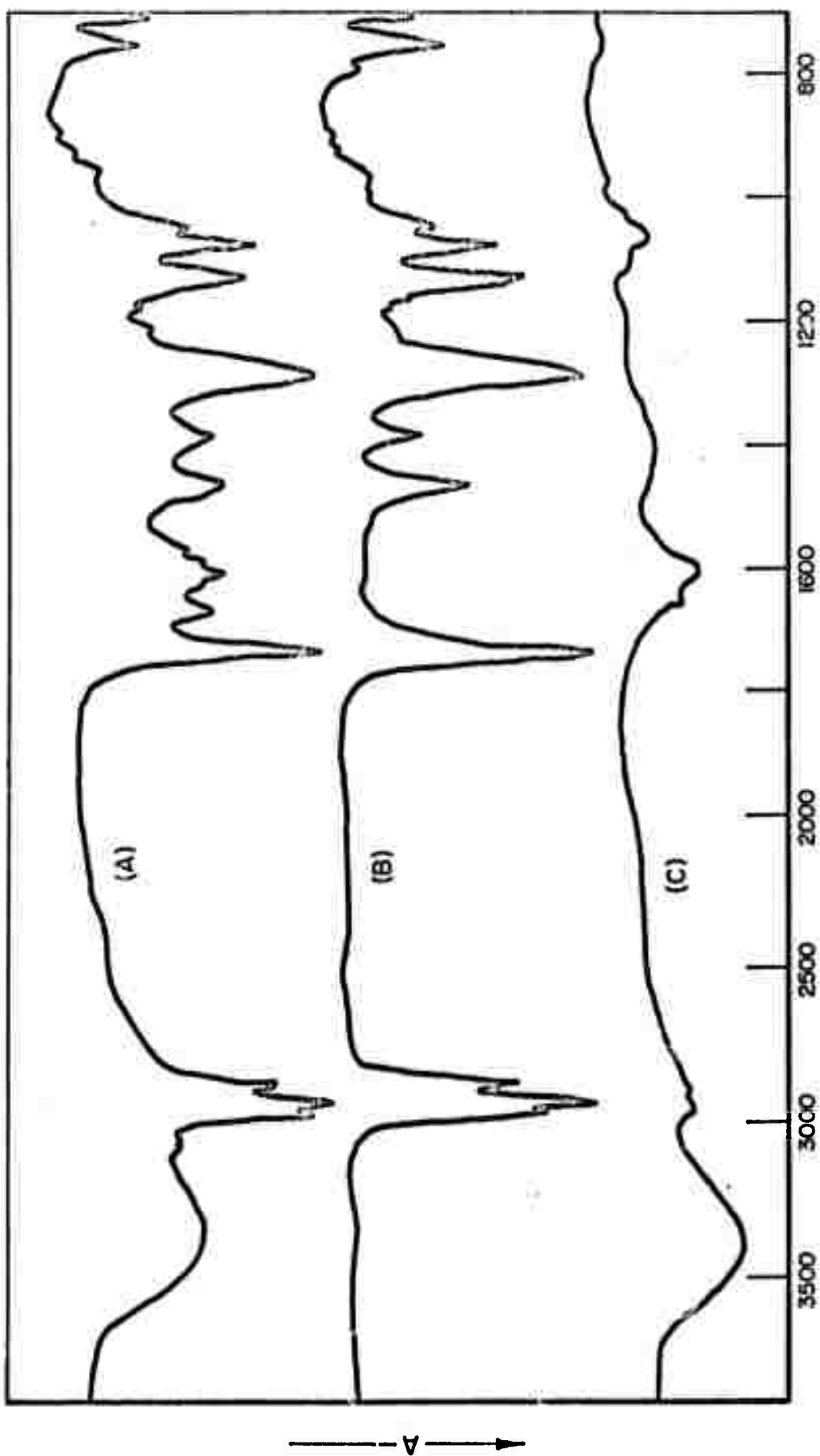


FIGURE 24. INFRARED SPECTRA OF (A) LW-Pr-2, (B) THE  $\text{CCl}_4$  SOLUBLE PORTION OF LW-Pr-2, AND (C) THE  $\text{CCl}_4$  INSOLUBLE PORTION OF LW-Pr-2

Liquid Water Extractions of Crushed GlassesInfrared Spectra

The infrared spectra of the residue of the water extraction of the seven types of crushed glass are placed in three groups as seen in Figures 25, 26, and 27. Figure 25 shows the spectra obtained from the water soluble residue of Nonex glass (A), 7052 glass (B), and cobalt glass (C). The spectra of this group of samples are characterized by a strong band in the 1350-1450  $\text{cm}^{-1}$  range and a strong band in the 1070 to 1180  $\text{cm}^{-1}$  region. For CG-N-1 and CG-C-1, the lower frequency band is the stronger while for CG-7052-1, the high frequency band near 1400  $\text{cm}^{-1}$  is the stronger. In Figure 26, the spectra of water soluble residue from uranium glass (A), Vycor glass (B), and quartz glass (C) are characterized by a very weak band in the 1400  $\text{cm}^{-1}$  region and a stronger band near 1075  $\text{cm}^{-1}$ . The intensities of the bands in this group of samples are much weaker than the intensities of the bands in the spectra shown in Figure 26. This intensity difference between the two groups of spectra (Figure 25 versus Figure 26) reflects the difference in the amount of residue obtained by water extraction. Much more material was extracted for CG-N-1, CG-7052-1, and CG-C-1 than for CG-U-1, CG-V-1, and CG-Q-1.

The spectrum of the water extract of pyrex glass is shown in the top spectrum (A) of Figure 27. The ratio of the band near 1400  $\text{cm}^{-1}$  to the one near 1075  $\text{cm}^{-1}$  is intermediate between that from the group of samples in Figure 25 and the group of samples in Figure 26. The amount of material extracted from CG-P-1 also is intermediate between the amounts of material extracted from the other two groups. This difference in amount is also reflected by the fact that the intensities of all the bands of CG-P-1 are also intermediate between the intensities of the bands of the other two groups. The lower spectrum of Figure 27 is of the residue of an amount of water equal to that used for the extraction which had previously stood in a round-bottomed flask for the same length of time as the extractions. Thus it is the system blank (CG-H<sub>2</sub>O-01) for the group of crushed glass experiments.

This spectrum CG-H<sub>2</sub>O-01 shows that the extremely weak bands cannot account for much of the spectra of the water soluble residues from the glasses, except possibly for the 1400  $\text{cm}^{-1}$  band of quartz.

Emission Analysis

Part of the emission analyses values for the residues from the crushed glass samples are given in Table 7. Compared to the system blank (CG-H<sub>2</sub>O-01), it can be seen that the elements listed in Table 7 can be extracted from some or all of the glasses in quantities substantially greater than the blank; with the possible exception of Ba. From Table 7 it is also apparent that the samples can be grouped by the amounts of various elements extracted, and these fall in the same groups as

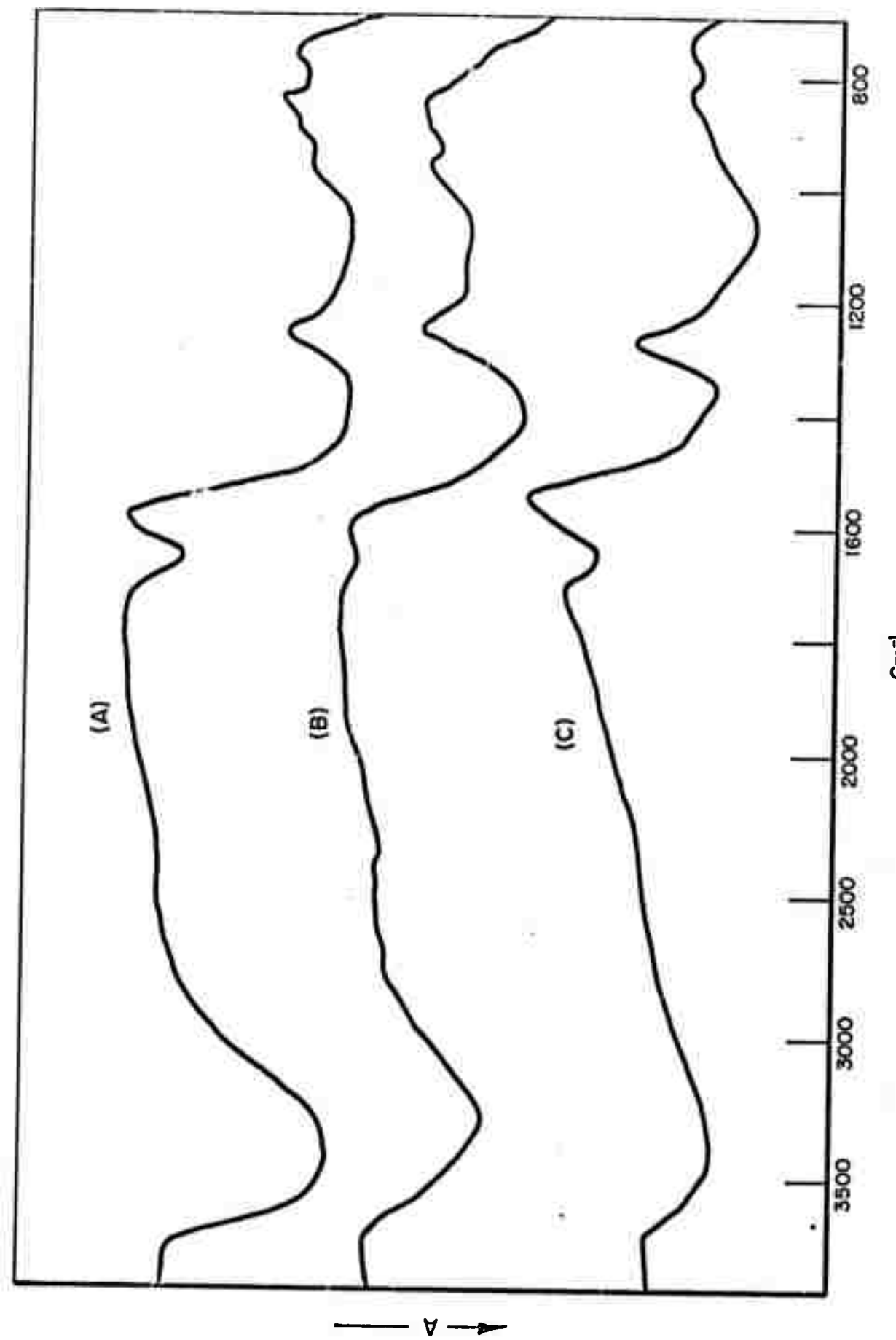


FIGURE 25. INFRARED SPECTRA OF (A) CG-N-1, (B) CG-7052-1, AND (C) CG-C-1

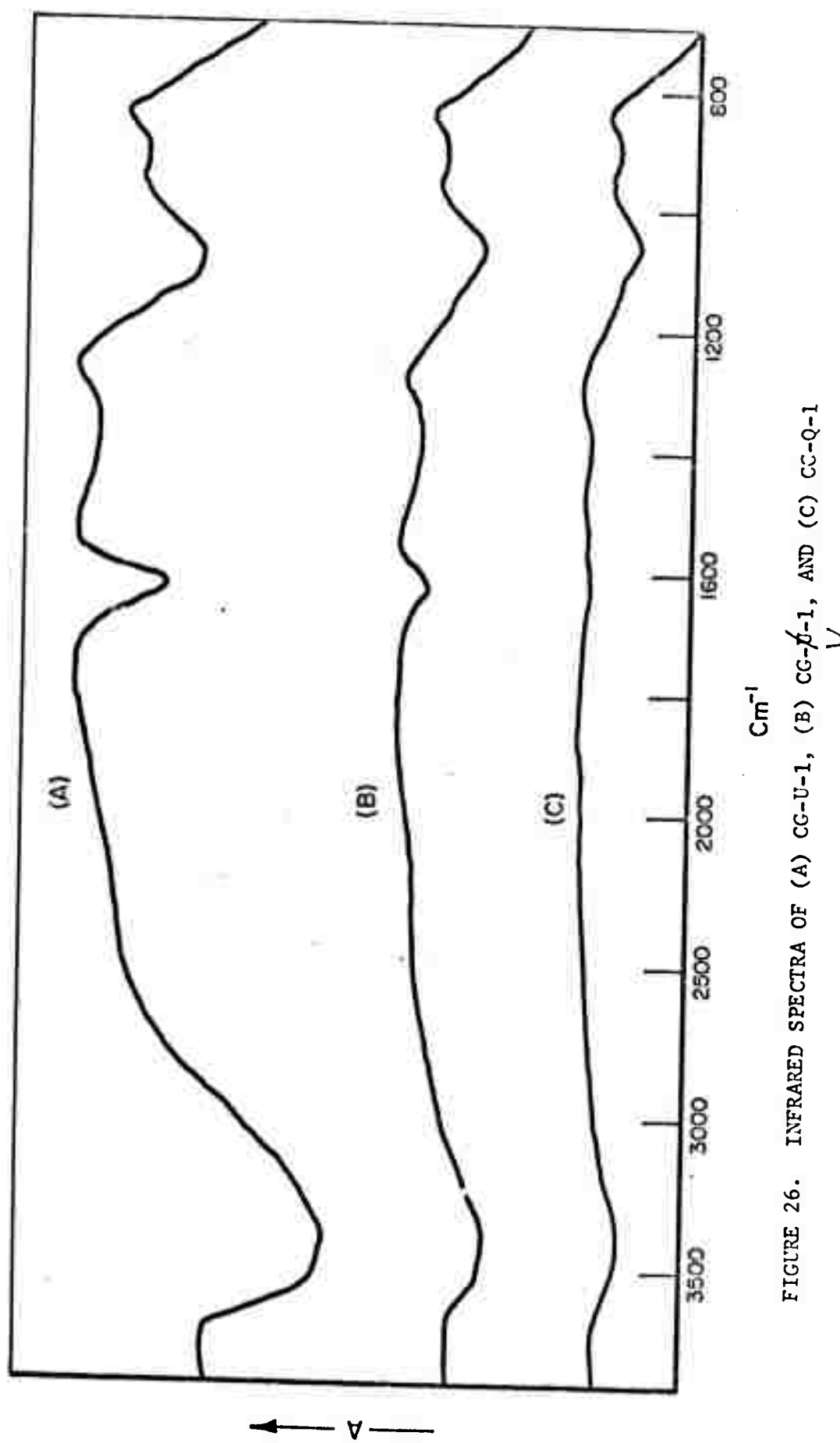


FIGURE 26. INFRARED SPECTRA OF (A) CG-U-1, (B) CG-J-1, AND (C) CC-Q-1

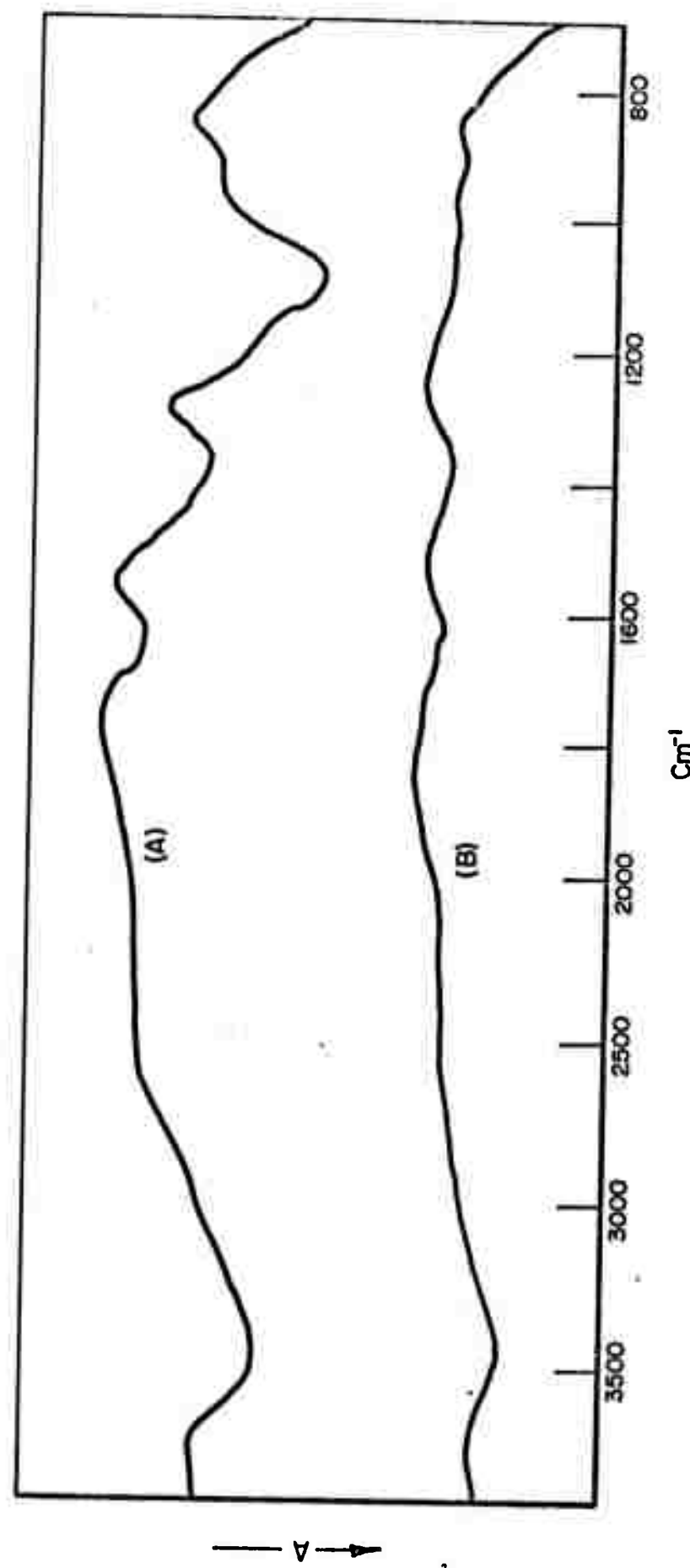


FIGURE 27. INFRARED SPECTRA OF (A) CG-P-1 AND (B) CG-H<sub>2</sub>O-01

the spectra were arranged (Figures 25, 26, and 27). Thus CG-N-1, CG-7052-1, and CG-C-1 have large amounts of B, while the rest of the extracts do not.

TABLE 7. PARTIAL EMISSION SPECTROGRAPHIC ANALYSES FOR WATER EXTRACTIONS OF CRUSHED GLASSES

Sample	Elements ( $\mu\text{g}$ )									
	Ba	B	Si	Al	Na	Ca	K	Co	Sb	As
CG-N-1	0.3	>100.0	>100.0	3.0	>100.0	7.0	>100.0	0.1	3.0	10.0
CG-7052-1	0.3	>100.0	50.0	0.5	100.0	5.0	>100.0	0.1	0.5	1.0
CG-C-1	0.3	>100.0	>100.0	3.0	100.0	5.0	>100.0	2.0	0.5	1.0
CG-P-1	0.1	15.0	30.0	0.1	50.0	1.0	1.0	0.1	0.5	1.0
CG-V-1	0.1	15.0	20.0	0.1	5.0	1.0	1.0	0.1	0.5	1.0
CG-Q-1	0.1	3.0	15.0	0.1	1.0	1.0	1.0	0.1	0.5	1.0
CG-H <sub>2</sub> O-01	0.1	2.0	3.0	0.1	1.0	0.5	1.0	0.1	0.5	1.0

The samples of the first group (CG-N-1, CG-7052-1, and CG-C-1) have the largest amounts of Si. CG-P-1 gives an intermediate value for Si, while the samples of the third group (CG-V-1 and CG-Q-1) give the lowest values for Si. The first group of samples shows the presence of some Al, while the rest of the samples apparently do not contain Al since the emission values are no greater than that of the system blank (CG-H<sub>2</sub>O-1). For Na, the differences are even more distinctive. The first group of samples has 100 or more  $\mu\text{g}$  of Na; while the second group has 50  $\mu\text{g}$ , and the third group has 5 or less  $\mu\text{g}$  of this element. Similar comparisons exist for most of the elements listed in Table 7. It is interesting to note that Co is detected in the residue from cobalt glass and that Sb and As are detected in the residue from Nonex glass.

#### Liquid Water Extraction of Glass Wool

The infrared spectra of the residues of the water extractions of glass wool are shown in Figure 28. Figure 28 (top) is the spectrum of a standard or blank (residue from 250 ml of water in a synex flask for 10 days). This spectrum (GW-H<sub>2</sub>O-1) is remarkably similar to the spectra of preparations of anomalous water yet it results from a simple water wash of a pyrex flask. The spectra of the residues from the water extraction of pyrex (GW-P-H<sub>2</sub>O-1) and quartz (GW-Q-H<sub>2</sub>O-1) glass wool are shown in Figure 28, middle and bottom respectively. The extraction from quartz glass wool gave a spectrum much like that of the blank. The spectrum from pyrex glass wool, however gave a strong 1680  $\text{cm}^{-1}$  band with practically no 1620  $\text{cm}^{-1}$  absorption. In the 400  $\text{cm}^{-1}$  range, the 1360  $\text{cm}^{-1}$  absorption is much stronger than the 1410  $\text{cm}^{-1}$  band much like the water washes of

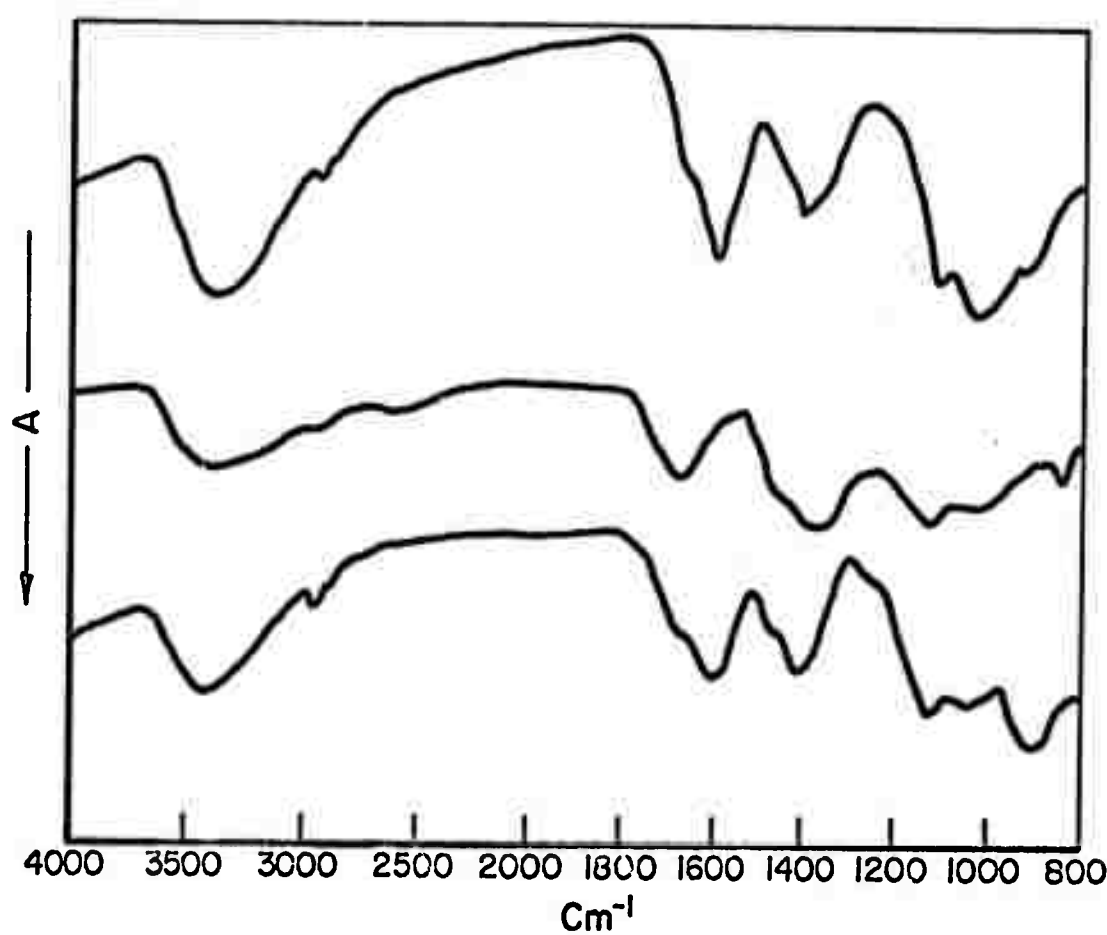


FIGURE 28. INFRARED SPECTRA OF GW-H<sub>2</sub>O-1 (TOP), GW-P-H<sub>2</sub>O-1 (MIDDLE), AND GW-Q-H<sub>2</sub>O-1 (BOTTOM)

of capillary tubes. However the important fact is that these washes give spectrum which are qualitatively similar to those of anomalous water preparations. This would indicate that at least most of the residue from anomalous water preparation consists of material extracted from glass.

### Carbonate Derivative

#### Analysis

The infrared spectra of the residue of the methanol or ethanol soluble portion of  $\text{NaHCO}_3$  are shown in Figure 29. Figure 29 (bottom) is the spectrum of the ethanol product while Figure 29 (top and middle) are two separate preparations of the methanol product. The spectra shown in Figure 29 are similar to spectra obtained by the University of Maryland (where the products were first<sup>(6)</sup> prepared). The methanol product varies slightly from preparation to preparation in one of three ways: (1) no  $\text{Na}_2\text{CO}_3$  absorption is present at  $880 \text{ cm}^{-1}$  (top Figure 29), (2) some  $\text{Na}_2\text{CO}_2$  absorption is present (middle Figure 29), or (3) both  $\text{Na}_2\text{CO}_3$  absorption at  $880 \text{ cm}^{-1}$  and an unknown absorption at  $865 \text{ cm}^{-1}$  are present. In any of these cases these differing absorptions are weak and most represent a very small portion of the sample. The major infrared bands are identical from preparation to preparation.

The major (strongest) bands of both the methanol and ethanol products have nearly identical frequencies indicating the same basic structural unit in each case.

It must be emphasized that none of the spectra in Figure 29 match reference spectra for sodium bicarbonate ( $\text{NaHCO}_3$ ). In these spectra (Figure 29) the strong  $1625 \text{ cm}^{-1}$  band and the CH stretching vibrations in the  $2900 \text{ cm}^{-1}$  range are of the most interest, for if this compound exists on glass, the strong  $1625 \text{ cm}^{-1}$  band would explain the remaining question in the infrared spectra of anomalous water. The CH bands would then have to be due to residual solvent or to a complex of this compound with the alcohol solvent. Thus the research shifted to the identification of this methanol product.

A sample of the methanol product was heated in air for five hours at  $100^\circ\text{C}$ . An infrared spectrum of this heated sample is shown at the top of Figure 30. While some of the original compound remains (see Tp bands at  $2960$ ,  $1625$ ,  $1090$ ,  $925$ , and  $830 \text{ cm}^{-1}$ ) most of the sample has been converted to sodium carbonate ( $\text{Na}_2\text{CO}_3$ ). Further heating at this temperature or shorter heating periods at higher temperatures will complete the conversion to  $\text{Na}_2\text{CO}_3$ . Conversion to  $\text{Na}_2\text{CO}_3$  upon heating is the known behavior of  $\text{NaHCO}_3$ , so the possibility existed that our methanol product was a different polymorph of  $\text{NaHCO}_3$  with some residual methanol. The bottom spectrum of Figure 30 shows the residue from the  $\text{CCl}_4$  extraction of the heated sample (shown at the top of Figure 30). As can be seen in Figure 30, this residue is not a spectrum of methanol, so if some residual methanol remains it can survive exposure to  $100^\circ\text{C}$  and not be extracted with organic solvents, i.e., it must be strongly bound or complexed to the methanol product.

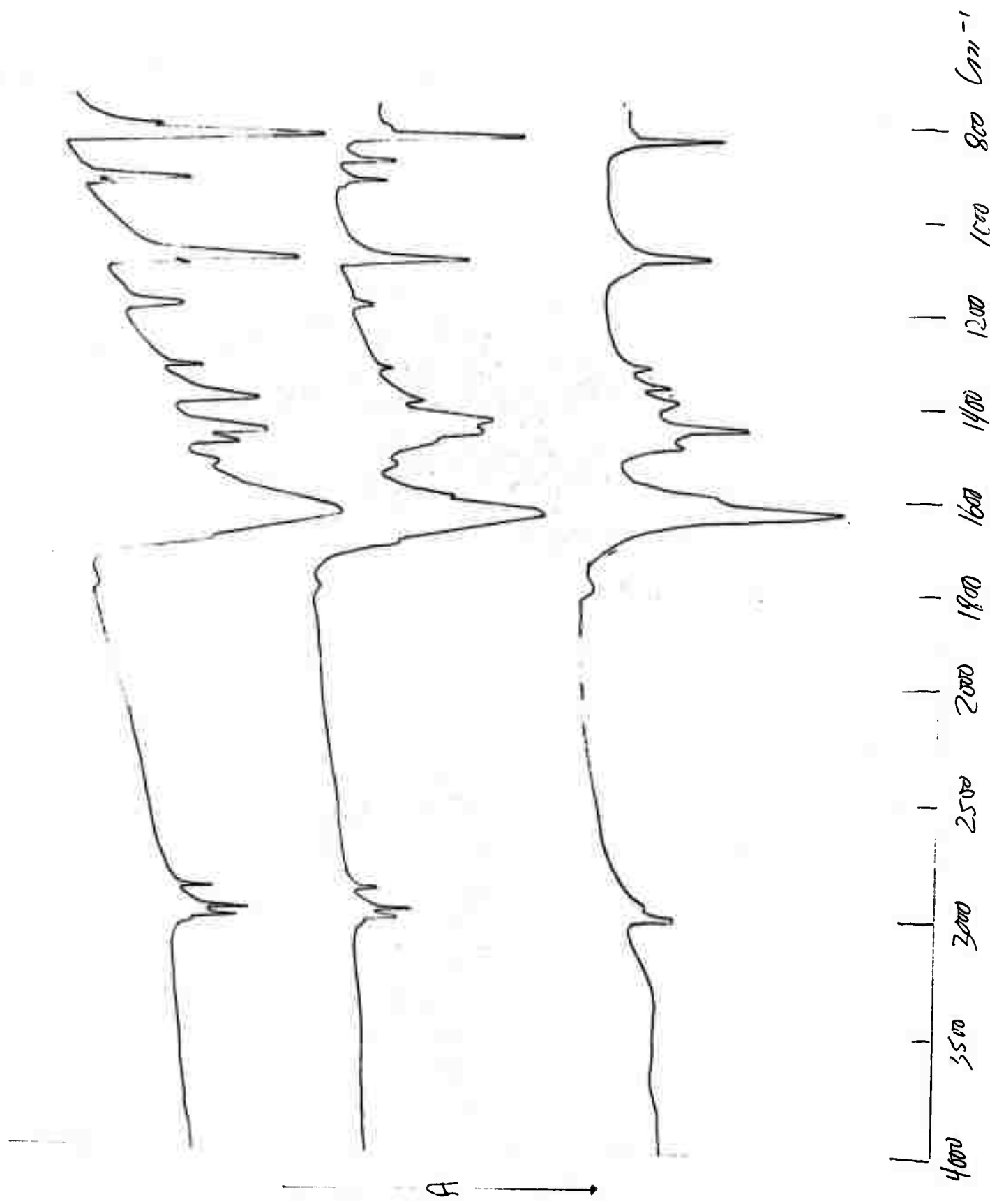


FIGURE 29. INFRARED SPECTRA OF  $\text{NaClO}_4$  IN  $\text{CHCl}_3$  (CRYSTAL, ANOTHER PREPARATION).

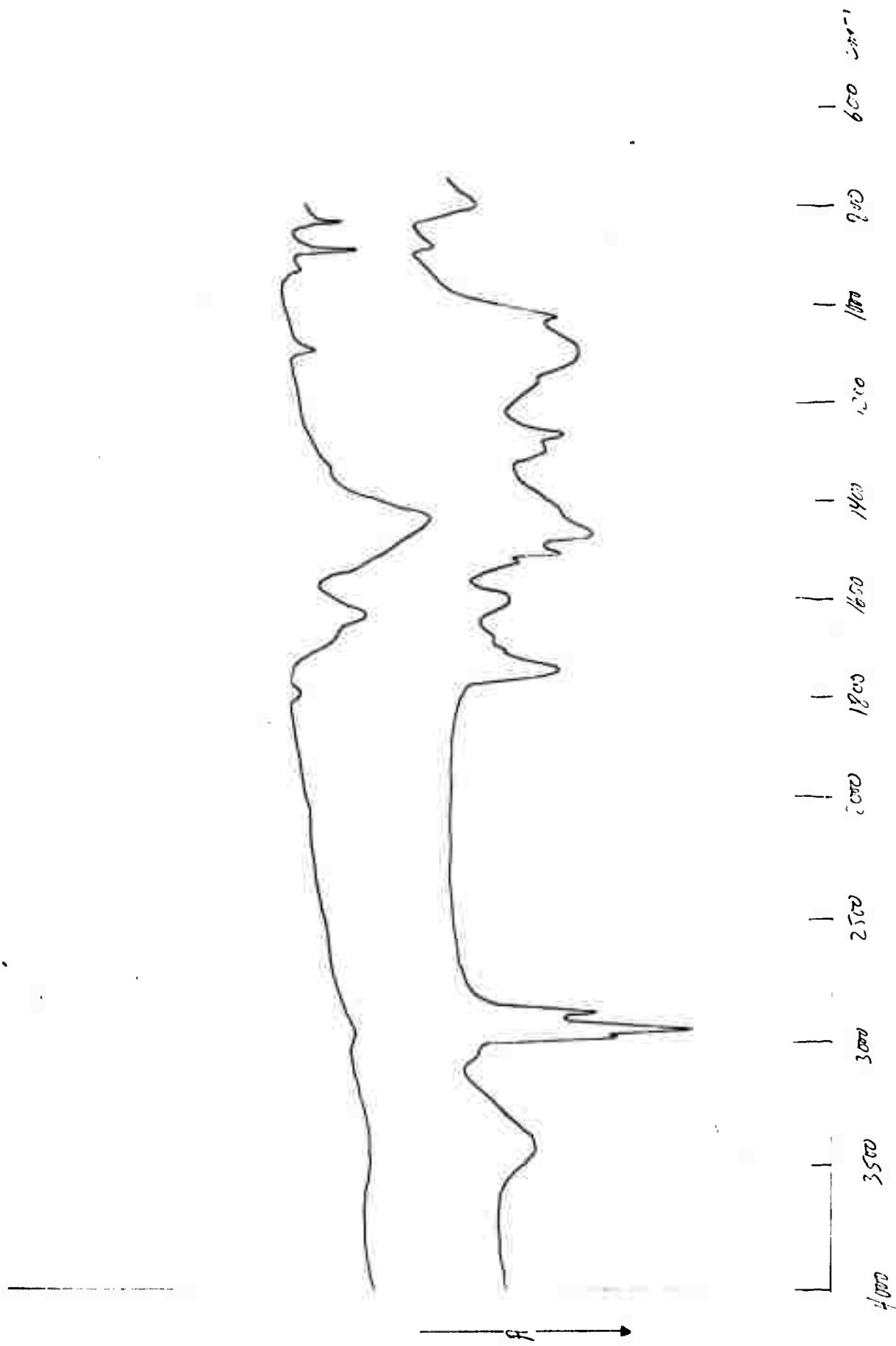


FIGURE 30. INFRARED SPECTRA OF  $\text{NaHCO}_3$  IN  $\text{CH}_3\text{OH}$  HEATED FOR FIVE HOURS AT 100°C (TOP) AND RESIDUE FROM  $\text{CCl}_4$  EXTRACT OF ABOVE SAMPLE (BOTTOM)

To test the possibility of complex formations, both thermal gravimetric (TGA) and mass spectrometry (MS) analyses were obtained on the methanol product. The TGA run is shown in Figure 31. This run which plots weight loss vs. temperature (programmed for a four degree temperature use per minute) shows that, upon heating, the sample immediately begins to lose weight. While there are several inflection points (change of rate of weight loss) before 120 C, it is near this point that the weight loss proceeds at a rapid rate. This rapid rate continues until near 190 C where further heating causes very little additional weight loss. At 230 C the total weight loss is 45.61 percent of the original weight. This weight loss is far too great to be accounted for solely on the basis of loss of  $\text{CH}_3\text{OH}$  from a 1:1  $\text{CH}_3\text{OH}-\text{NaHCO}_3$  complex although a  $\text{CH}_3\text{OH}$  clathrate is not excluded. An infrared spectrum of the residue remaining after this TGA run is shown in Figure 32 and represents almost pure  $\text{Na}_2\text{CO}_3$ .

The unknown methanol product (hereafter referred to as  $\text{NaHCO}_3$  in  $\text{CH}_3\text{OH}$ ) was then subjected to mass spectrometry analyses. This mass spectral studies were carried out using a mass spectrometer (Finnigan 1015) in which one can gradually heat the material and obtain mass spectra of the volatile decomposition product at various temperatures. The MS runs were programmed at the same rate (four degrees per minute) as the TGA runs. Since this MS unit is coupled to dedicated computer, it is possible to store the many MS runs made over the temperature range and retrieve the data in the form of either conventional mass spectra (amplitude or intensity vs. mass) or as amplitude (for any specified mass range) vs. temperature. The MS results (presented in the latter form) are shown in Figure 33. The amplitude or ion current generated by species in the 18-19 mass range are shown at the top of Figure 33. Thus masses of 18 or 19 ( $\text{H}_2\text{O}$ ) can be seen coming off near 33 C, near 55 C, and, with a weaker, broad peak, at about 72 C.  $\text{CO}_2$  (masses 44-45) is seen in Figure 33 (second from the top) coming off near 55 C, near 72 C and over the broad range near 110 C.  $\text{CH}_3\text{OH}$  (masses 31-32) is seen coming off (Figure 33, second from bottom) near 110 C and 140 C. The amplitude are not directly comparable (because of a normalization factor) from one mass range to another, but some quantitative measure can be achieved by comparison of the noise level of each trace. Thus it can be deduced that there is far less  $\text{CH}_3\text{OH}$  (masses 31-32) than either  $\text{H}_2\text{O}$  (masses 18-19) or  $\text{CO}_2$  (masses 44-45). This is confirmed by the plot shown at the bottom of Figure 33 which represents the total ion current for all masses coming off over this temperature range. As can be seen in the lower curve the  $\text{CO}_2$  and  $\text{H}_2\text{O}$  peaks at 33 C and 55 C can be weakly detected, but the  $\text{CH}_3\text{OH}$  peak at 110 C and 140 C are too small to be observed. The surprising feature of the lowest plot however, is that none of the products ( $\text{H}_2\text{O}$ ,  $\text{CO}_2$ , or  $\text{CH}_3\text{OH}$ ) are the major decomposition products with temperature. Instead, species which volatilize near 83 C make up the bulk of the decomposition products. A conventional mass spectrum (amplitude expressed as percentage of strongest peak vs. mass) of the product volatilizing at 83 C is shown in Figure 34. From this figure it can be seen that there are strong peaks with masses above 44-45. The strong peaks in the 28-32 mass range are due to  $\text{N}_2$  and  $\text{O}_2$  of air. The distribution of these peaks indicates the possibility of a complex mixture of hydrocarbon fragments and from the masses shown, the hydrocarbon are much bigger than the methyl groups which might be expected for the

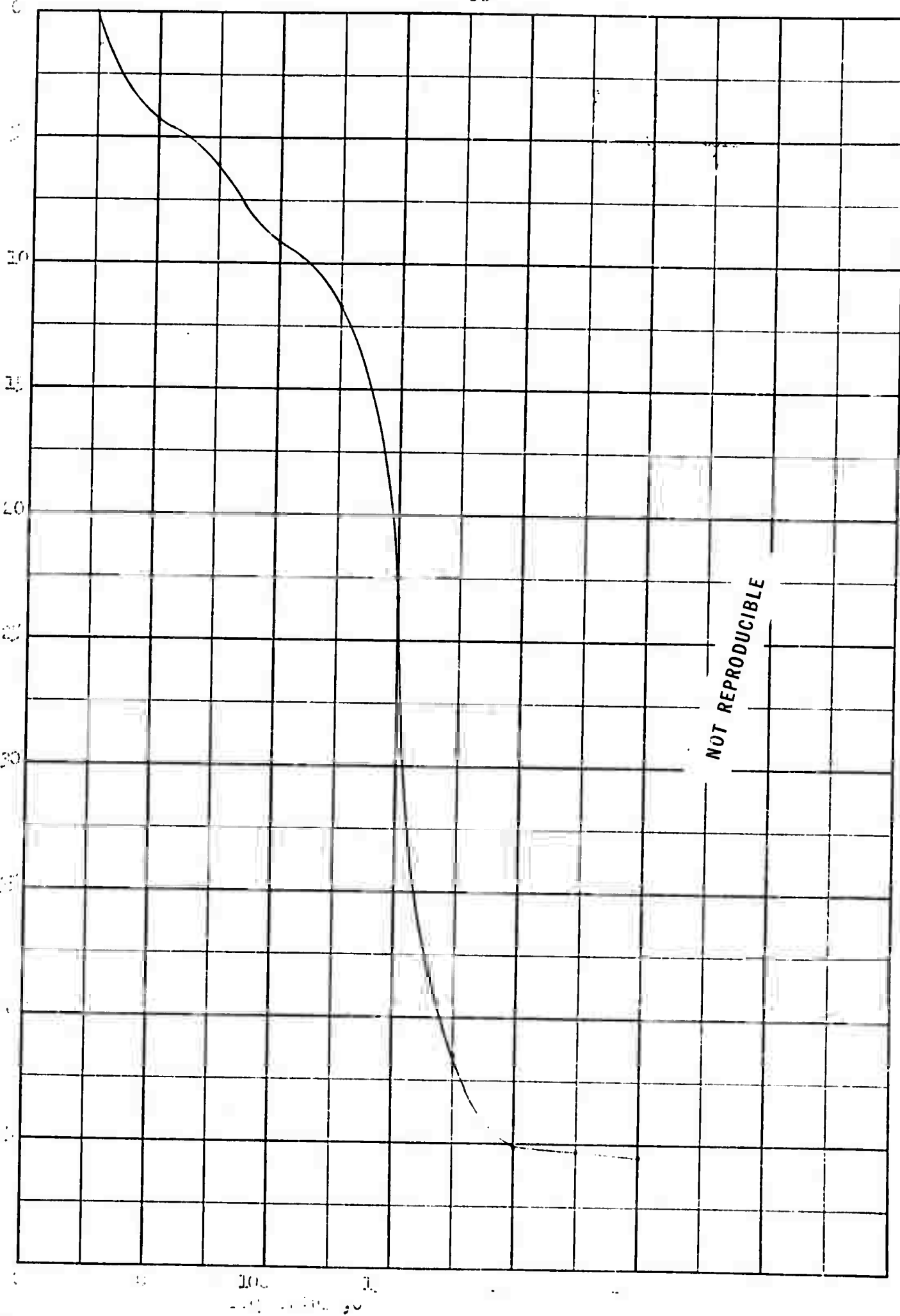


FIGURE 2.1. PIONEER GRAVIMETRIC ANALYSIS FOR OF THE  $\text{NaHCO}_3$  IN CEMENT PROFILE.

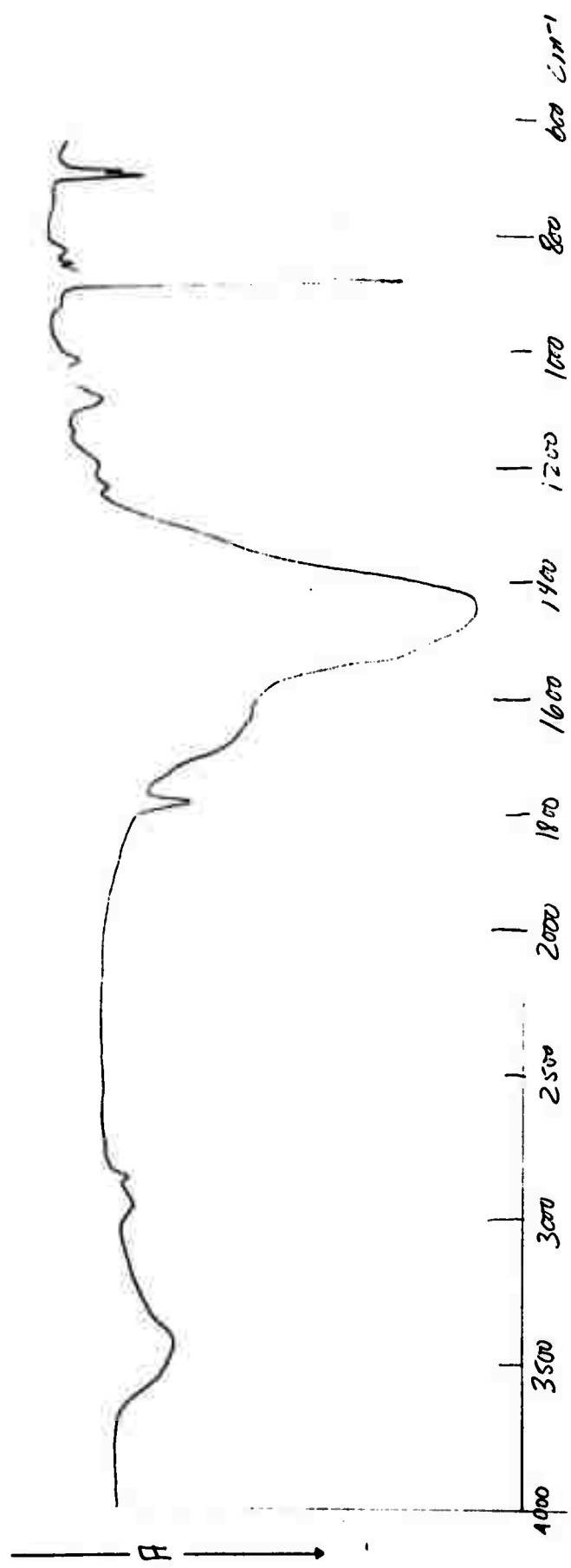


FIGURE 32. INFRARED SPECTRUM OF THE RESIDUE OF THE  $\text{NaHCO}_3$  IN  $\text{CH}_3\text{CH}$  PRODUCT  
AFTER TGA RUN SHOWN IN FIGURE 31

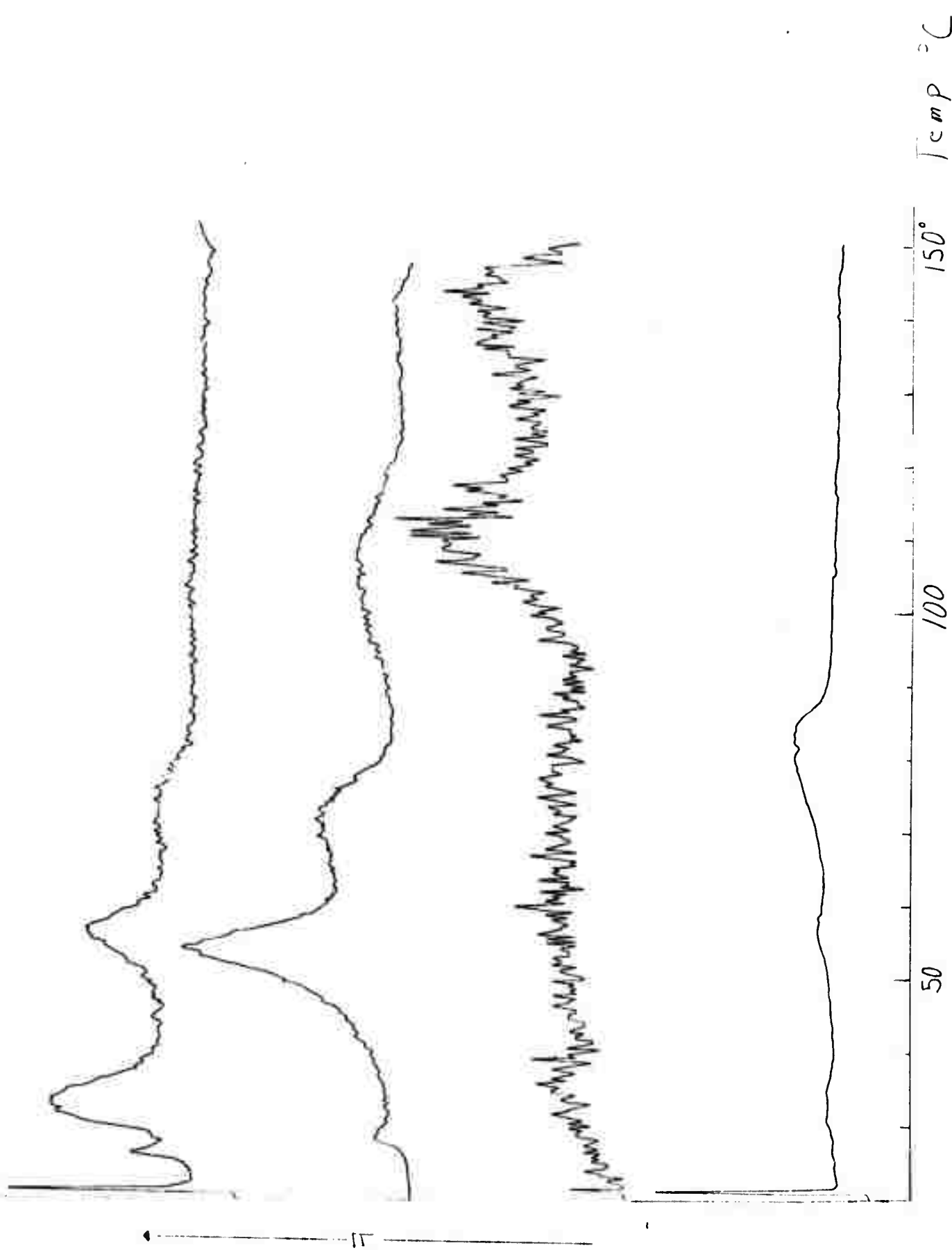


FIGURE 33. MASS SPECTRAL RESULTS (MASS SPECTRAL AMPLITUDE VS. TEMPERATURE) FOR THE  $\text{NaIICO}_3$  IN  $\text{CH}_3\text{OH}$  PRODUCT.  
 MASSES 18-19 (CROP), MASSES 31-32 (SECOND FROM TOP), MASSES 31-32 (SECOND FROM BOTTOM).

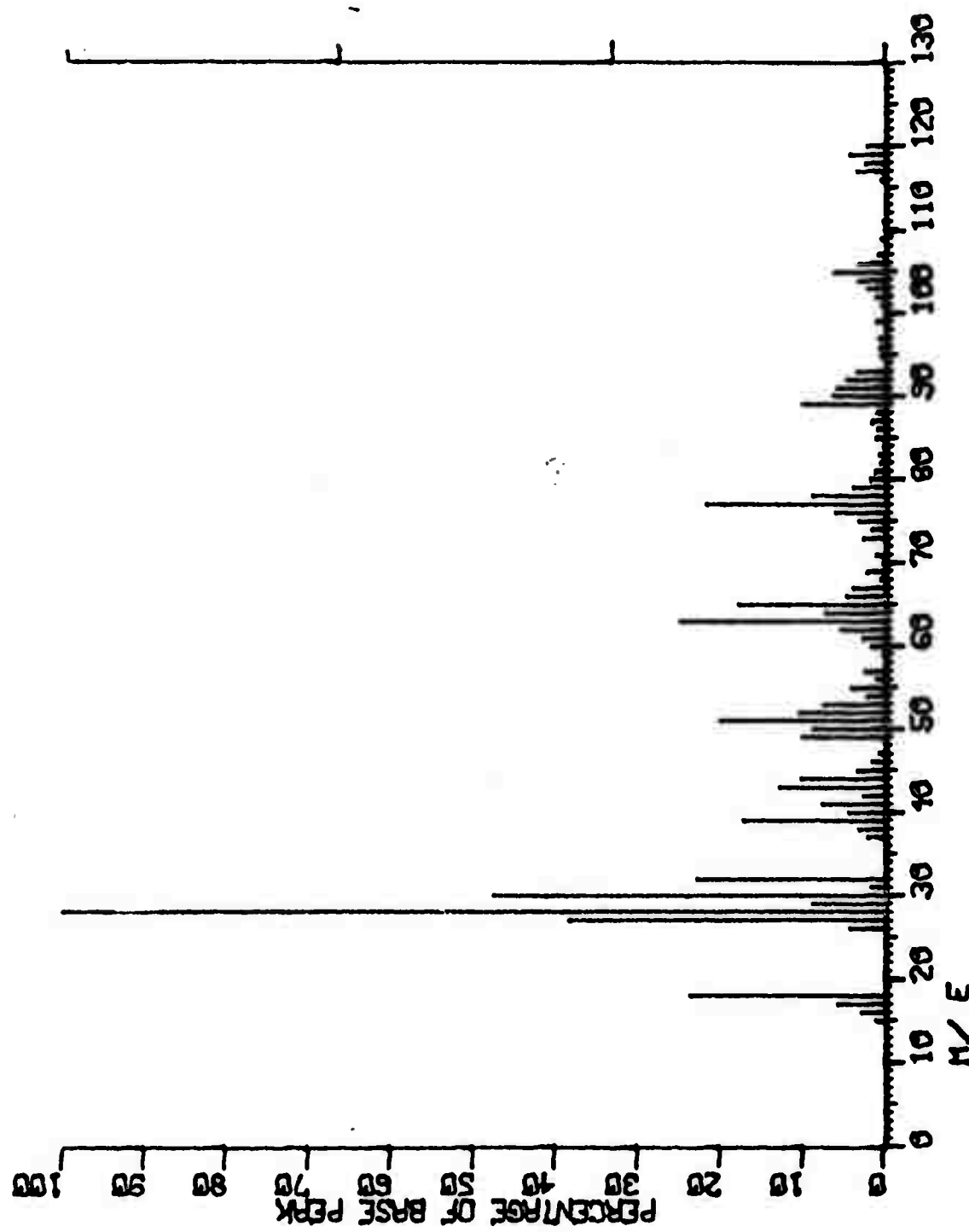


FIGURE 34. MASS SPECTRAL RESULTS FOR THE  $\text{NaHCO}_3$  IN  $\text{CH}_3\text{OH}$  PRODUCT AT 83 C

$\text{NaHCO}_3$  in  $\text{CH}_3\text{OH}$  product. Thus the mass spectral data strongly indicates that there is not enough  $\text{CH}_3\text{OH}$  for a  $\text{NaHCO}_3\text{-CH}_3\text{OH}$  complex or clathrate and that hydrocarbons (larger than  $\text{CH}_3$ ) are present (or formed with heat) in this  $\text{NaHCO}_3$  in  $\text{CH}_3\text{OH}$  product.

These results led to the use of a computer search system to compare the infrared spectrum of the  $\text{NaHCO}_3$  in  $\text{CH}_3\text{OH}$  product against 140,000 reference spectra. One compound (sodium methyl carbonate) was found to have nearly identical infrared frequencies (but different band intensities) with the unknown. Elemental analyses were then performed to ascertain if the unknown was indeed sodium methyl carbonate ( $\text{NaO-CO-OCH}_3$ ). Emission spectrographic analysis for the  $\text{NaHCO}_3$  in  $\text{CH}_3\text{OH}$  product are shown in Table 8 and compared to values for the starting sodium bicarbonate. Other elements besides those in the table were sought, but not detected. Table 8 demonstrates that the  $\text{NaHCO}_3$  in  $\text{CH}_3\text{OH}$  product could not be a metallic impurity in the original  $\text{NaHCO}_3$ .

TABLE 8. EMISSION SPECTROGRAPHIC ANALYSES

Sample	Elements (mg)						
	Mg	Si	Fe	Al	K	Ca	Na
$\text{NaHCO}_3$ in $\text{CH}_3\text{OH}$ Product	<10	10	<5	<5	10	<5	>>>100
$\text{NaHCO}_3$	10	<10	<5	<5	<10	15	>>>100

C, H, N, and Na analyses are shown in Table 9. As can be seen the observed values are low for carbon and hydrogen and high for sodium methyl carbonate. This leaves the possibility that either the product is not sodium methyl carbonate or that the bulk of the product is  $\text{NaO-CO-OCH}_3$ , but with a sodium-containing impurity present to cause the discrepancy in the elemental values. From the infrared spectrum of the  $\text{NaHCO}_3$  in  $\text{CH}_3\text{OH}$  product, one would have to conclude that the impurity is either noninfrared absorbing or has the identical frequencies of  $\text{NaO-CO-OCH}_3$ .

TABLE 9. C-H-N-Na ANALYTICAL RESULTS

Sample	% C	% H	% N	% Na
$\text{NaHCO}_3$ in $\text{CH}_3\text{OH}$ -1	20.2	2.5	<0.1	26.0
" " " -2	20.0	2.6	<0.1	25.3
" " " -3	21.6	-	-	-
Average (1, 2, 3)	20.6	2.6	<0.1	25.7
$\text{NaO-CO-OCH}_3$ (calc.)	24.5	3.1	0	23.5

In the course of the research it was soon noticed that samples of the  $\text{NaHCO}_3$  in  $\text{CH}_3\text{OH}$  product showed changes when left standing in air for a period of time. In order to study these changes, films of the  $\text{NaHCO}_3$  in  $\text{CH}_3\text{OH}$  product were laid on an infrared transmitting plate and an infrared spectrum recorded. This spectrum was similar to those shown in Figure 29. This film was then allowed to stand in air and spectra were recorded daily. Several of these spectra are shown on Figures 35 and 36. The spectrum in Figure 35a (recorded after standing in air three days) shows traces of a new band appearing at  $2940 \text{ cm}^{-1}$  on the side of the original  $2965 \text{ cm}^{-1}$  band. In addition new bands appear at  $1458 \text{ cm}^{-1}$  and  $870 \text{ cm}^{-1}$ , indicative of carbonate formation. After five days (Figure 35b) the  $2940 \text{ cm}^{-1}$  band is stronger than the  $2965 \text{ cm}^{-1}$  band and both the  $870$  and  $1448 \text{ cm}^{-1}$  bands have increased in intensity. After seven days (Figure 35c) the  $2965 \text{ cm}^{-1}$  band has almost disappeared, the  $870 \text{ cm}^{-1}$  band is very strong and the band in the  $1400 \text{ cm}^{-1}$  region has increased in intensity and shifted to  $1449 \text{ cm}^{-1}$ . All of the remaining bands of the  $\text{NaHCO}_3$  in  $\text{CH}_3\text{OH}$  product by now have obviously decreased in intensity. After ten days (Figure 36d) these changes are even more pronounced and in addition a new band has appeared at  $905 \text{ cm}^{-1}$ . By the end of 24 days (Figure 36e) virtually all of the bands of the original product have disappeared to be replaced mainly by sodium carbonate ( $1448$  and  $870 \text{ cm}^{-1}$ ) but also by a surprisingly large amount of CH ( $2940 \text{ cm}^{-1}$ ). This CH has changed from the  $\text{CH}_3$  ( $2965$ ) of the original sample to absorption bands typical of a hydrocarbon chain ( $\text{CH}_3$  at  $2965 \text{ cm}^{-1}$  and  $\text{CH}_2$  at  $2940 \text{ cm}^{-1}$ ). The unusual formation of a hydrocarbon chain from methyl groups suggests the possibility that the  $905 \text{ cm}^{-1}$  band could arise from olefinic unsaturation.

Since oxygen may accelerate or catalyze the decomposition, a fresh sample was placed on an infrared transmitting plate and allowed to stand in a vacuum instead of in air. Spectra were recorded daily, some of which are shown in Figure 37 and 38. Unlike the sample exposed to air, three days in a vacuum (Figure 37, top) did not show the formation of a new CH band at  $2940 \text{ cm}^{-1}$ , but did show carbonate formation ( $1435$  and  $880 \text{ cm}^{-1}$ ). After seven days, the spectrum (Figure 37, bottom) of the sample shows increasing amounts of carbonate and the appearance of a new CH band at  $2940 \text{ cm}^{-1}$ . After 12 days (Figure 38, top) the  $2940 \text{ cm}^{-1}$  band is readily discernible, but it is not until 24 days (Figure 38, bottom) that the CH intensity at  $2940 \text{ cm}^{-1}$  is stronger than that of the original CH band ( $2965 \text{ cm}^{-1}$ ). By this time the sample is mostly carbonate and apparently is much like the sample after standing 24 days in air (Figure 36, bottom). However closer examination reveals that there are distinct differences between the sample that decomposed in air and the sample that decomposed in a vacuum. This is demonstrated in Figure 39 which shows the spectra of a sample after 10 days in air (Figure 39, top) and 10 days in a vacuum (Figure 39, bottom). One obvious difference is that the rate of carbonate formation (or decomposition of the original sample) is not as great in the vacuum sample as in the air sample. A less obvious difference is that the carbonate absorption bands are at different frequencies ( $1448$  and  $870 \text{ cm}^{-1}$  in the air sample compared to  $1435$  and  $880 \text{ cm}^{-1}$  in the vacuum sample). Figure 40 shows a comparison of the 24 day air sample and vacuum sample which more clearly demonstrates the same difference in carbonate frequencies. Thus while both samples decompose to a carbonate, each decomposes

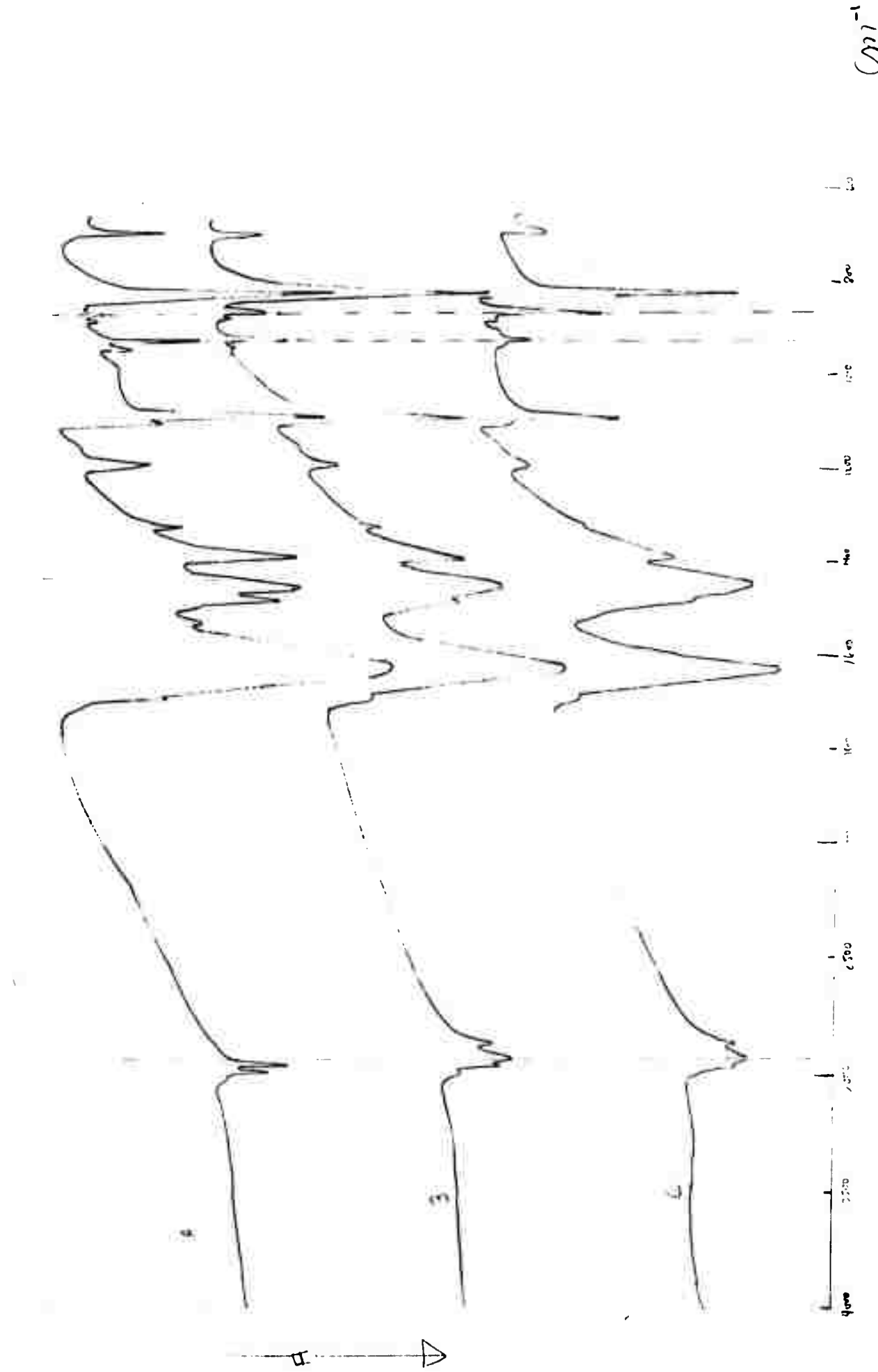


FIGURE 35. INFRARED SPECTRA OF THE  $\text{NaHCO}_3$  IN  $\text{CH}_3\text{OH}$  PRODUCT AFTER STANDING IN AIR FOR (A) 3 DAYS, (B) 5 DAYS, AND (C) 7 DAYS

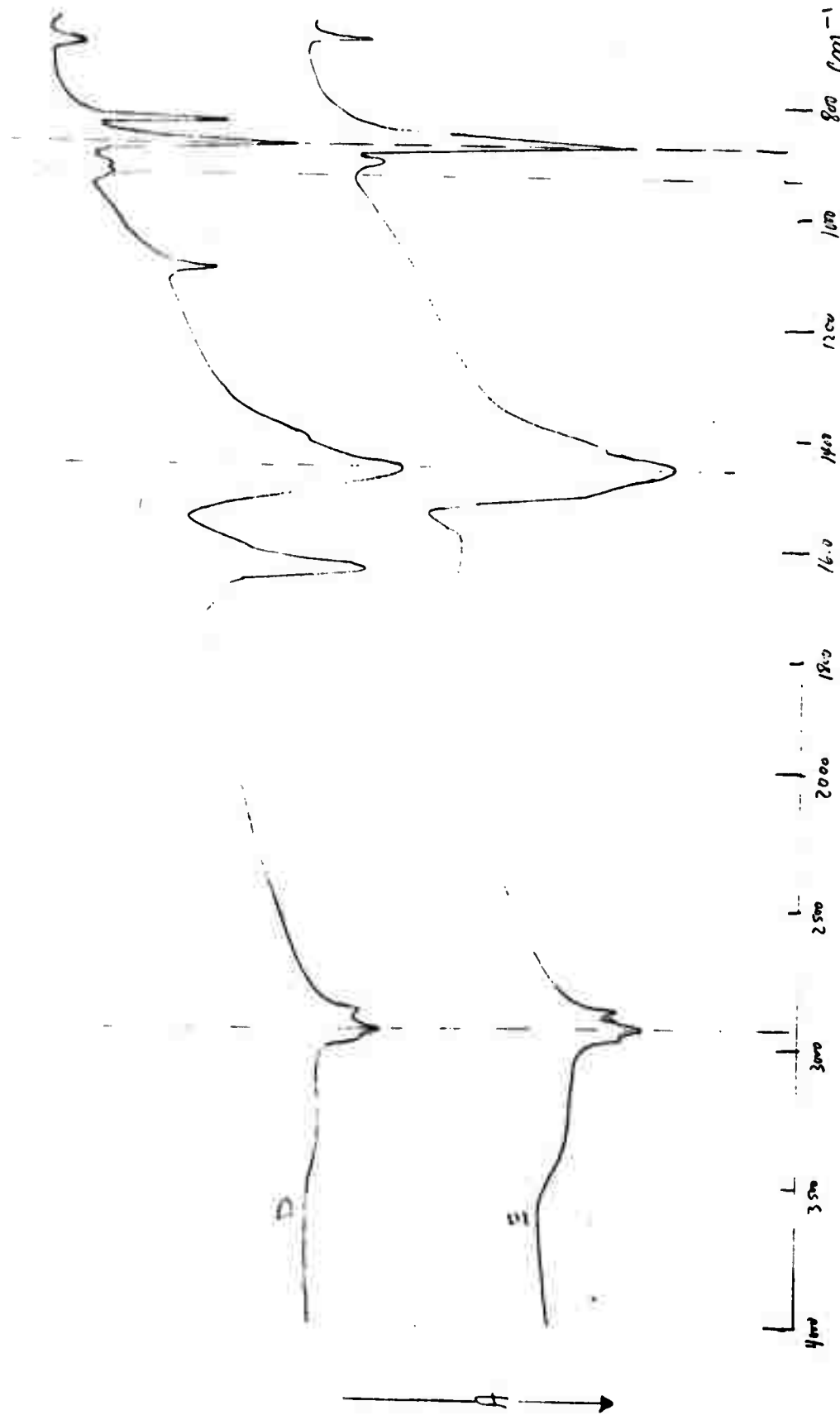


FIGURE 36. INFRARED SPECTRA OF THE  $\text{NaHCO}_3$  IN  $\text{CH}_3\text{OH}$  PRODUCT AFTER STANDING IN AIR FOR (D) 10 DAYS AND (E) 24 DAYS

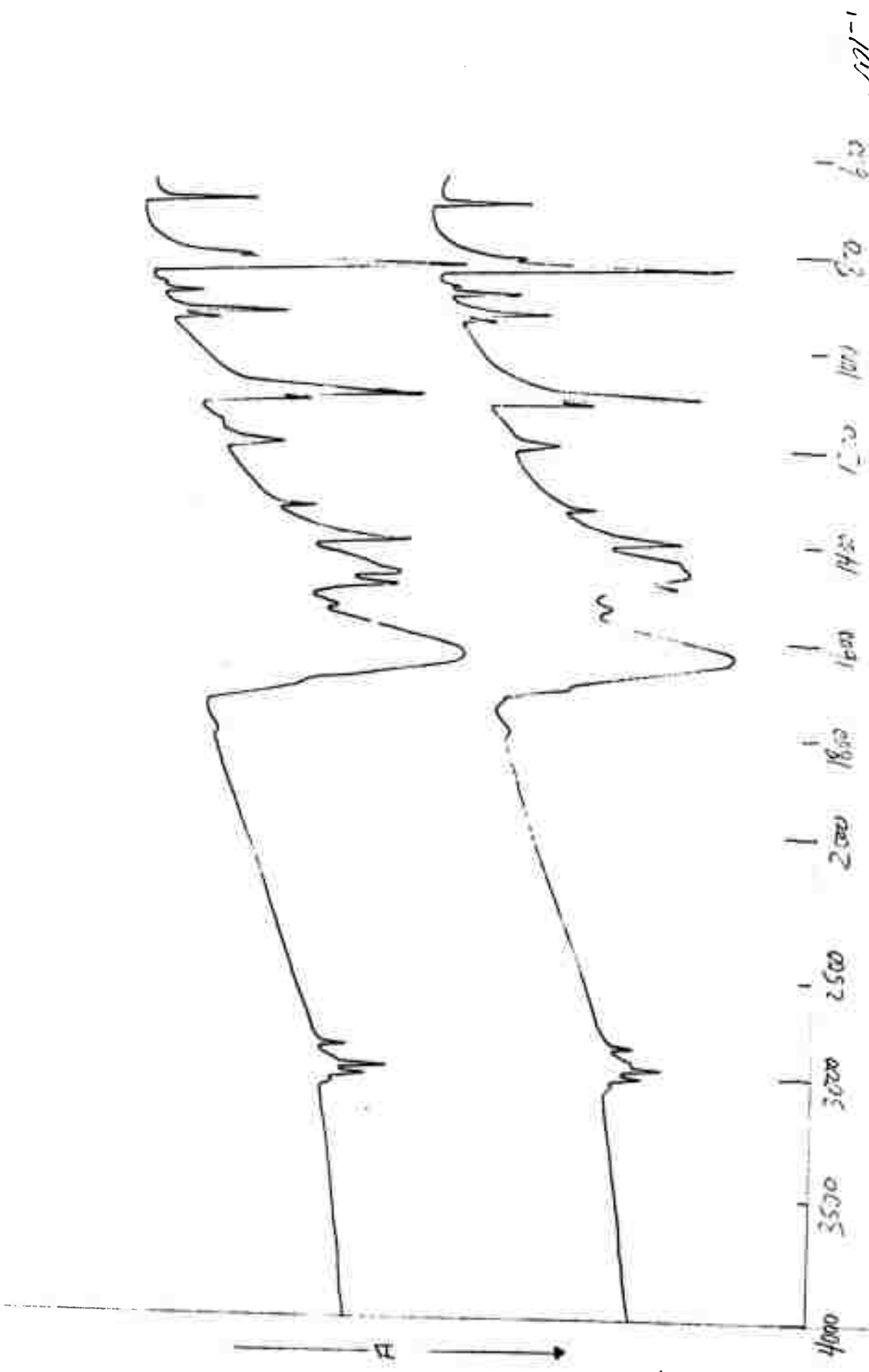


FIGURE 37. INFRARED SPECTRA OF THE  $\text{NaLiCO}_3$  IN  $\text{CH}_3\text{OH}$  PRODUCT AFTER STANDING IN A VACUUM FOR 3 DAYS (TOP) AND 7 DAYS (BOTTOM)

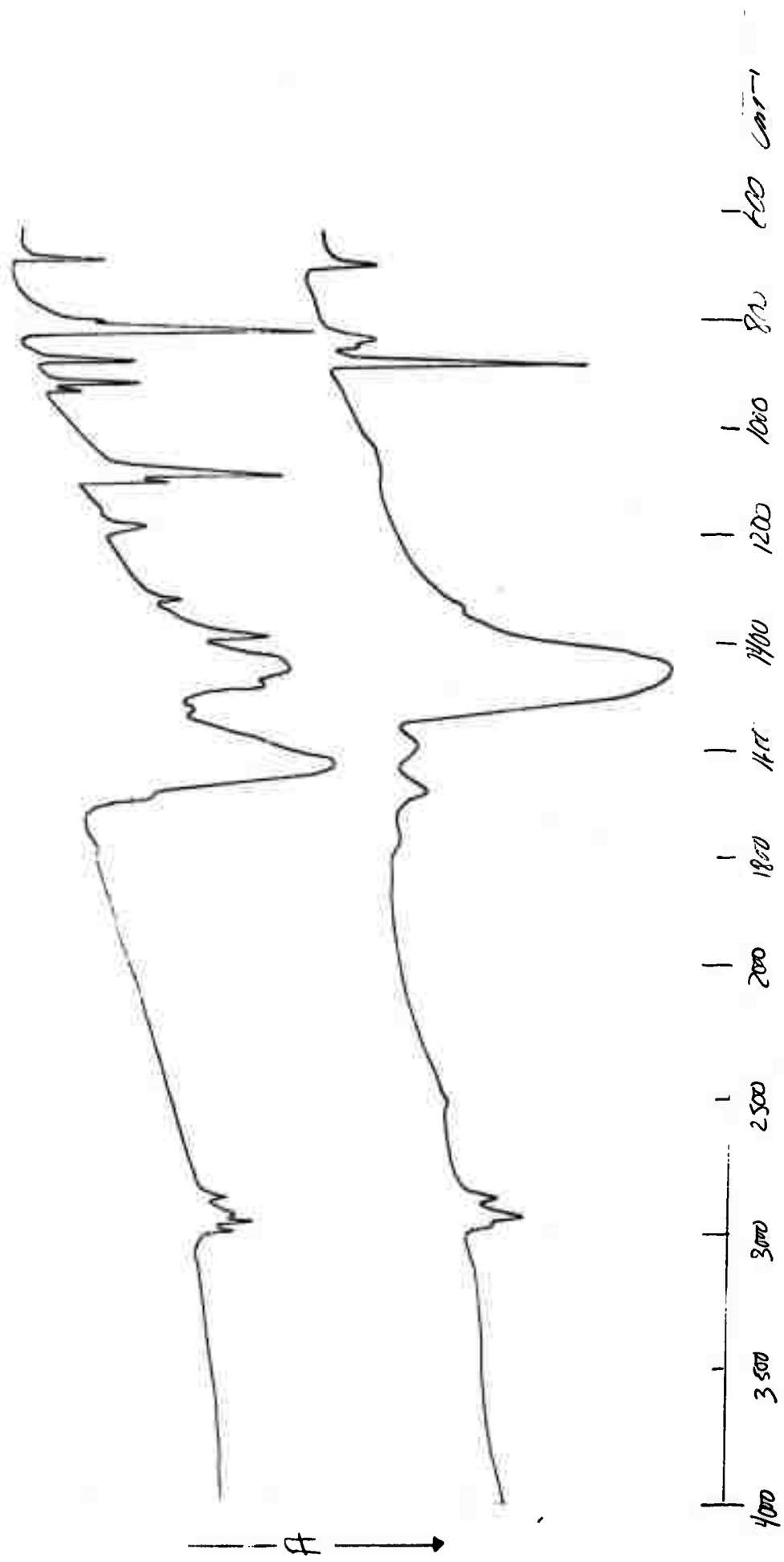


FIGURE 38. INFRARED SPECTRA OF THE  $\text{NaHCO}_3$  IN  $\text{CH}_3\text{OH}$  PRODUCT AFTER STANDING IN A VACUUM  
FOR 12 DAYS (TOP) AND 24 DAYS (BOTTOM)

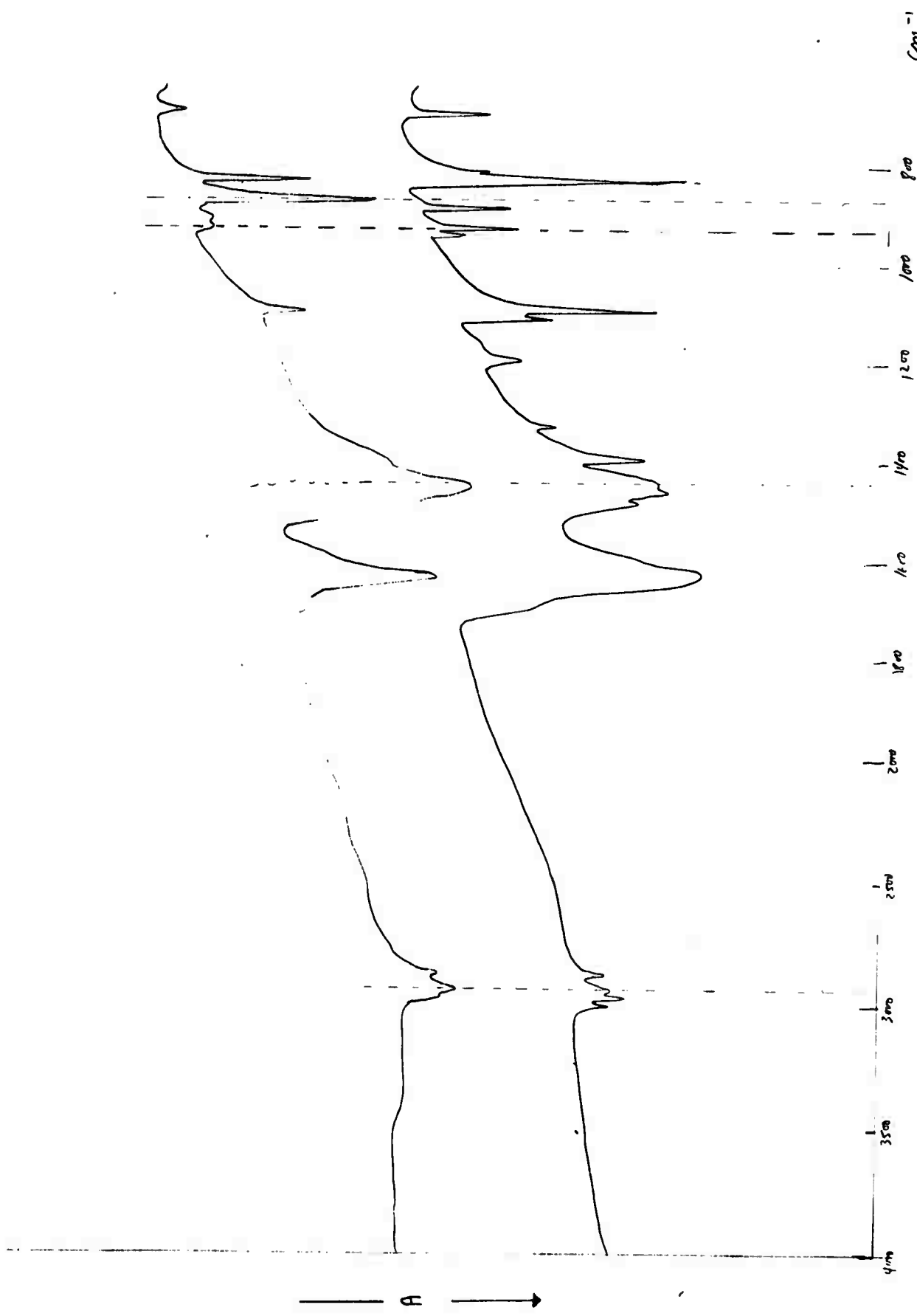


FIGURE 39. INFRARED SPECTRA OF THE  $\text{NaHCO}_3$  IN  $\text{CH}_3\text{OH}$  PRODUCT AFTER STANDING 10 DAYS IN AIR (TOP) AND 10 DAYS IN A VACUUM (BOTTOM)

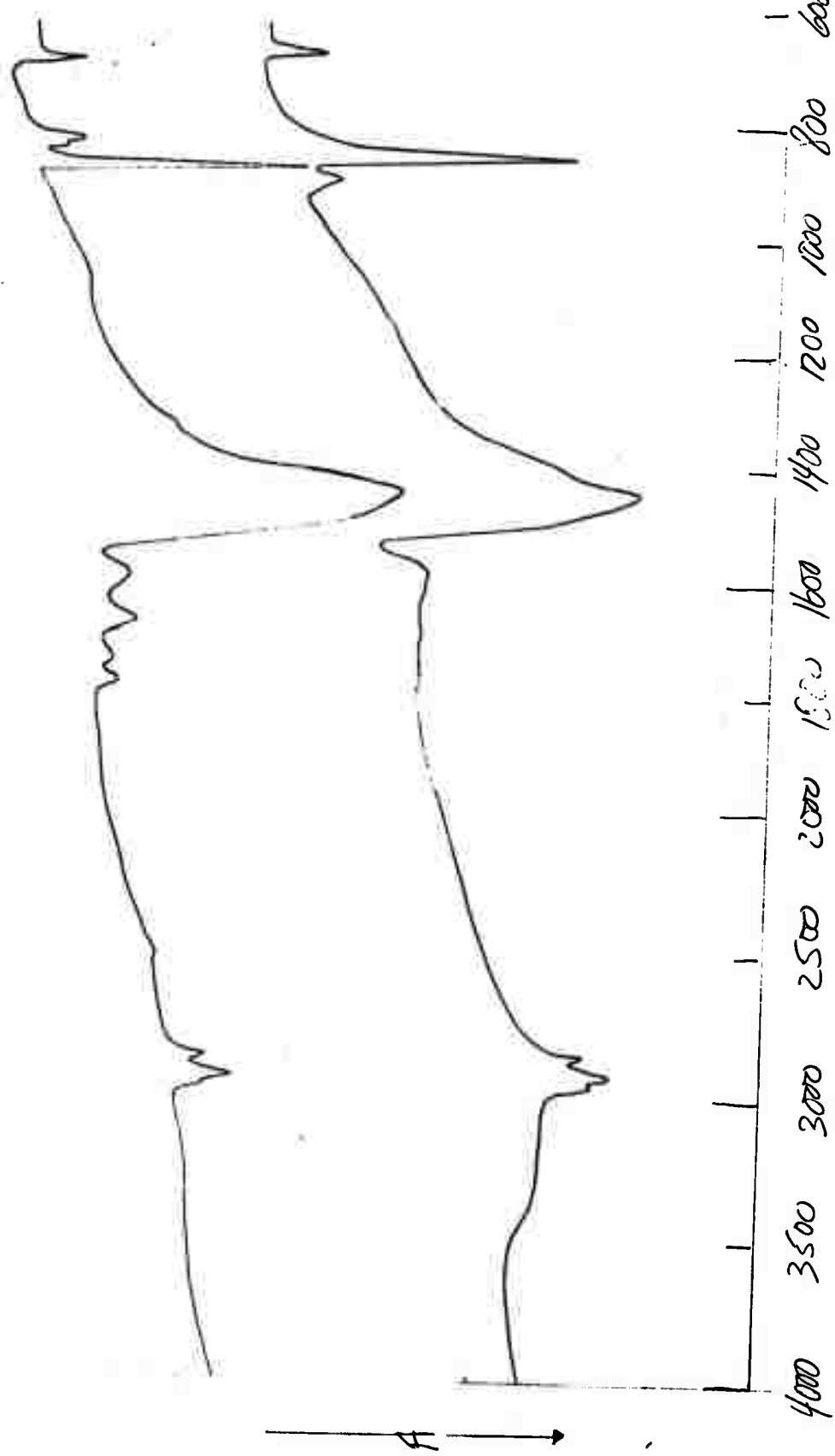


FIGURE 40. INFRARED SPECTRA OF THE NaHCO<sub>3</sub> IN CH<sub>3</sub>OH PRODUCT AFTER STANDING 24 DAYS IN AIR (TOP) AND 24 DAYS IN A VACUUM (BOTTOM)

to a different carbonate probably different polymorphic forms or species containing a different amount of water of hydration.

### Extraction

A fresh sample of the  $\text{NaHCO}_3$  in  $\text{CH}_3\text{OH}$  product was prepared, the spectrum of which is shown in Figure 41 (top). This sample was allowed to stand in air for a period of about 21 days. The spectrum of this 21 day old sample is shown in Figure 41 (bottom). From this spectrum it can be seen that while there is still some of the original sample left most of it had decomposed to sodium carbonate. Also not as much of the CH component ( $2940 \text{ cm}^{-1}$ ) was formed as in some of the previous samples (Figure 36E and 38, bottom). At this point (after 21 days), the sample was extracted first with  $\text{CCl}_4$  and then with  $\text{CHCl}_3$ . The spectra of the residue from the  $\text{CHCl}_3$  extract and the  $\text{CCl}_4$  extract are shown in Figure 42, top and bottom respectively. Only a small amount of residue was present in each extraction. While the spectrum of the  $\text{CCl}_4$  extract only shows weak absorptions, it is significant to note that only organics (as shown by the CH absorption near  $2900 \text{ cm}^{-1}$ ) are present, and these organics are hydrocarbon in nature with no polar groups (no C-O absorptions). The residue from the  $\text{CHCl}_3$  extract shows both  $\text{Na}_2\text{CO}_3$  absorptions and absorptions from the  $\text{NaHCO}_3$  in  $\text{CH}_3\text{OH}$  product. However the CH bands (near  $2900 \text{ cm}^{-1}$ ) are much stronger than in the original sample indicating extraction of a hydrocarbon-like material.

The residues from the  $\text{CCl}_4$  and  $\text{CHCl}_3$  extracts were combined and subjected to mass spectral analysis. The sample was heated at a programmed rate and high resolution mass spectra were taken at various temperatures. These mass spectra near 50 C, near 150 C, and 200 C are shown in Figures 43, 44, and 45 respectively. The primary difference seen in these figures is the expected one - as the temperature is raised more fragments of higher mass numbers are detected. However the important facts to be learned from the mass spectral data are not clearly apparent from the figures. The high resolution capability coupled with a computer programmed to handle these high resolution data allows one to predict the most probable empirical formula for each observed mass peak. From these empirical formulas it can be definitely shown that these samples are primarily a complex mixture of hydrocarbon (only C and H) of varying chain length ranging up to  $\text{C}_{20}$ . A small percentage (no greater than 10 percent) are fragments containing C, H, and O. At 40 C most of the hydrocarbon fragments are  $\text{C}_{12}$  or lower, while at 150 and 200 the fragments range upwards to  $\text{C}_{20}$ . Mass spectral data alone do not establish definitely that any of the hydrocarbon fragments are unsaturated, but the infrared data (Figures 35 and 36) makes some unsaturation appear highly likely. Thus the  $\text{NaHCO}_3$  in  $\text{CH}_3\text{OH}$  product (which originally contains only methyl groups) goes through a decomposition mechanism which involves converting  $\text{CH}_3$  groups to  $\text{CH}_3(\text{CH}_2)$  - hydrocarbon chains, some of which are likely unsaturated hydrocarbons.

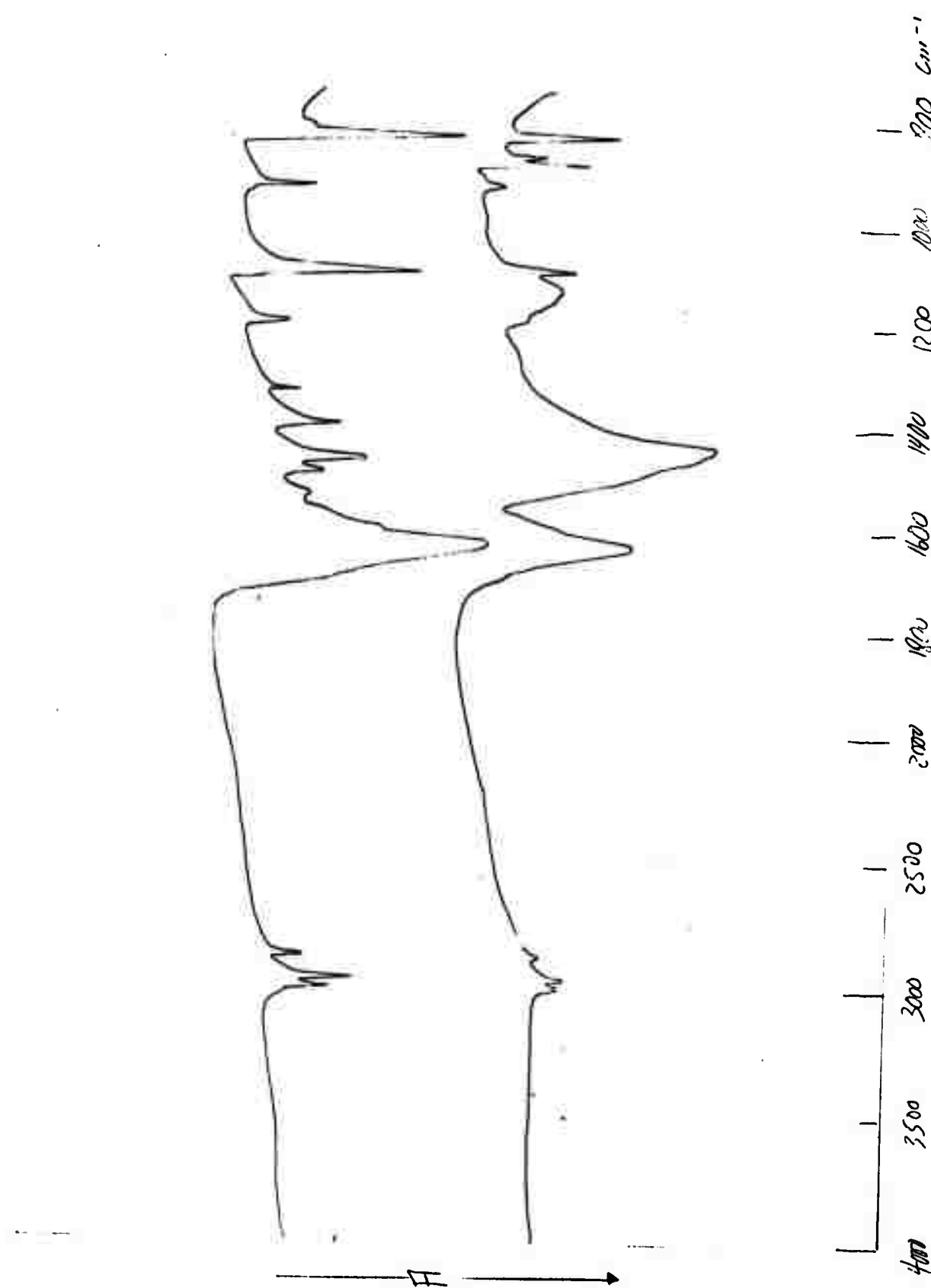


FIGURE 41. INFRARED SPECTRA OF THE NaHCO<sub>3</sub> IN CH<sub>3</sub>OH PRODUCT FRESH SAMPLE (TOP) AND AFTER 21 DAYS IN AIR (BOTTOM)

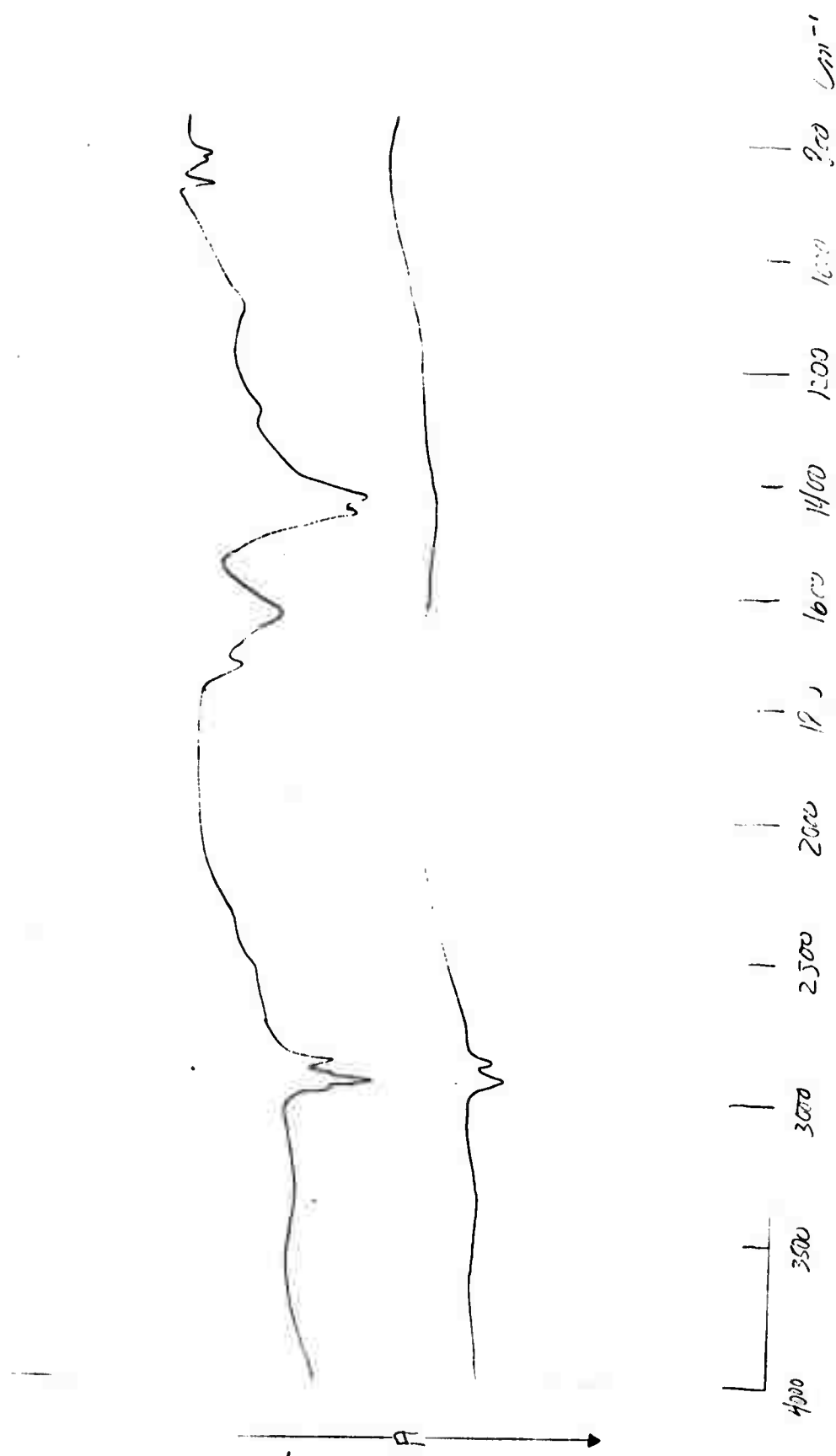


FIGURE 42. INFRARED SPECTRA OF THE NaHCO<sub>3</sub> IN CH<sub>3</sub>OH PRODUCT AFTER STANDING 21 DAYS IN AIR RESIDUE FROM CHCl<sub>3</sub> EXTRACT (TOP) AND RESIDUE FROM CCl<sub>4</sub> EXTRACT (BOTTOM)

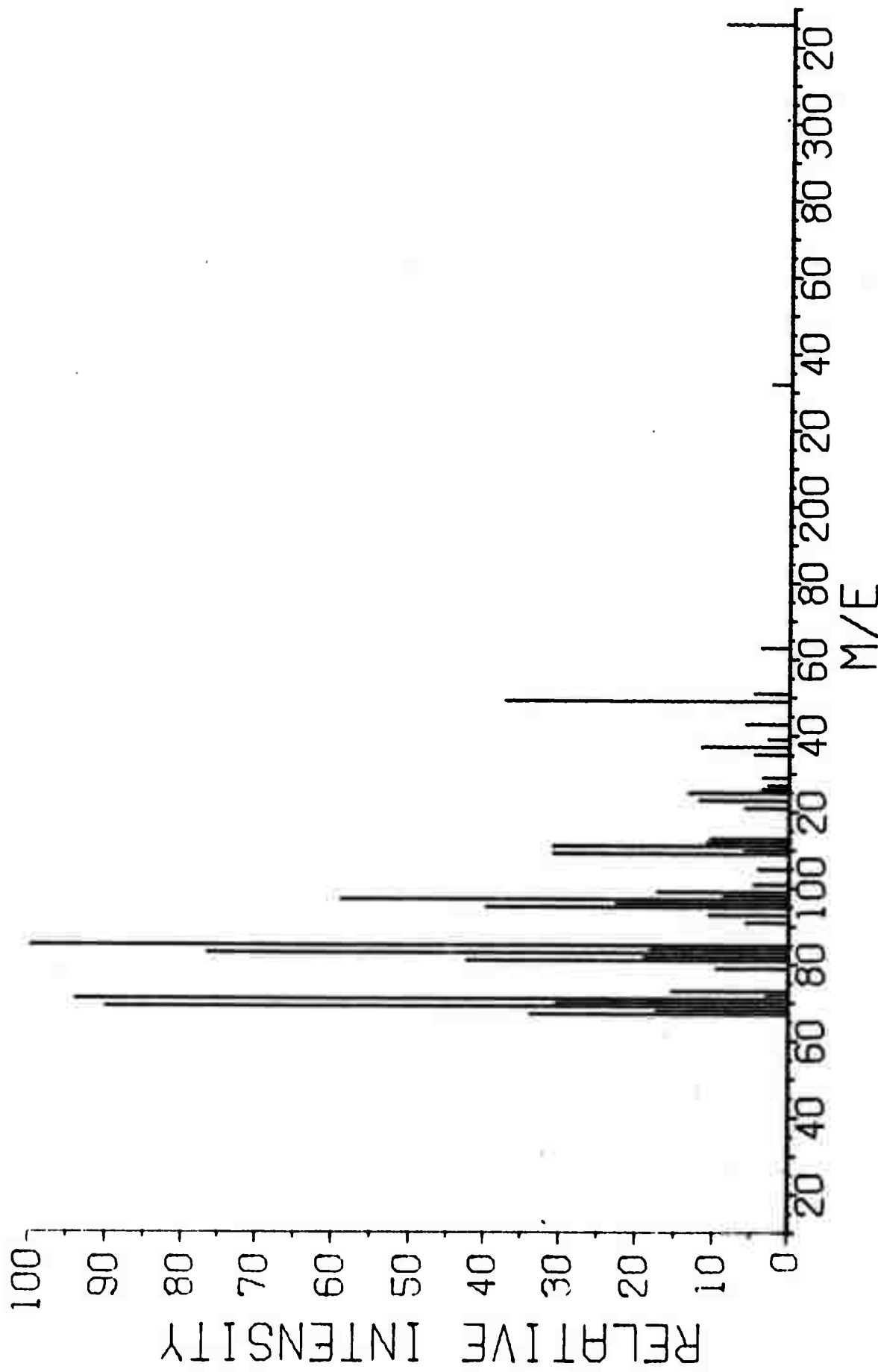


FIGURE 43. MASS SPECTRA OF THE RESIDUE FROM THE  $\text{CHCl}_3$  AND  $\text{CCl}_4$  EXTRACTS OF THE  $\text{NaHCO}_3$  IN  $\text{CH}_3\text{OH}$  PRODUCT AT 50°C

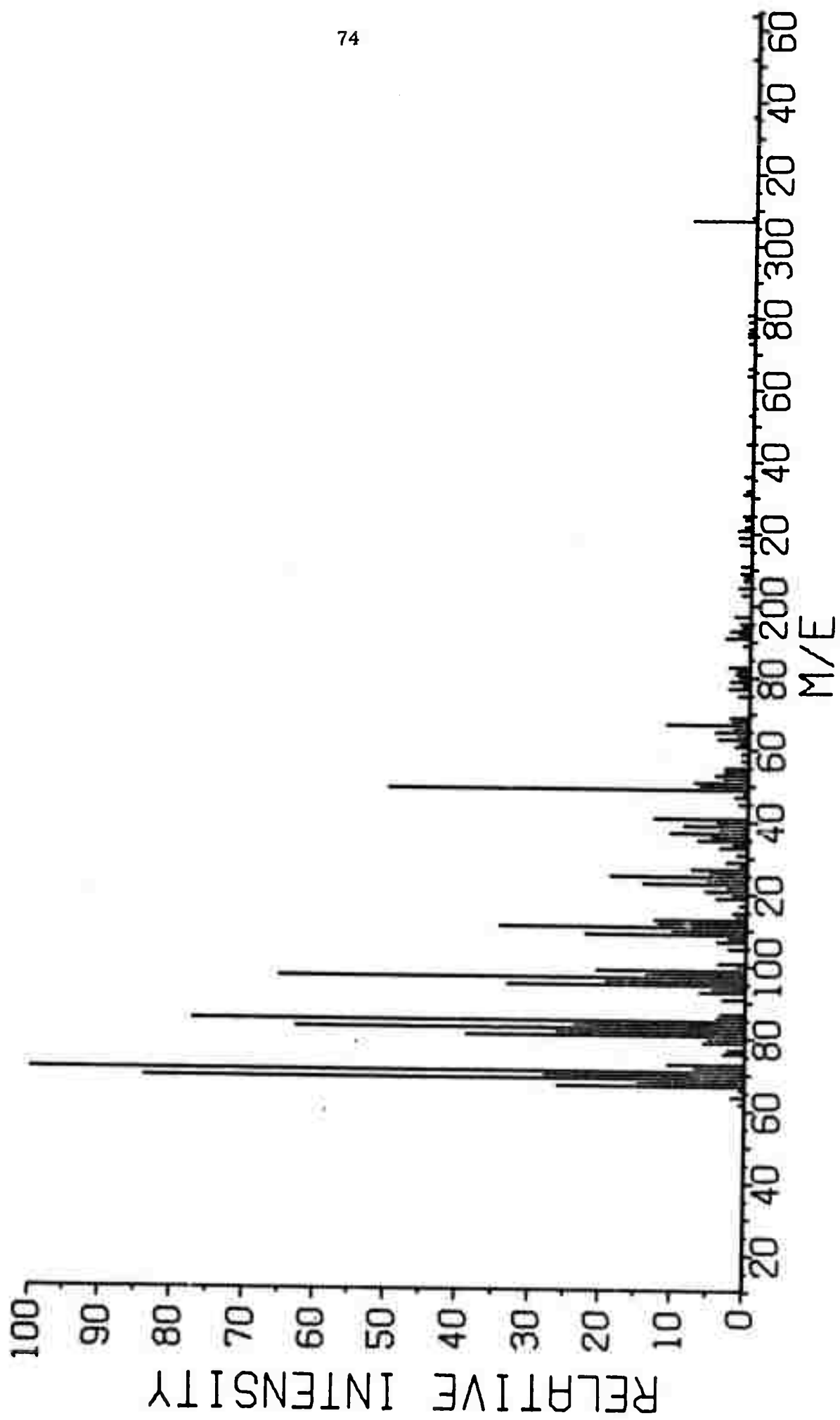


FIGURE 44. MASS SPECTRA OF THE RESIDUE FROM THE  $\text{CHCl}_3$  AND  $\text{CCl}_4$  EXTRACTS OF THE  $\text{NaLiCO}_3$  IN  $\text{CH}_3\text{OH}$  PRODUCT AT 150°C

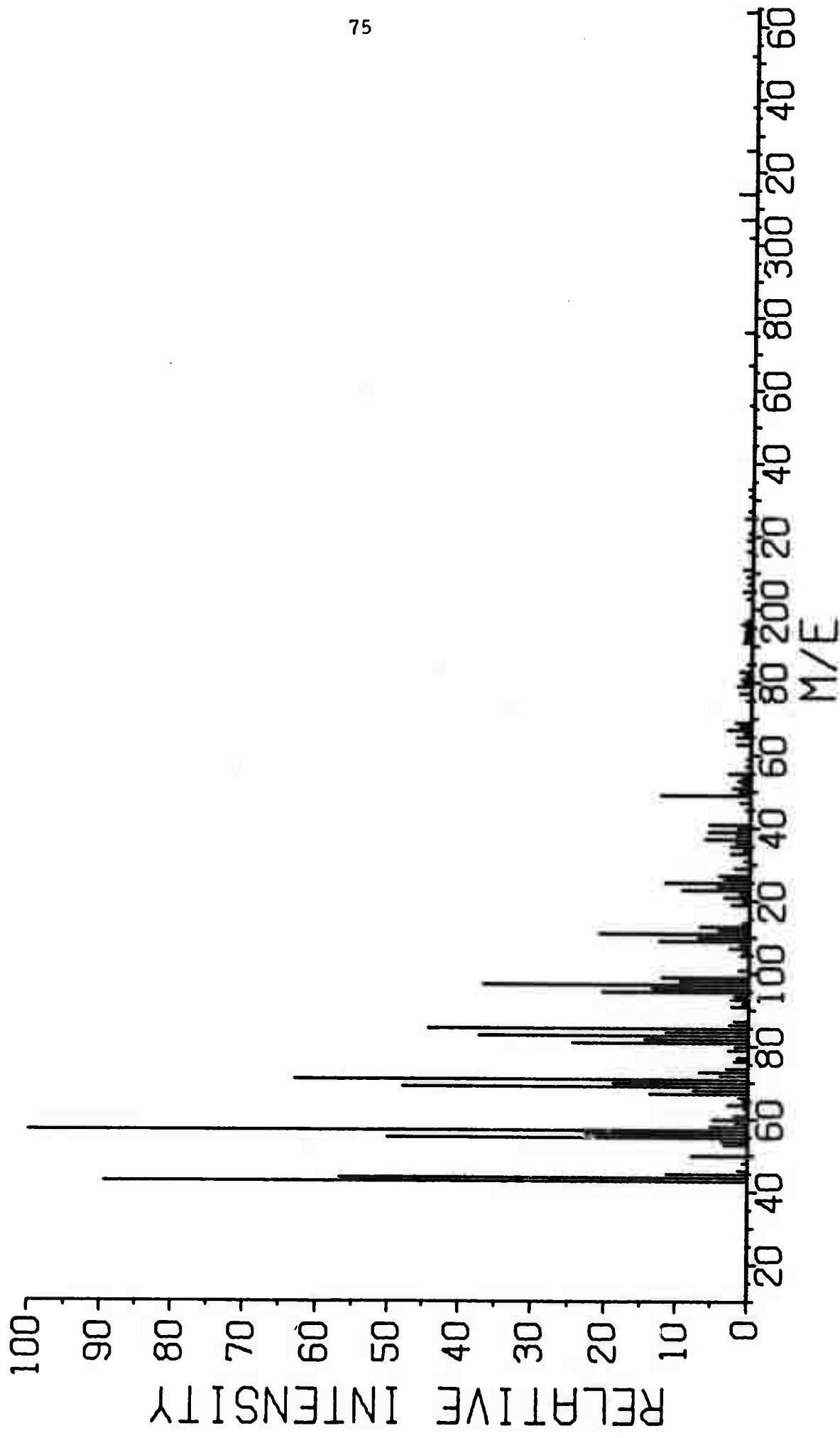


FIGURE 45. MASS SPECTRA OF THE RESIDUE FROM THE  $\text{CHCl}_3$  AND  $\text{CCl}_4$  EXTRACTS OF THE  $\text{NaIK(O}_2\text{)}_3$  IN  $\text{CH}_3\text{OH}$  PRODUCT AT 200°C

DISCUSSION

The results of this research lead to two important and major conclusions: (1) even though the infrared spectrum of anomalous water is not completely explained, the qualitative similarity of the elemental composition of the various water washes and preparations demonstrates that the material that has been called "anomalous water" consists mainly of material extracted from glass and residues from the water itself and (2) the chemistry of the formation and decomposition of the  $\text{NaHCO}_3$  in  $\text{CH}_3\text{OH}$  product coupled with some of the analytical results of the anomalous water research indicates the probability of the occurrence of unusual chemical reactions occurring in water-glass systems which may be of major importance.

The infrared spectrum of anomalous water consists of three absorption band complexes: one near  $1600 \text{ cm}^{-1}$ , one near  $1400 \text{ cm}^{-1}$ , and one in the  $1000-1150 \text{ cm}^{-1}$  region. The elemental composition detected for the various water washes and anomalous water preparations have established that the observed infrared frequencies between  $1040$  and  $1090 \text{ cm}^{-1}$  arise from Si-O vibrations and those between  $1120$  and  $1140 \text{ cm}^{-1}$  are S-O frequencies. In the  $1400 \text{ cm}^{-1}$  range, the frequencies above  $1400 \text{ cm}^{-1}$  could be explained as carbonate vibrations and those below  $1400 \text{ cm}^{-1}$  (near  $1360 \text{ cm}^{-1}$ ) as nitrate frequencies. The detection of carbon in all samples combined with the infrared evidence support the presence of carbonates and the identification of  $\text{H}_2\text{O-CP-3}$  as primarily sodium nitrate helps support the nitrate concept. This leaves the frequencies near  $1600 \text{ cm}^{-1}$  as the only infrared band to be explained. The infrared spectrum of the  $\text{NaHCO}_3$  in  $\text{CH}_3\text{OH}$  product shows a strong  $1620 \text{ cm}^{-1}$  frequency. Although this compound has not yet been isolated from the anomalous water material, it is certain that carbonates or derivatives of carbonates do exist in the anomalous water system. This coupled with the fact that hydrocarbons have always been detected in the preparations and the decomposition behavior of the  $\text{NaHCO}_3$  in  $\text{CH}_3\text{OH}$  product, suggests that a compound with a strong  $1600 \text{ cm}^{-1}$  band is present in the anomalous water system. Thus most of the infrared spectrum of anomalous water can be explained with assurance and reasonable suggestions can be advanced to explain the rest of the spectrum. None of the species postulated involve a form of water.

However, the single most important fact arguing against anomalous water being a form of water is that every water washing (whether of capillary tubes, crushed glass, or glass wool) and every preparation of anomalous water (whether from cleaned or uncleaned tubes) give similar infrared spectra and have qualitatively similar chemical constituents. It is impossible to believe that this arises from any cause other than the combination of extraction of materials from glass and the residue of water itself.

As stated previously, all preparations of anomalous water showed the presence of small amounts of organic material in the form of  $\text{CH}_2$  and  $\text{CH}_3$  groups. Other workers<sup>(4)</sup> have postulated that these organics resulted from the absorption of perspiration aerosols by glass. Under the "clean" conditions of our experiments this seemed unlikely. The behavior of the  $\text{NaHCO}_3$  in  $\text{CH}_3\text{OH}$  product offers another

explanation. Since during the decomposition of the  $\text{NaHCO}_3$  product, it has been shown that  $\text{CH}_3$  groups are converted to  $\text{CH}_3(\text{CH}_2)_2$  chains, it is possible arguing by analogy that carbon on glass can also be converted to hydrocarbon groups. Thus the isolation and study of the chemistry of this species could be of immense importance in many areas of science.

REFERENCES

- (1) T. F. Page, Jr., and R. J. Jakobsen, *J. Col. and Interface Science*, 36, 427 (1971).
- (2) Various speakers at the International Symposium on Anomalous Water, Lehigh University, June, 1970.
- (3) W. J. O'Brien, *Surface Science*, 25, 298 (1971).
- (4) D. L. Rousseau, *Science*, 171, 170 (1971); R. E. Davis, D. L. Rousseau and R. O. Board, *Science*, 171, 167 (1971); S. W. Rabideau and A. E. Florin, *Science*, 169, 48 (1970).
- (5) T. F. Page, Jr., and R. J. Jakobsen, unpublished work.
- (6) E. R. Lippincott, private communication.

APPENDIX A - SAMPLE NOTATION

LW-H <sub>2</sub> O-00	Blank, the residue obtained from just the water used for the liquid washings.
LW-H <sub>2</sub> O-01	First system blank for the liquid washings with water, i.e., water extract of baking dish, flask, and vial.
LW-H <sub>2</sub> O-02	Second system blank for the liquid washings with water.
LW-H <sub>2</sub> O-1	First liquid washing of pyrex capillary tubes with water.
.	.
.	.
.	.
LW-H <sub>2</sub> O-15	Fifteenth liquid washing of the same pyrex capillary tubes with water.
H <sub>2</sub> O-CP-1	First preparation of anomalous material from water using the cleaned pyrex tubes from LW-H <sub>2</sub> O-15.
.	.
.	.
.	.
.	.
H <sub>2</sub> O-CP-8	Eighth preparation of anomalous material from water using the same cleaned pyrex tubes as in H <sub>2</sub> O-CP-1.
H <sub>2</sub> O-UP-1	First preparation of anomalous material from water using uncleaned pyrex tubes.
.	.
.	.
.	.
H <sub>2</sub> O-UP-7	Seventh preparation of anomalous material from water using uncleaned pyrex tubes.
H <sub>2</sub> O <sub>2</sub> -P-1	First preparation of anomalous material from a 3 percent H <sub>2</sub> O <sub>2</sub> solution using pyrex tubes.
H <sub>2</sub> O <sub>2</sub> -P-1H	Sample H <sub>2</sub> O <sub>2</sub> -P-1 after heating in air at 400 C for 60 minutes.
LW-Pr-00	Blank, the residue obtained from just the propanol-1 used for the liquid washings.
LW-Pr-01	Blank, a propanol-1 extract of Saran wrap.

LW-Pr-1	First liquid washing of pyrex capillary tubes with propanol-1.
LW-Pr-2	Second liquid washing of pyrex capillary tubes with propanol-1.
VW-H <sub>2</sub> O-1	First vapor washing of pyrex capillary tubes with steam.
.	.
.	.
.	.
VW-H <sub>2</sub> O-12	Twelfth vapor washing of pyrex capillary tubes with steam.
CG-N-1	First water extraction of Nonex crushed glass.
CG-7052-1	First water extraction of 7052 crushed glass.
CG-C-1	First water extractoin of cobalt crushed glass.
CG-P-1	First water extraction of pyrex crushed glass.
CG-U-1	First water extraction of uranium crushed glass.
CG-V-1	First water extraction of Vycor crushed glass.
CG-Q-1	First water extraction of quartz crushed glass.
CG-H <sub>2</sub> O-01	Blank, residue from water extraction of flask used for crushed glass extractions.
GW-H <sub>2</sub> O-1	Blank, residue from water extraction of flask used for glass wool extractions.
GW-H <sub>2</sub> O-2	Second blank, residue from water extractions of flask used for glass wool extractions.
GW-P-H <sub>2</sub> O-1	First water extraction of pyrex glass wool.
GW-P-H <sub>2</sub> O-2	Second water extraction of pyrex glass wool.
GW-Q-H <sub>2</sub> O-1	First water extraction of quartz glass wool.
GW-Q-H <sub>2</sub> O-2	Second water extraction of quartz glass wool.

## APPENDIX B

TABLE B-1. NUMERICAL VALUES FOR THE RANGE OF THE RELATIVE INTENSITY DISTRIBUTION FROM ELECTRON MICROPROBE ANALYSIS

Sample	B	N <sub>a</sub>	C	Mg	O	K	Ca	C <sub>1</sub>	S	Si
W-H <sub>2</sub> O-1	0/15	125/160	50/200	25/160	800/1350	180/350	50/270	180/300, 500/1400S	50/250, 200/650S	200/700
W-H <sub>2</sub> O-2 Edge	0/5	80/225	100/350	20/50	380/850	50/125	25/120	50/1500	25/75	25/300
W-H <sub>2</sub> O-1 Edge	9/18	90/200	10/300	25/50	600/850	250/400	20/120S	600/1000S	120/350	25/130S
W-H <sub>2</sub> O-1 Inside	5/15	90/200	80/160	35/50	?	400/600C	20/100, 350S	1300/2500C	40/130, 250S	20/120, 350S
W-H <sub>2</sub> O-2 Edge	0/7	36/125	30/160	1/20	100/700	5000/6500CR	0/25	50/100	10/20	10/30
W-H <sub>2</sub> O-12 Edge	0/7	120/250	60/130	20/80	425/900	10/150	10/125	100/425	25/240	50/720
W-H <sub>2</sub> O-13 Edge	0, 7	80/200	50/100	50/120	450/700	50/235	25/350S	55/350E, 900/2200S	25/150	50/200
W-H <sub>2</sub> O-14 Edge	5/8	80/210S	80/130	10/35	400/1000	40/200	25/125	300/1300S	50/140	1000/1100E
W-H <sub>2</sub> O-14 Inside	1/5	60/180	60/110	8/20	190/350	20/40	0/5	50/350S	10/25	10/50
H <sub>2</sub> O-CP-1 Edge	1/5	100/300	80/280	50/250	500/800	200/420	160/460	100/500, 3000S	100/380	50/400, 600S
H <sub>2</sub> O-CP-1 Inside	1/5	180/300	150/350	20/65	500/700	100/300	10/30	50/150, 1460/3600S	100/380	15/33, 600S
H <sub>2</sub> O-CP-2 Edge	0/5	100/300	150/190	25/80	400/630	100/500	0/15	75/480	100/535	100/535
H <sub>2</sub> O-CP-3 Edge	0/5	50/175	130/450	50, 110	300/450	120/200, 375S	40/100, 160S	100/500	50/150	10/120
H <sub>2</sub> O-CP-1 Edge	"	40/200	125/340	50/260	200/850	100/180	100/600	120/320, 500/1900S	150/430	60/260
H <sub>2</sub> O-CP-2 Edge	0/5*	175/320,	200/350	40/75,	550/825,	60/150	15/40, 25/50E	200/1000, 3000S	100/550	40/12, 1000S
H <sub>2</sub> O-CP-1 Edge	0/5	25/325E	50/125E	650/1000E	290/550	300/700	10, 150	450/800	300/500	40/225, 400/1100E
H <sub>2</sub> O-2P-1 Inside	0/5	75/250	50/170	50/300	350/450	550/1300	45/60	300/760	200/550	25/40
H <sub>2</sub> O-2P-1H Black	0/5	50/100	100/950S	100/450S	200/900S	100/700S	50/250	50/1800S	90/400	120/1800S
H <sub>2</sub> O-2P-1H White	0/5	30/200	10/120	50/180	400/900E	100/450	15/250	120/350	100/550	20/50
W-Pr-1 Inside	0/7	25/320S	750/1700	5/25, 225S	60/160	30/140	0/15	300/600, 300/400CS	25/70	300/1250S
W-Pr-1 Inside	0/7	60/375S	300/1500	0/25, 175S	50/125, 900/	15/45	0/16, 65S	25/200, 400/2800S	10/65	600/1600S
Al Plate Blank Inside	0/2	0/5	9/15	0/15	30/90	10/12	0/5	0/3	0/5	0/5

NOTE: S = Spots or Particles

E = Edge

C = Center

CR = Large Crystals

## APPENDIX C

TABLE C-1. WEIGHTS (uG) OF ELEMENTS DETECTED BY EMISSION SPECTROGRAPHIC ANALYSIS

	Ba	B	Si	Mn	Fe	Mg	Sn	Ni	Al	Cu	Na	Ti	Ca	Cr	K	Co	Sb	As	Wt.	Wt.	
Li-W-H <sub>2</sub> O-1	2.6	15.0	10.0	<0.1	0.2	<0.5	<0.1	1.0	0.1	50.0	<0.1	5.0	<0.1	<50.0	--	--	--	--	136.2	36.2	
Li-W-H <sub>2</sub> O-2	6.1	3.0	3.0	<0.1	0.1	<0.5	<0.1	0.2	0.1	>100.0	<0.1	3.0	<0.1	>100.0	--	--	--	--	>210.7	>110.7	
Li-W-H <sub>2</sub> O-12	<0.1	6.2	2.0	<0.1	<0.1	<0.5	<0.1	0.1	<0.1	<1.0	<0.1	1.0	<0.1	<50.0	--	--	--	--	55.8	5.8	
Li-W-H <sub>2</sub> O-13	<0.1	0.3	2.0	<0.1	0.3	<0.5	<0.1	<0.1	<0.1	<0.1	<0.1	1.0	<0.1	<50.0	--	--	--	--	55.8	5.8	
Li-W-H <sub>2</sub> O-14	<0.1	2.6	5.0	<0.1	<0.1	<0.5	<0.1	0.2	<0.1T	10.0	<0.1	1.0	<0.1	<50.0	--	--	--	--	55.0	5.0	
Li <sub>2</sub> O-CP-1	<0.1	0.3	2.0	<0.1	0.1	0.5	<0.1	0.2	<0.1T	20.0	<0.1	2.0	<0.1	<50.0	--	--	--	--	68.9	18.9	
Li <sub>2</sub> O-CP-2	0.2	3.0	26.0	<0.1	1.0	<0.5	1.0	3.0	<0.1	30.0	<0.1	5.0	<0.1	10.0	<0.5	<0.1	<0.1	<0.1	73.7	63.7	
Li <sub>2</sub> O-CP-3	0.1	1.0	16.6	<0.1	1.0	<0.5	<0.1	1.0	0.3	20.0	<0.1	5.0	<0.1	2.0	<0.1	<0.1	<0.1	<0.1	43.6	41.6	
Li <sub>2</sub> O-CP-4	<0.1	5.0	10.0	<0.11T	0.5	<0.5	0.1	0.1	<0.1	30.0	<0.1	5.0	<0.1	<50.0	--	--	--	--	76.7	26.7	
Li <sub>2</sub> O-CP-5	0.1	1.4	7.0	<0.1	0.3	<0.5	<0.1	0.5	<0.1	10.0	<0.1	2.0	<0.1	1.0	<0.1	<0.1	<0.1	<0.1	24.2	23.2	
Li-W-H <sub>2</sub> O-1	<0.1	2.0	5.0	<0.1	<0.1T	0.5	<0.1	0.1	<0.1T	1.0	<0.1	1.0	<0.1	<50.0	--	--	--	--	66.9	16.9	
Li-W-H <sub>2</sub> O-2	<0.1	1.1	1.0	<0.1	<0.1	<0.5	<0.1	<0.1	<0.1T	<1.0	<0.1	0.3	<0.1	<1.0T	<0.1	<0.5	<1.0	<1.0	107.6	57.6	
Li-W-H <sub>2</sub> O-6	<0.1	0.1	0.1	<0.1	0.1	0.02	<0.5	<0.1	<0.1	30.0	<0.1	2.0	<0.1	1.0	<0.1	<0.1	<0.1	<0.1	52.6	2.6	
Li <sub>2</sub> O-CP-1	0.1	2.0	5.0	<0.1	<0.1T	0.5	<0.5	<0.1	0.2	<0.1T	1.0	<0.1	1.0	<0.1	<50.0	--	--	--	--	66.9	16.9
Li <sub>2</sub> O-CP-2	<0.1	1.0	1.0	<0.1	<0.1	<0.2	<0.5	<0.1	<0.1	<0.1T	<1.0	<0.1	0.3	<0.1	<1.0T	<0.1	<0.5	<1.0	<1.0	107.6	57.6
Li <sub>2</sub> O-CP-3	<0.1	0.1	0.1	<0.1	0.1	0.02	<0.5	<0.1	<0.1	10.0	<0.1	2.0	<0.1	1.0	<0.1	<0.1	<0.1	<0.1	24.2	23.2	
Li <sub>2</sub> O-CP-4	<0.1	1.0	1.0	<0.1	<0.1	0.5	<0.1	0.1	<0.1T	1.0	<0.1	1.0	<0.1	<50.0	--	--	--	--	66.9	16.9	
Li <sub>2</sub> O-CP-5	<0.1	0.1	0.1	<0.1	0.1	0.02	<0.5	<0.1	<0.1	<0.1T	<1.0	<0.1	0.3	<0.1	<1.0T	<0.1	<0.5	<1.0	<1.0	107.6	57.6
Li <sub>2</sub> O-CP-6	<0.1	0.1	0.1	<0.1	0.1	0.02	<0.5	<0.1	<0.1	10.0	<0.1	2.0	<0.1	1.0	<0.1	<0.1	<0.1	<0.1	65.5	5.5	
Li <sub>2</sub> O-CP-7	<0.1	2.0	5.0	<0.1	<0.1	0.5	<0.1	0.1	<0.1T	1.0	<0.1	1.0	<0.1	<50.0	--	--	--	--	52.6	2.6	
Li <sub>2</sub> O-CP-8	<0.1	1.0	1.0	<0.1	<0.1	0.5	<0.1	0.1	0.2	5.0	<0.1	5.0	<0.1	<0.5	<1.0	<0.5	<1.0	<1.0	24.0	10.0	
Li <sub>2</sub> O-CP-9	<0.1	1.0	1.0	<0.1	<0.1	0.5	<0.5	<0.1	0.5	<0.1T	2.0	<0.1	3.0	<0.1	<1.0	<0.1	<0.5	<1.0	23.3	22.3	
Li <sub>2</sub> O-CP-10	<0.1	2.0	10.0	<0.1	2.0	2.0	2.0	3.0	1.0	30.0	0.1	2.0	1.0	<50.0	--	--	--	--	107.3	37.3	
Li <sub>2</sub> O-CP-11	<0.1	1.0	10.0	<0.1	0.2	3.0	3.0	15.0	0.5	30.0	0.3	1.0	2.0	5.0	<0.1	<0.5	<0.1	<0.1	175.8	173.8	
Li <sub>2</sub> O-CP-12	<0.1	2.0	3.0	<0.1	<0.1	<0.1	<0.5	<0.1	<0.1	<0.1T	<1.0	<0.1	0.5	<0.1	1.0	<0.1	<0.5	<1.0	10.9	9.9	
Li <sub>2</sub> O-CP-13	<0.1	0.1	0.1	<0.1	0.1	0.02	<0.5	<0.1	0.1	<0.1T	100.0	<0.1	5.0	<0.1	>100.0	<0.1	<0.5	<1.0	<1.0	>350.2	>250.2
Li <sub>2</sub> O-CP-14	<0.1	0.1	0.1	<0.1	0.1	0.02	<0.5	<0.1	0.1	<0.1T	100.0	<0.1	5.0	<0.2	>100.0	2.0	<0.5	<1.0	<1.0	>315.9	>215.9
Li <sub>2</sub> O-CP-15	<0.1	1.0	1.0	<0.1	0.1	0.02	<0.5	<0.1	0.1	<0.1T	>100.0	<0.1	7.0	0.3	>100.0	<0.1	3.0	10.0	>426.1	>261.1	
Li <sub>2</sub> O-CP-16	<0.1	1.0	1.0	<0.1	0.1	0.02	<0.5	<0.1	0.1	<0.1T	50.0	<0.1	1.0	<0.1	<0.1	<0.5	<1.0	<1.0	10.9	9.9	
Li <sub>2</sub> O-CP-17	<0.1	1.0	1.0	<0.1	0.1	0.02	<0.5	<0.1	0.1	<0.1T	1.0	<0.1	1.0	<0.1	<0.1	<0.5	<1.0	<1.0	10.9	9.9	
Li <sub>2</sub> O-CP-18	<0.1	1.0	1.0	<0.1	0.1	0.02	<0.5	<0.1	0.1	<0.1T	1.0	<0.1	1.0	<0.1	<0.1	<0.5	<1.0	<1.0	10.9	9.9	
Li <sub>2</sub> O-CP-19	<0.1	1.0	1.0	<0.1	0.1	0.02	<0.5	<0.1	0.1	<0.1T	1.0	<0.1	1.0	<0.1	<0.1	<0.5	<1.0	<1.0	10.9	9.9	
Li <sub>2</sub> O-CP-20	<0.1	1.0	1.0	<0.1	0.1	0.02	<0.5	<0.1	0.1	<0.1T	1.0	<0.1	1.0	<0.1	<0.1	<0.5	<1.0	<1.0	10.9	9.9	
Li <sub>2</sub> O-CP-21	<0.1	1.0	1.0	<0.1	0.1	0.02	<0.5	<0.1	0.1	<0.1T	1.0	<0.1	1.0	<0.1	<0.1	<0.5	<1.0	<1.0	10.9	9.9	
Li <sub>2</sub> O-CP-22	<0.1	1.0	1.0	<0.1	0.1	0.02	<0.5	<0.1	0.1	<0.1T	1.0	<0.1	1.0	<0.1	<0.1	<0.5	<1.0	<1.0	10.9	9.9	
Li <sub>2</sub> O-CP-23	<0.1	1.0	1.0	<0.1	0.1	0.02	<0.5	<0.1	0.1	<0.1T	1.0	<0.1	1.0	<0.1	<0.1	<0.5	<1.0	<1.0	10.9	9.9	
Li <sub>2</sub> O-CP-24	<0.1	1.0	1.0	<0.1	0.1	0.02	<0.5	<0.1	0.1	<0.1T	1.0	<0.1	1.0	<0.1	<0.1	<0.5	<1.0	<1.0	10.9	9.9	
Li <sub>2</sub> O-CP-25	<0.1	1.0	1.0	<0.1	0.1	0.02	<0.5	<0.1	0.1	<0.1T	1.0	<0.1	1.0	<0.1	<0.1	<0.5	<1.0	<1.0	10.9	9.9	
Li <sub>2</sub> O-CP-26	<0.1	1.0	1.0	<0.1	0.1	0.02	<0.5	<0.1	0.1	<0.1T	1.0	<0.1	1.0	<0.1	<0.1	<0.5	<1.0	<1.0	10.9	9.9	
Li <sub>2</sub> O-CP-27	<0.1	1.0	1.0	<0.1	0.1	0.02	<0.5	<0.1	0.1	<0.1T	1.0	<0.1	1.0	<0.1	<0.1	<0.5	<1.0	<1.0	10.9	9.9	
Li <sub>2</sub> O-CP-28	<0.1	1.0	1.0	<0.1	0.1	0.02	<0.5	<0.1	0.1	<0.1T	1.0	<0.1	1.0	<0.1	<0.1	<0.5	<1.0	<1.0	10.9	9.9	
Li <sub>2</sub> O-CP-29	<0.1	1.0	1.0	<0.1	0.1	0.02	<0.5	<0.1	0.1	<0.1T	1.0	<0.1	1.0	<0.1	<0.1	<0.5	<1.0	<1.0	10.9	9.9	
Li <sub>2</sub> O-CP-30	<0.1	1.0	1.0	<0.1	0.1	0.02	<0.5	<0.1	0.1	<0.1T	1.0	<0.1	1.0	<0.1	<0.1	<0.5	<1.0	<1.0	10.9	9.9	
Li <sub>2</sub> O-CP-31	<0.1	1.0	1.0	<0.1	0.1	0.02	<0.5	<0.1	0.1	<0.1T	1.0	<0.1	1.0	<0.1	<0.1	<0.5	<1.0	<1.0	10.9	9.9	
Li <sub>2</sub> O-CP-32	<0.1	1.0	1.0	<0.1	0.1	0.02	<0.5	<0.1	0.1	<0.1T	1.0	<0.1	1.0	<0.1	<0.1	<0.5	<1.0	<1.0	10.9	9.9	
Li <sub>2</sub> O-CP-33	<0.1	1.0	1.0	<0.1	0.1	0.02	<0.5	<0.1	0.1	<0.1T	1.0	<0.1	1.0	<0.1	<0.1	<0.5	<1.0	<1.0	10.9	9.9	
Li <sub>2</sub> O-CP-34	<0.1	1.0	1.0	<0.1	0.1	0.02	<0.5	<0.1	0.1	<0.1T	1.0	<0.1	1.0	<0.1	<0.1	<0.5	<1.0	<1.0	10.9	9.9	
Li <sub>2</sub> O-CP-35	<0.1	1.0	1.0	<0.1	0.1	0.02	<0.5	<0.1	0.1	<0.1T	1.0	<0.1	1.0	<0.1	<0.1	<0.5	<1.0	<1.0	10.9	9.9	
Li <sub>2</sub> O-CP-36	<0.1	1.0	1.0	<0.1	0.1	0.02	<0.5	<0.1	0.1	<0.1T	1.0	<0.1	1.0	<0.1	<0.1	<0.5	<1.0	<1.0	10.9	9.9	
Li <sub>2</sub> O-CP-37	<0.1	1.0	1.0	<0.1	0.1	0.02	<0.5	<0.1	0.1	<0.1T	1.0	<0.1	1.0	<0.1	<0.1	<0.5	<1.0	<1.0	10.9	9.9	
Li <sub>2</sub> O-CP-38	<0.1	1.0	1.0	<0.1	0.1	0.02	<0.5	<0.1	0.1	<0.1T	1.0	<0.1	1.0	<0.1	<0.1	<0.5	<1.0	<1.0	10.9	9.9	
Li <sub>2</sub> O-CP-39	<0.1	1.0	1.0	<0.1	0.1	0.02	<0.5	<0.1	0.1	<0.1T	1.0	<0.1	1.0	<0.1	<0.1	<0.5	<1.0	<1.0	10.9	9.9	
Li <sub>2</sub> O-CP-40	<0.1	1.0	1.0	<0.1	0.1	0.02	<0.5	<0.1	0.1	<0.1T	1.0	<0									